Biochemical and Functional Characterization of Plastidial ADP-glucose Transporter

HvBT1 in Barley

by

Atta S. Soliman

A Thesis submitted to the Faculty of Graduate Studies of

The University of Manitoba

in partial fulfilment of the requirements for the degree of

DOCTOR OF PHILOSPHY

Department of Plant Science

University of Manitoba

Winnipeg, Manitoba

Canada

ACKNOWLEDGEMENT

TABLE OF CONTENTS

CHAPTER1: INTRODUCTION AND REVIEW OF LITERATURES

CHAPTER 2: BIOCHEMICAL AND MOLECULAR CHARACTERIZATION OF BARLEY PLASTIDIAL ADP-GLUCOSE TRANSPORTER (*HvBT1*)

CHAPTER 3. THE IMPACT OF PLASTIDIAL ADP-GLUCOSE TRANSPORTER (*HvBT1*) EXPRESSION ON STARCH SYNTHESIS IN BARLEY

CHAPTER4. DOWN-REGULATION OF THE PLASTIDIAL ADP-GLUCOSE TRANSPORTER (HvBT1) IMPAIRS STARCH ACCUMULATION AND ALTERS GRAIN COMPOSITION IN BARLEY.

LIST OF TABLES

LIST OF FIGURES

ABBREVIATIONS

AGPase: ADP-glucose pyrophosphorylase

ADP-Glc: ADP-Glucose

BT1: brittle 1

MCF: mitochondrial carrier family

DAA: days after anthesis

PBS: phosphate buffer saline

ORF: open reading frame

RC: rare codon

IPTG: isopropyl β-D-1-thiogalactopyranoside

3-PGA: 3- phosphoglyceric acid

FITC: fluorescein isothiocyanate

METS: mitochondrial energy transfer signature.

HvBT1: barley plastidial ADP-glucose transporter

SS: starch synthase

GBSS: granule-bound starch synthase

LSU: large subunit

SSU: small subunit

TLC: thin layer chromatography

RF: rate of flow

SEM: scanning electron microscope

WSC: water-soluble carbohydrate

3-PGA: 3-phosphogryceic acid

CTAB: cetyl tri-methyl ammonium bromide

SS: starch synthase

GBSS: granule-bound starch synthase

SBE1: starch branching enzyme1

PPi: inorganic phosphate

HPLC: high performance liquid chromatography

TLC: thin layer chromatography

HPAEC: high performance anion exchange chromatography

FOREWORD

The thesis has been written in manuscript format as outlined by the Department of Plant Science, Faculty of Agriculture and Food Sciences, University of Manitoba. The thesis is divided into five parts; general introduction and literature review followed by three manuscripts that contain the research parts in the thesis. Each manuscript contains an abstract, materials and methods, results and discussion. In addition, a general summary and conclusion, a list of references and appendices are included. The first manuscript (chapter #2), "Biochemical and molecular characterization of barley plastidial ADP-glucose transporter (HvBT1)", has been published in PloSOne (doi:10.1371/journal.pone.0098524). The second manuscript (chapter #3) and the third (chapter #4) have been submitted to Plant physiology and biochemistry and BMC Plant Biology, respectively.

ABSTRACT

Biochemical and Functional Characterization of Plastidial ADP-glucose Transporter HvBT1 in Barley

Atta Soliman. Ph.D, University of Manitoba, September, 2014.

Supervisor: Dr. Fouad Daayf.

Starch is the main storage biopolymer in cereal plants. Several enzymes and carrier proteins are involved in the starch biosynthesis process. ADP-glucose pyrophosphorylase (AGPase) has been characterized as a key factor in this process, which catalyzes the conversion of glucose 1-phosphate into ADP-glucose in the cytosol of the endospermic cell. The freshly synthesized ADP-glucose must be transported into amyloplasts by the activity of ADP-glucose transporter. In the current research, we have characterized HvBT1 biochemically in *E. coli* system. HvBT1 shows high affinity to ADP-glucose as a transport substrate in counter-exchange with ADP with affinities of 614 and 334 µM, respectively. The cellular and subcellular localization of HvBT1 indicated its target the amyloplasts envelopes. The comparison between two barley cultivars; Harrington and Golden Promise shed some light on the impact of HvBT1 on starch accumulation. Higher expression of AGPase and HvBT1 (10 fold) provide an ideal combination for improving starch yield, where starch content was higher by 2.5% in Harrington. Unlike Harrington, the expression of soluble starch synthase encoded genes was higher in Golden Promise which accumulates less starch. This result provided evidence of the importance of HvBT1 in starch synthesis process along with AGPase. Down-regulation of HvBT1 also provided a cement evidence of its effect on the starch accumulation process, where the knock down

lines showed 17% lower starch and altered starch composition. Also, as a result of decreasing starch, protein content increased in the transgenic grains by 4-5 % of its content in the wild type, while β-glucan was 37% lower than the wild type control. Down-regulation of HvBT1 led to decrease the grain yield by ~ 30% as a result of increase the grain size. Also, it seems to have pleotropic effects on other starch synthesis genes, where *AGPLs* was down-regulated while the plastidial SSU genes, *AGPS1b* and *S2* were up-regulated. Soluble starch synthases *SS2a* and *SS3a* were down-regulated, while *SS2b* was up-regulated in the transgenic plants. The accumulated evidences indicated that HvBT1 is a key factor in starch biosynthesis process.

CHAPTER 1: INTRODUCTION AND LITERATURE REVIEW

1.1. Introduction

Starch is considered to be the main storage form of carbohydrates in plants. As storage compound, starch has unique features which make it a more preferable compound for short and long term storage than soluble sugars. These features are the osmotic inactivity, storability in granules and difficulty to convert into a soluble phase, making it a stable molecule. Starch is synthesized and stored in the old leaves during the day time to be used later at night time for metabolic reactions and energy production (Geiger et al. 2000). Furthermore, starch has several benefits for human health; one of them being the development of resistant starches. Resistant starch is a fraction of starch or its degradation products which are transported from the small intestine into the large bowel. Starch is fermented in the large bowel by gut bacteria that produce short fatty acids' chains which decrease colon cancer (Topping and Clifton, 2001). Resistant starch is also important for human health since its digestion is slow providing the blood stream by modulate flow of glucose which reduces the insulin demand (Morell and Myers, 2005).

Most starch that is being used in human diet comes from cereal grains. Starch yield is tightly controlled by grain filling stage during normal plant development. Cereal grain development can be divided into two large stages; the enlargement stage and the filling stage. During the enlargement stage, the cell division is accelerated for zygote and endosperm and water influx into the cell, while in the second stage, the cell division slows down and storage molecules start to accumulate (Emes et al. 2003). Starch consists

of two major compounds; amylose and amylopectin, both consisting of glucose polymers. In amylose, the glucose monomers bind together by α 1,4- glucosidic bonds and produce a linear polymer, while amylopectin has another type of bonds; α 1,6- glucosidic bonds which make branches in the glucose polymers (Martin and Ludewig, 2007). Polyglucans are renewable and biodegradable compounds used by different industries. The most important and challenging issue for industry nowadays is to identify and characterize factors that enhance the effectiveness of starch accumulation and increase starch yield (Baroja-Fernandez et al. 2004). The increased demand on cereals reflects their importance worldwide for energy production, human and animal consumption, as well as other related food applications. The bioethanol production industry is growing and it is a worldwide concern (Morell and Myers, 2005).

The main source of the carbon which is used for the starch biosynthesis in plants comes from ADP-glucose. ADP-glucose is synthesized by ADP-glucose pyrophosphorylase enzyme (AGPase) in the cytosol of endospermic plants especially in the storage tissues and then imported into the amyloplasts through ADP glucose transporter protein localized at the amyloplast membrane. Moreover, ADP glucose sugar is imported in counter exchange with ADP (Bowsher et al. 2007). The majority of AGPase activity takes place in the plastids in non-endospermic species, but in cereals and some graminaceous species, 85–95 % of the AGPase activity takes place in the cytosol of endospermic cells in storage tissues, so the extra-plastidial form of AGPase results into ADP-glucose production in the cytosol (James et al. 2003). Starch biosynthesis requires the nucleotide sugar ADP-glucose which is considered as the glucosyl donor in the reaction catalyzed by starch synthase enzyme (Leorch et al. 2005). ADP-glucose

transporter protein is a transmembrane protein located in the amyloplast envelopes membrane and the polypeptide responsible for the binding site for the substrate (ADP-Glucose) is a 38 KDa fragment. Recent approaches focused on the low starch mutants from maize (*Brittle 1*) and barley (*Lys5*) which accumulate ADP glucose in the endospermic cell cytosol, have shown mutations in one or more of the amyloplast envelop transmembrane polypeptide (Browsher et al. 2007). In maize, the *brittle 1* gene (*ZmBT1*) which belongs to the mitochondrial carrier family (MCF), has a great effect on starch accumulation in cereals, particularly in maize (Kirchberger et al. 2007). The maize mutant that is deficient in *ZmBT1* gene accumulates 12 fold higher levels of ADP glucose in the endospermic cell cytosol than its wild type endosperm (Pien et al. 1996). There is also a maize homolog in potato (*Solanum tuberosum)* (*StBT1*) that has been identified and functionally characterized as a specific adenine nucleotide uniporter. The main function of this protein is to provide the cytosol and other cell compartments with ATP which is originally synthesized in the plastids (Leorch et al. 2005). In barley, the isolated plastids from *lys5* mutants were able to synthesize starch using glucose-1-phosphate, but they could not synthesize starch using ADP glucose sugar. This suggests that there is a lesion in the *lys5* locus for the plastidial ADP- glucose transporter protein. The gene which encodes for ADP glucose transporter (HvNST*)* belongs to carrier family proteins. In this approach, the most abundant plastidial envelopes membrane proteins isolated and purified showed homology with maize ADP glucose transporter *Brittle1*. These findings suggest a vital role of HvNST in starch accumulation (Patron et al. 2004). The existence of ADP glucose transporters in some cereal species such as maize and barley points to the existence of these transporters in all endospermic species (Martin and Ludewig, 2007).

1.1.1. Objectives of the work

1- Biochemically and molecular characterization of the barley plastidial ADP-glucose transporter HvBT1, using an *E. coli* expression system, and study the expression and localization of HvBT1.

2- Investigate the possible impact of *HvBT1* expression on other starch biosynthesis-related genes and starch accumulation in two malting barley cultivars; Harrington and Golden Promise.

3- Investigate the impact of down-regulation of *HvBT1* in barley Golden Promise using antisense approach on grain composition.

Literature Review

1.1.2. Barley

Barley (*Hordeum vulgare L.*) is one of the oldest cereal grain crops worldwide. It is believed that, in the most authentically reports, barley (*Hordeum spontaneum*) is the ancestor of our cultivated barley (*Hordeum vulgare L).* It is also believed that barley was domesticated in the Fertile Crescent in the Near East region that represents a part from Palestine, Israel, Turkey, Syria, Iraq and Iran (Harlan, 1978). There are more evidences for the multicentre of origin of cultivated barley includes North Africa and Asia. The DNA marker approaches have been applied to the remains of barley grains in archaeological sites Near Crescent to investigate the genetic divergences among different populations. The results indicated that Israel-Jordon region is the site of barley domestication and the Himalayan region could be the centre of diversifications of cultivated barley (Badr et al. 2000).

Barley was presumably first used as human food in ancient civilizations alongside with wheat, and it was considered as "the poor's men bread ". Thousands of years ago, barley has been cultivated in the old world such as North Africa, Asia and Europe and brought to North America by Columbus in 1494 (Newman and Newman 2006). Because of the prominence of wheat and rice, barley has been used for feed, malting and brewing. Recently, about two-thirds of the barley crop has been used for feed, one-third for malting and about 2% for food directly.

In Canada, Barley is growing mainly in the Prairie Provinces; Alberta, Saskatchewan and Manitoba, and the average annual production of barley in Canada is around 12.5

million tons. Barley products have much potential on the human health. Barley β-glucans act in lowering blood cholesterol and glycemic index. Barley is a rich source of tocols, including tocopherols and tocotrienols, which are known to reduce serum LDL cholesterol through their antioxidant properties. In addition, barley flour now is used to improve the nutritional quality of wheat bread without affecting the bread appearance and volume. Recently, barley research is refreshed to introduce barley cultivars serving in different industries for use of the starch and non-starch components in biofuel production and for human health benefits, respectively.

1.1.3. Grain composition

1.1.3.1. Starch content

Starch is the most important biopolymer in higher plants, which is used in human food additives and various industries such as bioethanol production as a raw material. Starch mainly contains two components; amylose and amylopectin. Amylose is a linear polymer of α- 1,4 linked D-glucopyranose and also some α- 1,6 linked glucan chain (Curá et al. 1995), while amylopectin is branched molecules composed of α- 1,4 linked glucose chains connected by α- 1,6 linkages (Hood, 1982).

1.1.3.2. Protein content

Barley grains contain approximately 8-13 % proteins on dry matter basis. There is a negative correlation between starch and protein contents in cereal grains. Seebauer *et al.* (2010) reported about inbred maize lines that accumulated high protein contents accompanied with low starch and high kernel weight. Also, Clarke *et al.* (2008) reported that the protein content increased in barley *SS2a* mutant, which accumulated less starch.

1.1.3.3. B- glucan content

Barley grain contains a wide range of β-glucans that may constitute 3 to 20% of the grain dry weight, depending on the genotypes and environmental effects (Munck et al. 2004; Fincher and Stone 1986). The cell wall of barley endosperm contains around 75% of the total β-glucan found in grains (Fincher and Stone 1986) which has high potentials in reducing blood cholesterol and improve human health (Kalra and Joad 2000; Léon et al. 2000). However, β-glucan has disadvantages in brewing process.

1.1.3.4. Lipid content

In cereal grains, lipids are found in various compartments such as aleurone layer, endosperm, embryos and represents 1-3% of the total grain weight (Morrison 1978; Joacobsen et al. 2005). In barley, lipids are mainly concentrated in the embryos (Price and Parsons 1979) and also make a complex with amylose especially lysophospholipids (Morrison 1993).

1.1.4. Starch biosynthesis enzymes

1.1.4.1. ADP-Glucose pyrophosphorylase (AGPase)

In cereals, ADP-Glucose pyrophosphorylase (AGPase) is located in the cytosol and plastids of the endospermic cells, whereas the activity of AGPase was reported to take place only in the plastids in other plant species. The total activity of AGPase in the cytosol is about 85-95 % in the cereal endosperm (Beckles et al. 2001). In the cytosol, AGPase converts glucose 1-phosphate using ATP into ADP-Glucose which represents the building blocks of starch synthesis (Stark et al. 1992). AGPase is a heterotetrameric enzyme that contains two small subunits (SSU) and two large subunits (LSU). The two

types of subunits are very essential for the normal activity of AGPase. The highest AGPase activity occurs in the plastids of the most plant cells (Bae et al. 1990). AGPase activity in the endosperm was confirmed in the most important cereal crops (Denyer et al. 1996; Sikka et al. 2001; Thorbjørnsen et al. 1996 and Tetlow et al. 2003). In case of the absence of the large subunits, the small subunits are able to perform the normal enzyme function but lack the allosteric regulation of the heterotetrameric form (Ballicora et al. 1995). The small subunits are catalytic subunits, whereas the large subunits are thought to modulate the enzymatic regulatory prosperities. In barley (*Hordeum vulgare L.*), AGPase small subunits are encoded by *HvAGPS1* gene. This gene encodes for two different transcripts for the small subunits of the ADP-Glucose pyrophosphorylase enzyme. Previously, it was assumed that *HvAGPS1a* encodes for small subunits in the cytosol, whereas *HvAGPS1b* encodes for plastidial small subunits (SSU). Another AGPase small subunit gene *HvAGPS2* was identified as the main gene responsible for the plastidial AGPase small subunits and has a role in AGPase activity in leaves (Rösti et al. 2006). Low starch barley mutant, Risø 16, showed 80% less starch as compared to the normal starch level in the parental line. This mutant has 31% of the normal activity of the AGPase (Johnson et al. 2003). The starch content has been greatly affected in maize mutants' *shrunken-2* and *btrittle-2* which have less than 2% of the normal AGPase activity and accumulate less than 25% of the normal starch yield (Tsai and Nelson 1996). In non-photosynthetic organs, starch is synthesized from the dominant photosynthetic molecule (sucrose) which is imported into the cytosol of developing storage organs. Sucrose is catabolised in the cytosol and mitochondria to produce starch synthesis precursors, glucose 6- phosphate and ATP (Comparot-Moss and Denyer 2009). Both

molecules are imported into the plastids via glucose phosphate/phosphate transporter and ATP/ADP transporter (Neuhaus and Wagner 2000).

1.1.4.2. Starch synthases

Starch synthase (SS) exist in all plants in multiple isoforms. Starch synthase isoforms have conserved functional domains. The C-terminal domain has two ADP-glucose (ADP-Glc) binding sites and a glucosyle transferase domain (Denyer et al. 2001). The N-terminal varies among isoforms and species. The main function of starch synthase (SS) is to catalyze the transfer of the glucosyle unit of ADP-Glc to the non-reducing end of the elongated glucan chain (Jeon et al. 2010). Those isoforms are also expressed in maize and wheat endosperm (Gao et al. 1998; Li et al. 2000). Those isoforms are encoded by multiple genes in cereals and their expressions are tissue-dependent. In maize, SSII has two isoforms (SSIIa and SSIIb) which are encoded by different genes. *SSIIa* gene is expressed mainly in the endosperm, while *SSIIb* is expressed in leaves. The Granule-bound starch synthase I (*GBSSI*) is expressed in different tissues by multiple genes (Harn et al. 1998; Tomlinson and Denyer, 2003). In wheat, there are multiple tissue-specific isoforms of GBSSI. Those isoforms are encoded by two types of genes; one gene is expressed in the endosperm and pollen grains, while the other one is expressed in the pericarp (Vrinten and Nakamura 2000). In Arabidopsis, there are four starch synthase isoforms (GBSS1, SS1, SSII, SSIII and SSIV) have been identified. Ten starch synthase isoforms have been characterized in rice (Hirose and Terao 2004; Ohdan et al. 2005).

1.1.4.2.1. Granule-bound starch synthase (GBSS)

In cereals, there are two forms of GBSSs; GBSSI and GBSSII. This class of starch synthases is associated with the starch granules unlike other classes of starch synthases which are found partially or entirely in the soluble phase in the plastids (Tomlinson and Denyer 2003). The main function of this class of SS is to elongate the amylose chains in the growing starch granules. Moreover, GBSSI has a role in amylopectin biosynthesis through elongating the long glucans in potato and rice (Denyer et al. 1996; Hanashiro et al. 2008). GBSSI is expressed mainly in storage organs, while the GBSSII is expressed in non-storage tissues and is responsible for transitory starch accumulation (Vrinten and Nakamura, 2000). In cereal, GBSSI is encoded by genes located in *waxy* locus. Mutations in *waxy* locus led to change in starch composition but not in starch content. The loss of GBSS activity results in low amylose content or lacking amylose completely in starch and produce *waxy* starch (Fujita et al. 2001; Visser et al. 1991). In barley, the *wx* mutants showed about 9% reduction of amylose content. This reduction is a result of the deletion of a part of *wx* promoter and 5' untranslated region of GBSSI gene in some low amylose cultivars. On the other hand, amylose is completely undetectable in starch in some barley waxy mutants (Patron et al. 2002).

1.1.4.2.2. Soluble starch synthase

1.1.4.2.2.1. Starch synthase I (SSI)

Starch synthase I (SSI) unlike other starch synthases, is unique and there is no known isoforms for it. Using anion exchange chromatography analysis, SSI represented the major soluble proteins in rice endosperm, where its activity was about 70% of the total SS activity (Fujita et al. 2006). The main role of SSI is to elongate the short amylopectin chains with DP < 10. Studies on cereal mutants and transgenic plants demonstrated that

SSI shows high affinity to the short amylopectin chains and work on chains A and B1 as substrates until reach a critical length (Commuri et al. 2001; Guan et al. 1998; Jeon et al. 2010). Analysis of some rice *SSI* mutants showed reducing of the chains DP 8-12, while the chains with DP 6-7 and 16-19 increased. These data demonstrate that SSI works only on the short chains with DP 6-7 and generates chains with DP 8-12 (Fujita et al. 2006). Analysis of Arabidopsis *SSI* mutants showed that the deficiencies in the SSI activity had no effect on starch granules, seed size, or shape (Delvalié et al. 2005). These results demonstrate that there are other SS isoforms which are able to compensate the reduction of the SSI activity. In cereal, *SSI* is expressed in the early stage of seed development (5-10 DAP). The decreasing activity of SSI is assumed to be a result of entrapping of the proteins in the growing granules, which would make it not accessible to the substrates (Peng et al. 2001).

1.1.4.2.2.2. Starch synthase II (SSII)

In monocot, there are two isoforms of SSII; SSIIa and SSIIb. SSIIa is functional in endospermic tissues while SSIIb is mostly functional in photosynthetic tissues (Tetlow and Emes 2011). SSII isoforms are located in the granules along with GBSSI in different cereal species. In maize, two SSII isoforms are characterized *in vitro,* which showed affinity to different substrates and kinetic properties (Imparl-Radosevich et al. 2003). Studies on different cereal crops demonstrated that the loss of function of SSII reduced the starch content and affect the amylopectin chain length and granule morphology. The loss of SSII activity results in alternations of the granule size and shape in wheat *sgp1* and barley *sex6* mutants (Morell et al. 2003; Yamamori et al. 2000). Maize *sugary2* (*su2*) mutant which lack SSIIa activity showed increased frequency of short chains of the

amylopectin (DP 6-11) and decreasing of the abundance chains (DP 13-20). The same effect has been observed in different mutants of barley and wheat (Morell et al. 2003; Zhang et al. 2004; Yamamori et al. 2000).

1.1.4.2.2.3. Starch synthase III (SSIII)

Starch synthase III is the second abundant SS in terms of the activity in the endosperm of maize and rice (Cao et al. 1999). In rice, two isoforms of SSIIIs were identified; SSIIIa and SSIIIb, which are expressed in endosperm and leaf tissues, respectively (Dian et al. 2005). The main role of the SSIIIs is to elongate the long glucan chains of amylopectin molecules (Fujita et al. 2007). The rice *ssIIIa* mutant showed reduction of glucan chains with DP 6-8, DP 16-20 and DP $\geq$ 30 and increase in the intermediate chains. The analysis of the rice *ssIIIa* mutants revealed that SSIIIs are involved in amylopectin synthesis from intermediate chains (Ryoo et al. 2007; Fujita et al. 2007). In maize, the *du1* mutants produced endosperm with a dull appearance. The glassy endosperm phenotype leads to the abnormal starch granule morphology (Gao et al. 1998). On the other hand, changes in the starch granule morphology and crystallinity, along with a reduction in the distribution of long-glucan chains, have been observed (Ryoo et al. 2007). This observation demonstrates the role of SSIII in amylopectin synthesis through elongating the long glucan chains. In potato, expressing the antisense from SSIII led to change in the long glucan chain distribution and affects the amylopectin structure and consequently starch granule morphology (Abel et al. 1996; Lioyd et al. 1999).

1.1.4.2.2.4. Starch synthase IV (SSIV)

The complete function of the SSIV in the contribution of the glucan chain length in cereals is still unknown. In rice, two genes of SSIV; *SSIVa* and *SSIVb* have been identified and expressed constantly during grain filling. This finding suggested the possible role of these genes in starch synthesis in the endosperm (Hirose and Terao 2004; Dain et al. 2005). In Arabidopsis, *ssIV*/dull mutant has been identified but not in other plant species. This mutant showed severe growth deficiency and display not only reduction in the number of starch granules per plastid but also increasing the starch granule size. These results suggested that possible role of SSIV in the priming of starch granule formation (Roldán et al. 2007). Another study on Arabidopsis *ssIV* mutant reported that SSIV is necessary for establishing and priming new starch granules. The function of SSIV in priming the starch granules can be partially compensated by SSIII. The loss of function of both SSIV and SSIII results in inhibition of starch granules (Szydlowski et al. 2009).

1.1.4.2.3. Starch branching enzymes (SBEs)

The function of this type of enzymes is to catalyze the formation of branch points by cleaving the- (1, 4) polyglucan linkage and connect the chains via α- (1, 6) linkage. BEs belong to α- amylase superfamily and able to create α- (1, 6) linkages on the glucan chains (Jespersen et al. 1993). There are two major classes of SBEs: SBEI (SBEb) and SBEII (SBEa). The differences between the two classes result in the glucan chain length and substrate specificity. SBEI shows high affinity to branching amylose molecules, while SBEII shows high affinity to amylopectin (Guan and Preiss 1993). Analysis of SBEIa mutant (*sbe)* in rice showed significant reduction in the abundance of long glucan chains of amylopectin, while short and intermediate glucan chains increased. On the other

hand, the *sbe1* mutant starch showed high resistance to gelatinization because of higher proportion of long glucan chains (Satoh et al. 2003). In cereal, there are two isoforms of SBEII; SBEIIa and SBEIIb. *SBEIIa* is expressed mainly in photosynthetic tissues, while *SBEIIb* is expressed in the endosperm. In wheat, the double mutant of *SBEIIa* and *SBEIIb* produced high amylose starch phenotype (Regina et al. 2005). High amylase starch phenotype in maize has been produced as a result of a mutation in SBEIIb (Yun and Matheson 1993). Suppression of all SBE genes in barley produces amylose only starch (Carciofi et al. 2012) that indicates the essential role of the SBE in amylopectin synthesis and structure.

1.1.4.2.4. Starch de-branching enzymes (DBEs)

Two classes of starch branching enzymes (DBEs) have been characterised; isoamylase (ISA) and pullulanase (PUL). These types of enzymes hydrolyze the ɑ-1.6 linkages of polyglucans. Both groups of enzymes have preferred substrates.

1.1.4.2.4.1.Isoamylase (ISA)

The impact of isoamylase on starch granules has been investigated via mutations in ISA genes. In maize, the *sugary1* (*su1*) mutant, which is deficient in ISA1 activity was isolated from cDNA of developing kernels that showed effect on the endosperm, where more short chains of amylopectin were detected along with phytoglycogen accumulation (James et al. 1995; Burton et al. 2002; James et al. 2003). In rice, transgenic plants expressing antisense of ISA1 produced *sugary*-amylopectin as in maize. The *su1* function was restored by transforming rice *su1* mutant with the wheat ISA gene, where the access phytoglycogen was substituted by amylopectin (Fujita et al. 2003; kubo et al. 2005). An

Arabidopsis mutant lacking all DBE proteins was not capable of forming starch granules, but highly branched glucans (Streb et al. 2008). It has been reported that the main function of ISA was to edit the highly branched chains or remove the unappropriate positioned branches of amylopectin and maintain cluster structures (Buléon et al. 1998; Nakamura 2002).

1.1.4.2.4.2.Pullulanase (PUL)

Pullulanase (PUL) debranches pullulan and amylopectin, unlike ISA, which debranches phytoglycogen and amylopectin (Nakamura et al. 1996). PUL is assumed to act on starch degradation during grain germination. Recent data from rice and maize indicated that PUL has been detected in developing grains, where PUL gene showed high expression during grain development (Nakamura et al. 1996; Beatty et al. 1999). Gene expression data indicated that PUL is involved in the starch biosynthesis process as ISA. Confirmation of PUL's function was obtained from rice PUL-deficient mutants. The double mutant *pul/su1* showed higher increase in the short chains than *pul* mutant alone (Fujita et al. 2009). In maize, the PUL-deficient mutant *zpu1-204* did not show significant differences in starch composition, while the double mutant *zpu-2041/su1* showed high accumulation of phytoglycogen in the endosperm (Dingers et al. 2003). Starch composition has not been affected by mutations in ISA or PUL on equal foot, but PUL is assumed to compensate for ISA and is involved in starch biosynthesis in cereal endosperm (Jeon et al. 2010).

1.1.4.2.5. Starch phosphorylase

There are two types of starch phosphorylase enzymes in plants, plastidial Pho1 and cytosolic Pho2. This group of enzymes catalyzes the removal of glucosyl units from the non-reducing ends of amylopectin chains and the forming of glucose 1-phosphate. Generally, starch phosphorylase is assumed to act on the degradation of phosphorolytic glucan (Steup 1988). Recently, Pho1 has been assumed to function on the surface of the starch granule, modifying starch structure and releasing glucose 1-phosphate to be recycled by starch synthase in building glucan chains (Tetlow et al. 2004). In rice, *pho1* mutant showed abnormal endosperm by accumulating small starch granules (Satoh et al. 2008). In wheat, starch phosphorylase Pho1 proteins increased in conjunction with other starch branching and starch synthase protein levels (Tickle et al. 2009). Pho1 synthesizes long chain malto-oligosaccharides (MOS) from glucose 1-phosphate, which provide evidence for its function in the glucan initiation process (Jeon et al. 2010).

1.1.5. Sugar transporters

1.1.5.1. Sucrose transporters

Sucrose is the primary product of photosynthesis in plants. It is partitioned from the synthesis location and assimilated to sink and storage tissues. Sucrose could be stored in form of starch or fatty acids or degraded into various metabolites. Sucrose moves passively from cell to cell through plasmodesmata or positively in different tissues through a sucrose transporter protein (Sauer 2007). Sucrose transporter is essential for plant growth and development, where it works for allocation of assimilates from sources to sinks. Sucrose transporter proteins could interact with other metabolic pathways and other developmental process to coordinate the whole plant communication. Studying the

function of sucrose transporter, sucrose facilitator and sucrose-like proteins has opened a new area of research for the role of cell compartmentations on metabolism and signalling of sucrose transporter in plants (Kühn, 2010). The genome sequence analysis and phylogenetic approaches provided more information about the members of the Major Facilitator Superfamily (MFS). Different sucrose transporter genes have been identified form different species. Nine sucrose transporter genes from Arabidopsis and five form rice have been identified (Aoki et al. 2003). The genome sequence analysis of some monocotyledonous plants has divided the sucrose transporter into five groups. The monocot sucrose transporter has been classified into two distinct groups (VI and V) (Braun and Slewinski 2009). The monocot sucrose transporter proteins are highly specific, unlike dicot *SUTs* (Sivitz et al. 2007). Many *SUT* genes have been identified and characterized from sugarcane, barley and rice. In sugarcane, *SUT* gene is expressed in maturing stems and assumed that it plays an essential role of sucrose accumulation in stalks (Reinders et al. 2006). In rice, down-regulation of *OsSUT1* using antisense technique affected the gain weight, germination and seedlings development (Furbank et al. 2001; Ishimaru et al. 2001). *OsSUT1* is involved in retrieving of sucrose from apoplasm (Scofeid et al. 2007). The monocot sucrose transporter group I was functionally characterized in different cereal plants. The barley sucrose transporters *HvSUT1* and *HvSUT2* are responsible for sucrose loading in phloem and sink tissues (Weschke et al. 2000).

1.1.5.2. Adenine nucleotide transporter

The most important differences between photosynthetic and non-photosynthetic plastids are the presence and absence of the photophosphorylation process, respectively.

17

Heterotrophic plastids require ATP energy molecules which can be generated from cytosolic organelles by substrate phosphorylation (Emes and Neuhaus 1997). ATP/ADP transporter was identified as a second type of eukaryotic adenylate carrier proteins (Kampfenkel et al. 1995). ATP/ADP transporter from Arabidopsis (*AtAAPT1*) was characterized biochemically in *E. coli* which confirmed the functional prosperities of transporting ATP in counter exchange with ADP (Tjaden et al. 1998). Plastidial ATP/ADP transporter proteins possess 11 to 12 membrane domains and exist in all higher and lower plant species (Winlker and Neuhaous 1999; Linka et al. 2003). In potato (*Solanum tuberosum*), a homolog of BT1 was identified as a mitochondrial carrier protein by phylogenetic analysis. The difference between BT1 from maize and potato is that maize *ZmBT1* has been characterized as ADP-Glucose transporter protein, while *StBT1* has been characterized as adenine nucleotide uniporter that can transport various types of nucleotides; AMP, ADP and ATP. Expression of *StBT1* in *E. coli* system led to functional integration of StBT1 protein in the *E. coli* cell membrane and transport of adenine nucleotides (Leorch et al. 2005). Arabidopsis plant (*Arabidopsis thaliana*) possesses two isoforms of ATP/ADP transporter (*AtNTT1* and *AtNTT2*). *AtNTT1* is a sugar induced form expressed mainly in stems and roots, whereas *AtNTT2* is expressed in various Arabidopsis tissues (Reiser et al. 2004). Recently, a new Arabidopsis ATP transporter (*AtPM-ANT1*) has been identified and characterized. The function of this transporter was identified as exporting ATP molecules that work as extracellular signal molecules. These signal molecules are required for pollen maturation and anther dehiscence (Rieder and Neuhaous 2011)

1.1.5.3. ADP-Glucose transporters

1.1.5.3.1. Structure and function

The ADP-glucose transporter is a member of the mitochondrial carrier family. This family works as carriers for different metabolites. ADP-glucose transporter does not show high similarities at the DNA or protein levels with the nucleotide sugar transporters which belong to drug metabolite transporter super family (Patron et al. 2004; Tjaden et al. 2004). The prediction of the ADP-glucose transporter protein structure showed that the protein is one polypeptide chain and works as a monomer. It contains six membrane domains connected by inter loops inside and outside the membrane. The N- and C-terminals are located in the cytosolic side of the membrane (Swissprot data base). In the endospermic cell, the majority of ADP-glucose is synthesized in the cytosol and `should be imported to amyloplasts for starch biosynthesis (Comparot-Moss and Denyer 2009). ADP-glucose transporter is assumed to be a key factor in starch biosynthesis process. It has a potential effect on the plastidial ADP-glucose content in the amyloplasts and subsequently on the starch accumulation and quality (Tjaden et al. 1998; Clarke et al. 1999). Importing ADP-glucose into amyloplasts cannot be carried out by ATP/ADP transporter, because it is highly specific to nucleotides but not to nucleotides sugars (Emes et al. 2003). The *BT1* locus in maize encodes a protein with 38-42 kDa localized in maize amyloplast envelopes and is believed to have a role in the transport of ADP-glucose (Sullivan et al. 1995; Shannon et al. 1998). Study on wheat endosperm amyloplasts has demonstrated the presence of the ADP-glucose transporter proteins in the amyloplast envelopes (Emes et al. 2001). Different barley low-starch mutants were tested for starch accumulation. It was assumed that the ADP-glucose transporter gene is located in the *Lys5* locus on the chromosome 6H. Two of the low starch mutants showed an

amino acid substitution in the conserved domain for all members of the carrier proteins family of. This finding strongly supports the idea of the ADP-Glucose transporter gene is located in the *Lys5* locus. Starch analysis of the low starch mutants showed high accumulation of ADP-Glucose in the endospermic cell cytosol (Patron et al. 2004).

1.1.5.3.2. Characterization of ADP-Glucose transporter

The transport activity of different phosphorylated sugars was investigated using the amyloplast envelop membrane. The maize amyloplast envelop proteins were functionally reconstituted in the proteoliposomes. The results showed that the amyloplasts are able to transport glucose 6-phosphate, hexose phosphate and ADP-glucose which work as substrates for starch biosynthesis (Möhlmann et al. 1997). Maize ADP-glucose transporter (*ZmBT1*) was the first characterized homolog in cereal plants. The heterologous expression of this gene in *E. coli* led to functional integration of the expressed protein to the plasma membrane of *E. coli* cells. The transport assay with the radiolabeled substrate; (^{14}C) ADP-Glc showed that the ability of the expressed protein to transport the substrate in in counter exchange of ADP with affinity of 850 and 465 μM of ADP-Glc and ADP, respectively (Kirchberger et al. 2007). In wheat, ADP-glucose transporter was characterized using the reconstituted amyloplast envelops proteins in proteolosomes. The uptake of the ADP-glucose was correlated with the ADP and AMP as in counter-exchange substrates (Bowsher et al. 2007).

1.1.6. Plant transformation

Transformation of cereal crops is still genotype-dependent. A few numbers of cultivars from different cereal crops are suitable for transformation process. Barley Golden

Promise is one of the model cultivars which can be used to study the function of different pathways in cereals. The advantages of using barley for transformation are the less genomic complexity than wheat and high callus induction and regeneration. The most elite cereal cultivars are still recalcitrant for transformation because of their resistance to *Agrobacterium* infection and tissue culture (Emes et al. 2001). Successful transformation depends on the gene expression cassette, the technique of DNA transfer and the tissue culture techniques which used to produce fertile transgenic plants (Repellin et al. 2001).

1.1.6.1. Transformation techniques

1.1.6.1.1.   Direct gene transfer

1.1.6.1.1.1. Biolistic DNA transfer system

The biolistic transformation or particle bombardment was the most common method for transformation of cereal crops. The main objective of this technique is to investigate the transient gene expression. Successful transformation of cereal crops using this method has been reported to produce stable transgenic plants (Danilova, 2007). The transformation of the woody plants using *Agrobacterium* has many limitations because of the bacterial host range and poor tissue culture conditions. The biolistic transformation can overcome the first barrier of *Agrobacterium* transformation. A successful attempt of using biolistic-mediated transformation was performed on a fruit tree (*Feronia limonia L.*). Transient expression of GUS gene and stable transgenic plants have been obtained by Purohit et al. (2007).

One of the disadvantages of the biolistic delivery system is the high copy number in the transgenic plants. The high copy number in the genome of same cell leads to gene

silencing and instability. In maize, the transgenic plants obtained from using the biolistic gene delivery system resulted in copy number from 1-20 copies. The best performance was found in maize plants that carried copies ranging from 1- 4 (Walters et al. 1992) and 3-8 copies (Brettschneider et al. 1997). The size of the introduced genes is another limiting factor of using the biolistic gene delivery system. The DNA fragments larger than 10 kb could be difficult to be introduced by this system because of poor adhering to the gold particle and damage during the bombardment. However, transformation of DNA fragments smaller than 10 kb showed high rate of success in many studies (Register et al. 1994; Tang et al. 2000). Commercial barley cultivars are still difficult to use as a material for transformation. Improving transformation approaches can help dragging the elite cultivars to genetic transformation. Shoot meristematic culture was used for biolistic-mediated transformation of oat and barley commercial cultivars. The transgenic plants showed stability over generations (Zhang et al. 1999).

1.1.6.1.1.2. PEG – mediated transformation

The first transgenic cereal plant was produced by the direct DNA transfer using the protoplast (Toriyama et al. 1988). The use of protoplast cells eliminates the barriers related to some properties of plant cells. Stable transformed plants from different cereal plants have been produced via protoplast transformation. Stable transformation from barley (*Hordeum vulgare L.*) was first obtained using PEG-mediated DNA transfer. Cell suspension is the relevant plant material to obtain protoplasts for stable transformation (Lazzeri et al. 1991; Nobre et al. 2000). In rice, fertile transgenic plants were obtained using PEG-mediated transformation of protoplast from cell suspension (Kayashimoto et al. 1990). Chloroplasts have also been used for PEG-mediated DNA transfer in tobacco.

1.1.6.1.1.3. Electroporation- mediated transformation

Electroporation is a direct method of introducing DNA into plant protoplasts. The potential advantages of electroporation are high DNA delivery rate, the viability of the electroporated cells, applicable for single cell (protoplast) and cell clusters and low cost over other transformation techniques (Prasanna et al. 1997; Sorokin et al. 2000). The disadvantage of using electroporation is the high rate of damage to the DNA constructs due to the electric pulsing (Danilova, 2007) and undesirable mutations (Somaclonal variations) in the culture of cell suspension and protoplasts (Lorz and Lazzeri 1992). The great success obtained using electroporation led the use of more plant materials other than protoplasts. Different parameters were optimized to improve the efficiency of electroporation such as mechanical wounding and enzymatic treatment of the explants to facilitate the DNA uptake (Vain et al. 1995). Several optimizations were conducted to increase the efficiency of electroporation method. Gürel and Gozukimizi (2000) investigated the optimal conditions for electroporation of barley mature embryos. The conditions for successful mature barley embryo electroporation are found to be 500 v/cm and 500 µFd capacitance, as these conditions produced healthy geminating seedlings. Other parameter tested is culture duration of the embryos before electroporation. The best culture duration was found to be 3 days-old culture that produced the highest germination frequency. Other studies on main cereal crops indicated the potentials of the electroporation as a method for plant transformation. Successful transformation has been obtained using electroporation of rice embryos (Tada et al. 1990), maize embryos and pollen grains (Songstad et al. 1993; Leedell et al. 1997) and wheat embryos (Kloti et al. 1993; He and Lazzeri, 1998). Further optimization of electroporation-mediated

transformation has been conducted on rice immature embryos, which indicated the possible application of this technique for genetic transformation as well as to investigate the genetic regulation in embryos (Yu-jun and Jie, 2008).

1.1.6.1.2. Indirect gene transfer

1.1.6.1.2.1. *Agrobacterium*-mediated transformation

Agrobacterim tumefaciens is a soil-born plant pathogen which mainly infects dicotyledonous plant species. It infects plant roots and produces crown gall tumor disease. The genus of *Argrobacterium* contains different species which have different host range disease symptoms: for example, *A. tumefaciens* causes crown gall disease, *A. radiobacter* is avirulent species, *A. rhizogenes* causes root hairy disease, while *A. rubi* cause cane gall disease. Another *Agrobacterium* species; *A. vitis* was recently investigated that makes disease in grape and other limited plant species (Gelvin, 2003; Otten et al. 1996). *Agrobacterium tumefaciens* has high ability to transfer a foreign DNA (T-DNA) to the plant cell nucleus. This T-DNA integrates to host cell genome (Binns and Thomashaw 1988). *Agrobacterium* T-DNA contains different genes: oncogenes and opine synthesis genes. The oncogenes encode enzymes that are involved in hormone synthesis that enhance tumor formation. Opine synthesis genes encode for enzymes that involve in opine biosynthesis. Opines are mixture of amino acids and sugars used by *Agrobacteriun* cells as carbon and nitrogen sources (Gustavo et al. 1998; Zupan and Zambrysky, 1995). Ti plasmid is the major genetic factor which determines the host range (Thomashow et al, 1980). Different *vir* genes are known on Ti plasmid which determines the plant host range for each species. In maize, *virH* gene increases the ability

of *Agrobacterium* to induce infection. Other *vir* genes induce hypervirulance in some other strains (Jarshow et al. 1991).

1.1.6.1.2.2. Factors affecting *Agrobacterium* infection

Different factors affect *Agrobacterium*-plant interaction. *Vir* genes in *Agrobacterium* cells are activated during the co-cultivation with the plant cells. This type of signalling genes are constitutively expressed in *Agrobacterium* cells at low levels. *Vir* genes mainly include two distinct genes; *VirA* and *VirG* (Satchel and Nester 1986; Winans et al. 1988). *VirA* genes encode membrane-bound sensor kinase proteins that are autophosphorylated at conserved histidine residues and transfer the phosphate to the *VirG* proteins that act as a cytoplasmic regulator. The VirA/VirG system can be auto-controlled or controlled by the host plant using different exudates (Brencic and Winans 2005). Phenolic compounds, pH and monosaccharaides in the co-cultivation media contribute to the efficiency of *Agrobacterium*-plant interaction. Co-cultivation temperature is also essential for the transfer of the T-DNA from *Agrobacterium* cells into plant cells. Studies on *Agrobacterium*-plant interaction revealed that the efficiency of T-DNA transfer is higher at low temperature (19 °C) and reduced significantly at high temperature (31°C) (Fullner and Nester 1996). Acteosyringone, a phenolic compound, plays an important role in increasing the T-DNA transfer efficiency. In dicotyledonous species, mechanical damage such as wounding causes the release of phenolic compounds, which act as inducers for the *Vir* genes in *Agrobacterium*. These phenolic exudates help *Agrobacterium* cells to recognize the host plant and transfer T-DNA into the plant cells. In monocot species, *Agrobacterium* does not recognize the host because monocots fail to produce phenolic compounds which *Agrobacterium* cells need to recognize the host. So adding

acetosyringone to the cultivation media improves the transformation efficiency in monocotyledonous cells (Messens et al. 1990). It is reported that low pH and low PO_4 can induce the *Vir* genes and increase the transformation (Winans 1990). Another factor that affects *Agrobacterium*-plant interaction and increase transformation efficiency is the surfactant, i.e., silwet L77 (Whalen et al 1991).

1.1.6.1.2.3. Optimization of *Agrobacterium*-mediated transformation

Agrobacterium-mediated transformation is the relevant choice for plant transformation. This method has many advantages over other methods regarding to the low copy number, more stability over generations and reduces gene silencing associated with the integration position of the T-DNA (Shou et al. 2004; Barkat et al. 1997). *Agrobacterium*-mediated transformation has advantage of introducing different constructs in the same cell. This feature helps to remove the antibiotic marker genes from the transgenic plants and eliminate the restriction of marketing the transgenic plants (Miller et al. 2002; Matthews et al. 2001).

There are still restrictions of using *Agrobacterium*-mediated transformation approach in cereal crops. The transformation in cereal crops is still genotype-dependent and restricted to certain tissues as explants (mature and immature embryos) (Shrawat and Lorz 2006). Also the culture conditions of *Agrobacterium* and plant tissue culture need more improvement to allow transformation of recalcitrant cultivars (Cheng et al. 2004). Most barley transformations are done on immature embryos, derived calli and microspores as explants, due to their high regeneration capacity (Zhang et al. 2000). Another application of *Agrobacterium*-mediated transformation in barley is sequence

analysis of T-DNA and barley genomic DNA junctions. This approach helps to understand the mechanism of integration of the foreign DNA to plant genome. On the other hand, it allows tracking the T-DNA in plant cells to study its fate and the factors which affect the DNA delivery (Fang et al. 2002). Improving the regenerability and decrease the albinism were the main objectives of the study by Cho et al. (1998). The loss of regenerability and production of albino plants are the main obstacles for improving the plant transformation of the North American barley cultivars such as Harrington cultivar. In this study, the tissue culture conditions were optimized to increase the regenerability due to change in the developmental status in the culture. Increasing the concentration of ammonium nitrate in the growth medium led to increase efficiency of *Agrobacterium*-mediated transformation (Boyko et al. 2009). Different protocols have been established for *Agrobacterium*- mediated transformation in different cereals. In wheat, high transformation efficiency has been obtained using *Agrobacterium tumefaciens* AGL1 strain. Immature embryos are the best explants that can be used to generate transgenic wheat plants. The transformation protocol is relevant for durum, spring and winter wheat cultivars. The transformation efficiency which has been calculated based on the PCR reaction on the transgenic wheat lines was ranged between 0.3–9 % (Wu et al. 2009). In barley, the protocol for *Agrobacterium*-mediated transformation has been optimized by Harwood et al. (2009). In this protocol, barley immature embryos as explants and *Agrobacterium tumefaceins* AGL1 strain have been used. The importance of this protocol comes from the number of the fertile transgenic barley plants obtained that allows studying the gene function. Other protocols have been established for wheat transformation using *Agrobacterium* via floral dip and in planta inoculation. The

transformation ratios obtained from Floral dip and in planta inoculation are 0.9 – 10 % and 5%, respectively (Agarwal et al. 2009; Risacher et al. 2009).

CHAPTER 2: BIOCHEMICAL AND MOLECULAR CHARACTERIZATION OF BARLEY PLASTIDIAL ADP-GLUCOSE TRANSPORTER (HVBT1)

2.1 Abstract

In cereals, ADP-glucose transporter protein plays an important role in starch biosynthesis. It acts as a main gate for the transport of ADP-glucose, the main precursor for starch biosynthesis during grain filling, from the cytosol into the amyloplasts of endospermic cells. In this study, we have shed some light on the molecular and biochemical characteristics of barley plastidial ADP-glucose transporter, *HvBT1*. Phylogenetic analysis of several BT1 homologues revealed that BT1 homologues are divided into two distinct groups. The HvBT1 is assigned to the group that represents BT homologues from monocotyledonous species. Some members of this group mainly work as nucleotide sugar transporters. Southern blot analysis showed the presence of a single copy of *HvBT1* in barley genome. Gene expression analysis indicated that *HvBT1* is mainly expressed in endospermic cells during grain filling; however, low level of its expression was detected in the autotrophic tissues, suggesting the possible role of HvBT1 in autotrophic tissues. The cellular and subcellular localization of *HvBT1* provided additional evidence that HvBT1 targets the amyloplast membrane of the endospermic cells. Biochemical characterization of *HvBT1* using *E. coli* system revealed that HvBT1 is able to transport ADP-glucose into *E. coli* cells with an affinity of 614.5 µM and in counter exchange of ADP with an affinity of 334.7 µM. The study also showed that AMP is another possible exchange substrate. The effect of non-labeled ADP-glucose and ADP on the uptake rate of [α-^{32}P] ADP-glucose indicated the substrate specificity of HvBT1 for ADP-glucose and ADP.

2.2. Introduction

Starch is the main storage compound in grains of cereal crop. Its biosynthesis is catalyzed by a number of enzymes. ADP-glucose pyrophosphorylase (AGPase) converts glucose-1- phosphate, using ATP, into ADP-glucose (ADP-Glc) that acts as the building block of starch. This enzyme is located in the endospermic cells of cereal grains and it has a total activity of about 85% to 95% in the cytosol of such cells (James et al. 2003). The majority of ADP-Glc is synthesized in the cytosol and imported into the amyloplasts by ADP-glucose transporter located on the membrane of the amyloplasts. In wheat, the ADP-glucose transporter was characterized *in vitro* using reconstituted amyloplast envelope proteins in the proteoliposomes. The results of this study showed that ADP-glucose was transported in counter exchange of AMP and ADP (Bowsher et al. 2007). In maize, the brittle1 (BT1) mutant is deficient in four amyloplast envelope proteins. One of the defective proteins was *ZmBT1* that encodes ADP-glucose transporter (Cao et al. 1995; Cao et al. 1996). This mutant showed a low rate of ADP-Glc uptake into isolated amyloplasts, as compared to the control ones (Shannon et al. 1996). Using the radioactive (^{14}C) ADP-Glucose as a substrate, the *ZmBT1* heterologously expressed in *E. coli* was able to transport ADP-glucose with high affinity in counter exchange with ADP (Kirchberger et al. 2007)**.** Endospermic amyloplasts isolated from *lys5* mutant of barley, which is deficient in amyloplast envelope proteins showed reduced ADP-glucose uptake (Patron et al. 2004). In non-graminaceous species, two BT1 homologues were identified and characterized, *AtBT1*from Arabidopsis*,* and *StBT1* from *potato*. Characterization of *StBT1* using an *E. coli* expression system showed high affinity to AMP, ADP and ATP (Leroch et al. 2005).

The phylogenetic analysis of the BT1 protein revealed that maize *ZmBT1* and barley *HvNST1* belong to the mitochondrial carrier family (MCF) (Patron et al. 2004; Picault et al. 2004). In cereals, ADP-glucose transporter protein possesses six membrane spanning domains. The C-terminus and N-terminus of these proteins are located inside the amyloplasts (Patron et al. 2004). It was presumed that BT1 homologues are localized in plastids' membranes in autotrophic and heterotrophic tissues and are involved in transporting nucleotides or nucleotide sugars. Recently, subcellular localization analysis of maize and Arabidopsis plants expressing *ZmBT1* and *AtBT1* homologues, respectively, showed dual localization of the two MCF members on the mitochondrial as well as the plastidial membranes. Another finding is that the transit peptide in N-terminal targets plastids, while the sequence targeting mitochondria is localized within internal domains (Bahaji et al. 2011).

The present study characterized barley ADP-glucose transporter, HvBT1, using *E. coli* expression system via monitoring the direct transport of ADP-Glc through the intact *E. coli* cells' plasma membrane. The expression of *HvBT1* in different tissues and the cellular and subcellular localizations of HvBT1 were investigated. In addition the study examined the effect of expressed HvBT1 protein on *E. coli* cell growth and protein expression.

2.3. Materials and methods

2.3.1. Plant Material

Barley (*Hordeum vulgare L.*) Harrington plants were grown a greenhouse condition (under 8 h dark/16 h light photoperiod). Spikes were harvested after 2- 20 days after anthesis (DAA) and frozen immediately in liquid nitrogen until used for RNA extraction.

2.3.2. Amplification and cloning of *HvBT1*

RNA was extracted using RNeasy Plant Mini Kit (Qiagen, Hilden, Germany). The genomic DNA was digested in columns using RNase-Free DNase I Kit (Qiagen). The purity and integrity of the RNA was determined using agarose gel electrophoresis and NanoDrop spectrophotometer (Thermo Fisher Scientific, Waltham, MA, USA), respectively. The cDNA was synthesized using Revert Aid First Strand cDNA Synthesis Kits (Thermo Scientific). The open reading frame (ORF) of *HvBT1* was amplified using gene specific primers, which were designed based on the reported DNA sequence (GenBank ID: AY560327.2). The amplified ORF was cloned in the pGEM-T-Easy plasmid and introduced into *E. coli* DH5α (Invitrogen, Carlsbad, CA, USA). Following plasmid isolation, the target sequence was verified by sequencing (Macrogen, Rockville, MD, USA) and blast searched against the GenBank database. The resulting ORF was amplified using specific primers flanked by restriction sites for Nde1 (5'-CGTcatatgGCGGCGGCAAT-3') and BamH1 (5'-TAggatccTCATGGTCGATCACCG-3') and cloned into the bacterial expression plasmid pET16b (Novagen, Darmstadt, Germany) in Nde1 and BamH1 restriction sites and further verified by DNA sequencing.

2.3.3. Southern blot analysis

Genomic DNA was extracted using the CTAB method from 2 g frozen leaf tissue and treated with RNase A to eliminate RNA contamination. The genomic DNA was digested

using XhoI, BamHI, SalI and KpnI (do not cut *HvBT1* sequence). Then, the digested products were separated on 0.8% agarose gel. Denaturation and neutralization were performed according to the standard protocol (Sambrook et al. 1989). After transferring the DNA into the nylon membrane (GE Healthcare, Little Chalfont, UK), DNA fragments were fixed to the membrane using UV crosslinker (Stratagene, La Jolla, CA, USA). Gene Images Alkphos Direct Labeling and Detection system (GE Healthcare) was used for preparation of the probe (700 bp). Pre-hybridization, hybridization, and washing, and all the procedures were performed according to the manufacturer's instructions. The chemiluminescent signal was generated and detected using CDP-Star reagent.

2.3.4. Quantitative Real-time RT- PCR

Quantitative Real-Time PCR was achieved using C1000 Thermal Cycler (Bio-Rad, Hercules, CA, USA) and SSo Fast Eva Green Super mix (Bio-Rad) according to the manufacturer's instructions. Actin was used as a quantitative normalizer. The *HvBT1* specific sense, (5'-TGTACGACAACCTCCTCCAC-3'); and antisense, (5'-GCAGTGTCTCGTAGGCGTAG-3') primers and *β-Actin* sense, (5'-CCAAAAGCCAACAGAGAGAA-3') and antisense, (5'-GCTGACACCATC ACCAGAG-3') were used for qRT-PCR. The results were analyzed using $2^{-\Delta\Delta C_T}$ method (Livak and Schmittgen 2001).

2.3.5. Cellular localization of *HvBT1* transcripts

RNA in-situ Hybridization was used to investigate the cellular localization of *HvBT1*. Barley caryopsis (8 DAA) were collected and immersed immediately in 4%

paraformaldehyde in PBS buffer (pH 7.4) on ice. The caryopsis was cut from both ends to facilitate buffer penetration and exchange. Then the caryopsis was purged under vacuum for 15 min. The rest of the procedures were performed according to Belmonte et al. (2006). The probe was prepared using DIG-RNA labeling Kit (Roche). Briefly, the full length cDNA was amplified and cloned into pGEM-T-Easy plasmid (Promega, Madison, WI, USA). The ORF was amplified using M13 forward and reverse primers located in the upstream and downstream of T7 and SP6 promoter regions, respectively. The PCR products were used as templates for T7 and SP6 RNA polymerase reactions. Sense and antisense probes were hydrolyzed using bicarbonate buffer (60 mM Na_2Co_3 and 40 mM $NaHCo_3$) to reach to 150 bp length. Pre-hybridization, hybridization, and color development were done according to Canton et al. (1999) and Tahir et al. (2006), respectively.

2.3.6. Subcellular localization of HvBT1 protein

Subcellular localization of HvBT1 was investigated using transient expression of HvBT1 fused with YFP in Arabidopsis protoplast. Plant binary vector pEarleyGate 101 containing the yellow fluorescent protein (YFP) was prepared using Gateway LR clonase reaction (Invitrogen, USA). The coding sequence of *HvBT1* was cloned into pENTR-1A entry plasmid at EcoRI and XhoI restriction sites. The *HvBT1* specific primers were designed to include the restriction sites of EcoRI and XhoI. The stop codon of *HvBT1* ORF was removed by excluding it from the reverse primer of *HvBT1* to generate continuous ORF that includes both *HvBT1* and *YFP* in the binary plasmid. Phusion DNA polymerase was used to amplify the coding sequence of *HvBT1* from pGEM-T-Easy

plasmid. The PCR product was digested using EcoRI and XhoI. The digested PCR product was cloned in pENTR-1A plasmid using T4 DNA ligase (Fermentas, Thermo Scientific, CA). LR clonase reaction was performed using pENTR-1A:*HvBT1* and pEarleyGate101 according to the manufacturer's instruction. The insertion and the orientation of *HvBT1* in pEarleyGate101::*HvBT1* were verified by PCR and sequencing (Macrogen, USA). The transient expression was performed on Arabidopsis protoplasts by introducing the pEarleyGate101::*HvBT1* plasmid into protoplasts using PEG-mediated transformation according to Yoo et al. (2007). The immunolocalization of HvBT1**::**YFP in the fixed Arabidopsis protoplasts was performed using anti-YFP Tag (Mouse monoclonal) primary antibody (Applied Biological Materials Inc., Canada) with dilution of 1:1000. Fluorescein conjugated anti-Mouse IgG (FITC) (Applied Biological Materials Inc., Canada) was used as secondary antibody with dilution of 1:200. The immunolocalization procedures were performed according to Lee and Hwang (2011).The HvBT1-YFP expression was monitored using confocal laser scanning microscope (Zeiss, Oberkochen, Germany) with excitation wavelengths of 488 nm with broad pass 505-530 nm, and 488 nm with long pass 650 nm for HvBT1**::**YFP and chlorophyll, respectively. FITC was detected with excitation of 495 nm and BP of 528 nm according to the manufacturer's instructions.

2.3.7. *HvBT1* codon optimization

In *E. coli*, the rare codons (RCs) are defined as synonymous codons, which are decoded by low abundant tRNA (rare tRNA). The RCs affect the translation rate of

eukaryotic proteins due to the unavailability of the rare tRNA [19]. One of the most limiting steps during expression of eukaryotic genes in *E. coli* is the codon bias. The low usage codons for particular amino acids disrupt the expression of most eukaryotic genes. Gene synthesis methods are able to optimize the DNA sequences by substituting rare codons with other ones that are common in *E. coli's* translation machinery system. The four problematic amino acids (Proline, Arginine, Leucine and Isoleucine) have more than one codon, thus the challenges are to choose the right codons for these amino acids that can be recognized by the *E. coli* translation machinery and provide the same amino acid sequence up on translation. To this end, the codons of the nucleotide sequence of the target gene were optimized to *E. coli* translation system. The newly synthesized sequence was cloned into pET16b plasmid (Novagen), which has His- tag at the N- terminus to produce fused protein that facilitates protein purification.

2.3.8. *Escherichia coli* strains and growth conditions

Two *E. coli* strains, Rosetta2 (DE3) plysS and C43 (DE3) (Lucigen, Middleton, WI, USA) were used in this study to investigate the optimal conditions for protein expression and the possible toxic effects of the ADP-glucose transporter protein (HvBT1). Bacterial transformation was performed according to the strain specificity and the manufacturer instructions. Bacterial cells harboring pET16b::*HvBT1*, the original (org) or the optimized sequences (opc), and the control cells harboring the empty pET16b plasmid were grown at 37°C overnight in 5 ml 2xYT medium supplied with 100 µg /ml carbenicillin. This culture was used to inoculate fresh 2xYT culture medium which was then incubated at 37°C for 2 h to reach OD 600 = 0.6. The expression of *HvBT1* was then induced by

adding IPTG (final concentration 0.5 mM) and incubation at 20°C overnight. The cells were centrifuged at 5000 g and resuspended in the transport buffer (50 mM potassium phosphate, pH 7.2) followed by incubation on ice.

2.3.9. Inhibitory effect of the expressed HvBT1

Escherichia coli cells of strains C43 and Rosetta2, harboring different copies of *HvBT1* (org or opc) were grown in 2xYT medium supplied with 100 µg/mL carbenicillin. After the cell density reaches to OD_{600} ~0.6, the expression of *HvBT1* was induced by adding IPTG (final concentration of 0.5 mM) and incubation at 20°C. The growth rate of cells was monitored over time using spectrophotometer. The same procedures were repeated using 2xYT agar plates. A single colony was spread on agar plates supplied with IPTG (0.5 mM final concentration) and without IPTG as a control, and then incubated at 30°C for 2 days.

2.3.10. Membrane protein extraction and SDS-PAGE

His-tagged HvBT1 protein was extracted and purified with HOOK His Protein Spin purification kit (G-Biosciences, St. Louis, MO, USA) according to the manufacturer's instructions with minor modification. The cell pellets were placed in liquid nitrogen to disrupt the cell wall and then re-suspended in PE LB–Lysozyme buffer provided with the kit with complete protease inhibitor (Roche Applied Science). The cells were incubated at 37°C for 60 min and further disrupted by ultrasonication (250 W, 4 x 30 s, 4°C). Unbroken cells and cell debris were collected using centrifugation at 4°C, first at 15,000 g for 20 min and then at 50,000 g for 90 min. The membrane protein fractions

(supernatant) were mixed with nickel chelating resin. The rest of the procedures were performed according to the manufacturer's instructions. After elution, His-tagged HvBT1 protein was desalted with Sephadex G50 and the purified membrane protein was subjected to SDS-PAGE analysis according to Laemmli et al. (1970).

2.3.11. Transport assay using *E. coli* C43 (DE3) strain harboring pET16b::*HvBT1* (opc)

The transport assay was performed using intact *E. coli* cells. IPTG-induced *E. coli* cells harboring either *HvBT1* recombinant plasmid or the empty one (control) were resuspended in potassium phosphate buffer (pH 7.2). The transport assay was initiated by adding [α-^{32}P] ADP-Glc or [α-^{32}P] ADP as transport substrates to the reaction mixture. [α-^{32}P] ADP-Glc was enzymatically synthesized using a modified protocol of Ghosh and Preiss (1966) and Rösti et al. (2006). The procedures of the assay were as follow: ADP-glucose pyrophosphorylase (AGPase) was extracted from the leaf tissues of two weeks old barley seedlings (0.5 g) with extraction buffer containing 50 mM HEPES (pH 7.4), 2 mM MgCl$_2$, 1 mM EDTA and 1mM DTT. The mixture was centrifuged at 10,000 *g* for 15 min at 4°C. The supernatant was used directly in the assay. The direct ADP-glucose synthesis was conducted in assay buffer (0.2 mL) containing 100 mM HEPES (pH 7.6), 15 mM MgCl$_2$, 0.025 % (w/v) BSA, 0.5 units inorganic pyrophosphatase from baker's yeast (Invitrogen), 0.5 mM glucose 1- phosphate, 1.5 mM ATP, 15 mM 3-PGA and 4 µL [α-^{32}P] ATP (3000 Ci [111TBq]/mmol) (Perkin Elmer). Supernatant containing AGPase (20 µL) was added to the assay buffer and incubated at 37°C for 20 min and the reaction stopped by boiling the mixture for 2 min at 95°C. The mixture was used without further

dilution for making working stock. [α-^{32}P] ADP was enzymatically synthesized from [α-^{32}P] ATP (3000 Ci [111 TBq]/moll) (PerkinElmer). In brief, 3-4 μL of [α-^{32}P] ATP was added to 20 μL reaction mixture that contains 20 mL of 50 mM HEPES-KOH (pH 7.2), 5 mM $MgCl_2$, 1 mM glucose, 1 unit of hexokinase, and 10 mM unlabeled ATP. The mixture was incubated for 60 min at room temperature. Hexokinase was deactivated by heating for 2 min at 95°C (Tjaden et al. 1998). The uptake experiment was carried out at 30°C. The uptake was terminated by quick transfer the cells to 0.45 μm filter under vacuum. The filter was washed with 3-4 mL cold potassium phosphate buffer (pH 7.2) to remove unimported radiolabelled substrate. The filter was transferred to scintillation cocktail (5 mL) and the amount of ^{32}Puptakenwas quantified in a liquid scintillation counter ((Beckman, Brea, CA, USA).

Efflux experiment of the putative [α-^{32}P] ADP-Glc substrate was conducted in intact IPTG-induced *E. coli* cells harboring *HvBT1* and empty plasmid as a control. The cells were pre-incubated with 1μM [α-^{32}P] ADP-Glc in 50 mM potassium phosphate buffer (pH 7.2) for 5 min at room temperature. The uptake buffer was diluted 1000 times using ADP-Glc, ATP, ADP and AMP at a final concentration of 1 mM and incubated for indicated time points. The uptake reaction was stopped by quick filtration in 0.45 μm filters under vacuum. The filter was washed by adding 3-4 mL ice cold potassium phosphate buffer and then placed in scintillation cocktail (5 mL). The radioactivity of ^{32}P was monitored at the indicated time points as described above (Kirchberger et al. 2007). The efflux of intracellular [α-^{32}P] ADP was conducted in induced *E. coli* cells harboring*HvBT1*. The cells were incubated with 1μM [α-^{32}P] ADP for 5 min and the rest of the procedures were performed as described above for [α-^{32}P] ADP-Glc. Non-labeled

ADP-Glc and ADP dilution (1000 times) were used to enhance the export of $[\alpha\text{-}^{32}\text{P}]$ ADP.

2.3.12. Bioinformatics analysis

BT1 protein sequences (29 amino acid sequences) were collected using the BLASTp program (Altschul et al. 1997) and were aligned with ClustalX program (Thompson et al. 1997). The phylogenetic tree was generated by MEGA 5.2 program (Tamura et al. 2011) and the tree was annotated with Corel Draw (Corel Corporation Ltd., Ottawa, Canada)

2.4. Results

2.4.1. Bioinformatics analysis of HvBT1

The phylogenetic tree divided BT1 proteins into two main groups. The first group represented monocotyledonous species including wheat, barley, maize and rice and the second group represented both monocotyledonous and dicotyledonous species (Figure 2.1). The first group consists of subgroups for BT1 homologues that are classified mainly based on their biochemical functions. The HvBT1 (GenBank ID: AAT12275) is classified in a distinct subgroup (orange color) that includes BT1 homologues from *T. aestivum* and *T. urartu*. Comparison of the amino acid sequence of HvBT1 with that of other BT homologues showed high similarity with BT homologue from *Triticum aestivum* (GenBank ID:ACX68637; 97% similarity or 92% identity), *Triticum urartu* (GenBank ID: EMS62502; 99% similarity or 88% identity). *Aegilopus tauschii* (GenBank ID: EMT17313; 99% similarity or 89% identity) and *Aegilopus crassa*

(GenBank ID: ACX68638; 97% similarity or 90% identity). The HvBT1 homologue also showed similarity with homologues from *Zea mays* (GenBank ID: NP001105889; 92% similarity or 66% identity) and, *Zea mays* (GenBank ID: ACF78275; with 92% similarity or 71% identity). Other subgroups in the phylogenetic tree include BT1 homologues that function as either nucleotide sugar transporter or adenine nucleotide transporter. The second group consists of BT1 homologues from both monocotyledonous and dicotyledonous species. This group is divided into two main distinct subgroups. One of the subgroups includes BT1 from monocotyledonous species that mainly function as either nucleotide sugar transporter or adenine nucleotide transporter. The second subgroup includes BT1 homologues from only dicotyledonous species that mainly function as nucleotide carrier proteins. The BT1 homologues from dicotyledonous species showed low similarity to HvBT1.
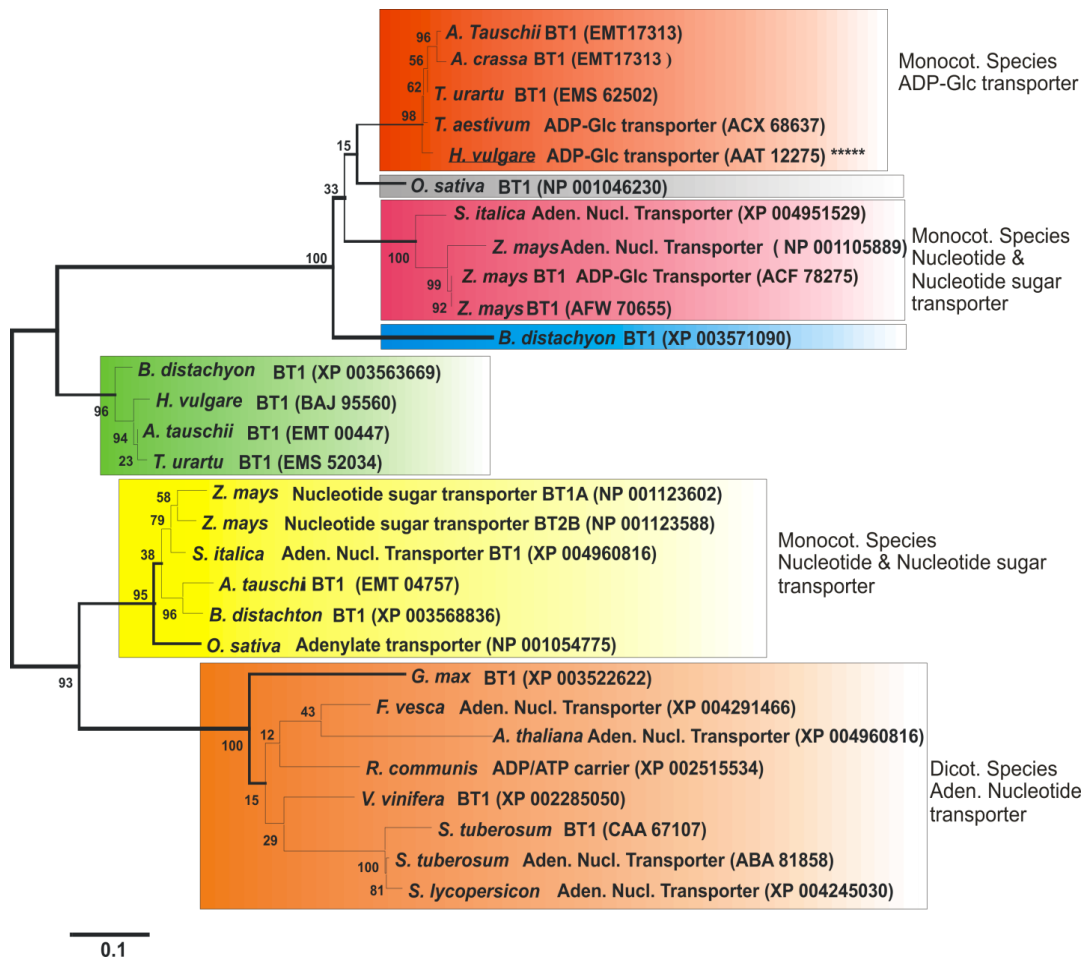
Figure 2.1. Phylogenetic analysis of BT1 proteins.

The BLASTp (Altschul et al. 1997) program was used to retrieve sequences that were related to BT1. The amino acid sequences were aligned with the Clustal X program (Thompson et al. 1997). Phylogenetic estimates were created by the Molecular Evolutionary Genetic Analysis program package (MEGA 5.2) (Tamura et al. 2011). The gaps were eliminated from the analysis in MEGA by using complete deletion setting. The phylogenetic tree was generated with the Maximum Parsimony (PARS), Neighbour joining (NJ; setting JTT model), and Maximum likelihood (ML) methods. MEGA 5.2 was also used for determining the best fit substitution model for ML analysis; thus for ML analysis the JTT+G model was applied and for all programs the bootstrap option was selected (1000 replicates) in order to obtain estimates for the confidence levels for the major nodes present within the phylogenetic trees. The phylogenetic tree was annotated

with Corel Draw^{TM} (Corel Corporation Ltd., Ottawa, Canada). The phylogenetic tree divided BT1 homologues into two main groups represent monocotyledonous and mono and dicotyledonous species. HvBT1 was located in the first group within a distinct subgroup (Orange color) with *T. aestivum* (GenBank ID: ACX 68637) which was characterized as ADP-glucose transporter (Bowsher et al. 2007). Another subgroup (Red color) assigned for monocot species including Z. *mays* (GenBank ID: ACF 78275) which characterized as ADP-glucose transporter. The second group was dedicated for both mono and dicotyledonous species. Dicotyledonous species were assigned in a distinct subgroup (Brown color).They are mainly function as nucleotide transporter as *S. tuberosum* (GenBank ID: ABA 81858) and *A. thaliana* (GenBank ID: XP 004960816) were characterized as adenine nucleotide transporter (Leroch et al. 2005; Kirchberger et al. 2008).

Southern blot analysis of HvBT1

The restriction analysis of barley genomic DNA with XhoI, BamHI, SalI and kpnI (Figure 2.2) revealed that only one distinct band can be produced by digestion with different restriction enzymes which do not cut inside *HvBT1* sequence. This result indicated that there is one copy of *HvBT1* in barley genome.
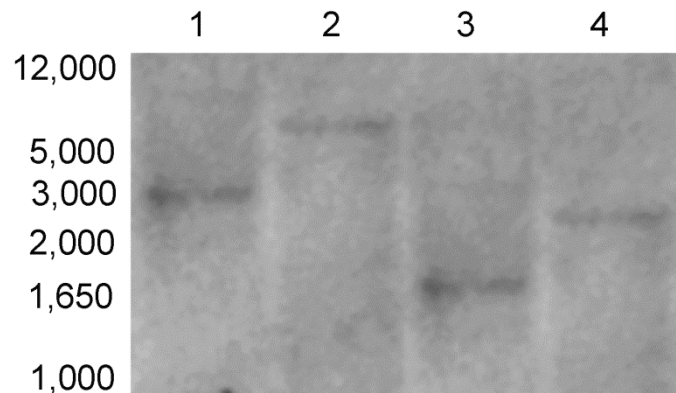
Figure 2.2. Southern blot analysis of barley *HvBT1*.

Barley nuclear DNA was digested with **1:** BamHI, **2:** SalI, **3:** XhoI and **4:** KpnI and subjected to southern blot analysis. DNA probe was prepared with 700 bp of *HvBT1* cDNA and used for hybridization. Molecular weight of the standard DNA ladder was indicated in the image.

2.4.3. Expression analysis of *HvBT1*

The expression profile of *HvBT1* was investigated in different tissues such as stems, leaves and seeds using quantitative real-time PCR and *β-Actin* in different tissues. Our showed the presence of high abundance of *HvBT1* transcripts in the endosperm at

different stages of grain filling. The maximum transcript level was detected at 14 to 16 DAA. The transcripts of *HvBT1* were also detected in the leaf and stem tissues but at lower levels when compared to that found in the endosperm (Figure 2.3).
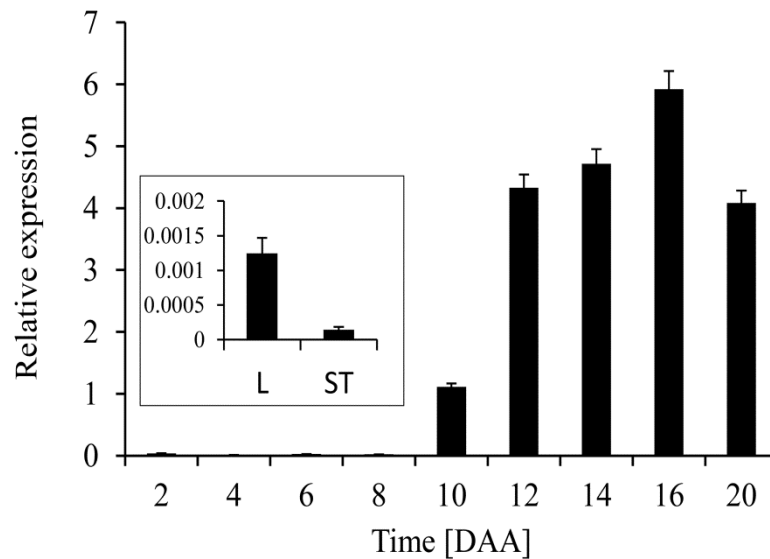
Figure 2.3. Real-time PCR analysis of *HvBT1* in different barley tissues.

Quantitative real-time RT-PCR was used to determine the expression level of *HvBT1* in different tissues using gene specific primers. *β-actin*, a housekeeping gene from barley, was used as an internal control. The relative expression level of *HvBT1* transcripts was normalized by β-actin expression level. Different head samples during grain filling (2-20 DAA) were assessed and samples from autotrophic tissues; stem and leaf also assessed (small scale).

2.4.4. Cellular and subcellular localization of *HvBT1*

Cellular localization of *HvBT1* transcripts was detected by RNA in-situ hybridization. Our results indicated a strong signal of alkaline phosphatase (in case of the antisense

probe) reflecting high accumulation of *HvBT1* transcripts in the starchy portion of developing caryopsis (Figure 2.4). Subcellular localization of the HvBT1::YFP fused protein showed that HvBT1 protein is targeted to the chloroplast membranes (Figure 2.5A). This result was validated by immunolocalization of HvBT1::YFP, where the fluorescence of FITC was detected in the chloroplast envelopes (Figure 2.5B).

Figure 2.4. Cellular localization of *HvBT1*.

Cellular localization of HvBT1 was assayed using RNA- in situ hybridization. **A:** shows hybridization with the sense probe which produces a very faint signal. **B:** shows antisense probe hybridization which produces high signal of alkaline phosphatase. (es), embryo sac; (al) aleurone and (em) embryo. The signal was detected strongly in embryo sac, which accumulates the endosperm.
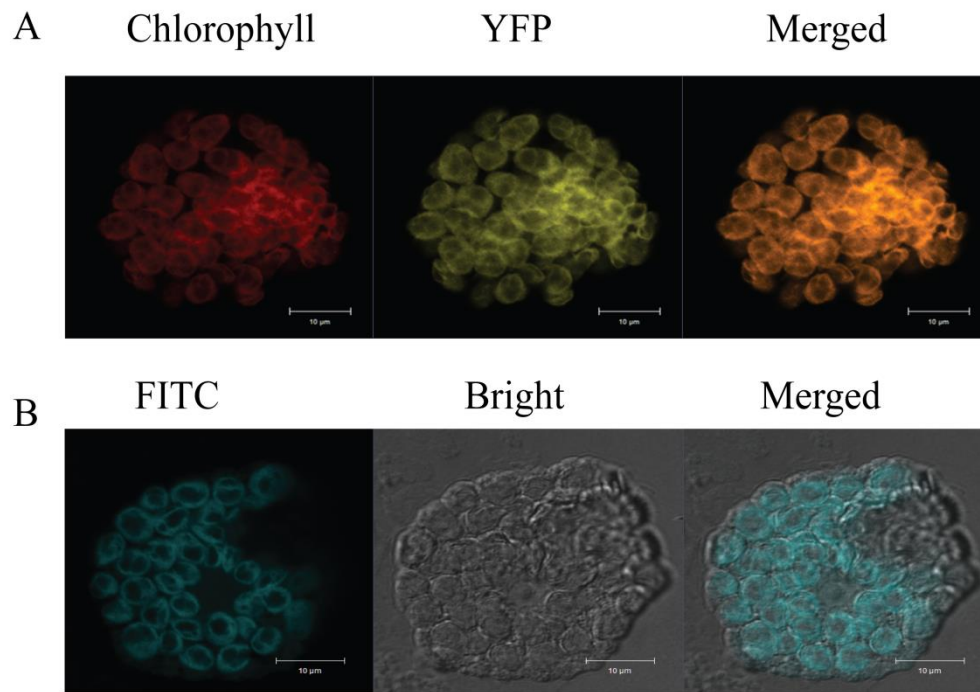
Figure 2. 5. Subcellular localization of HvBT1::YFP

Subcellular localization of HvBT1 was visualized by confocal laser scanning microscope. **A:** transient expression of HvBT1::YFP in living protoplasts; chlorophyll autoflorescence (red color), YFP fluorescence (yellow color) and merged image (orange color).**B:** immunolocalization of HvBT1::YFP was detected using anti-YFP antibody and visualized by the fluorescence of FITC-conjugated antibody. FITC fluorescence (blue color), bright field and merged image which show the localization of HvBT1::YFP on the chloroplast membranes.

2.4.5. Heterologous expression of HvBT1 in *E. coli* cells

SDS-PAGE analysis of the purified HvBT1 membrane protein showed that both *E. coli* strains C43 and Rosetta2 harbouring the optimized ORF of *HvBT1* are able to express the HvBT1 protein with expected mass of ~ 45 KDa (Figure 2.6). Meanwhile,

Rosetta2 harbouring the original ORF was also capable of expressing HvBT1 at very low level. The Rosetta 2 strain cells harbouring either org or opc ORFs of *HvBT1* showed growth inhibition, while the cell growth appeared to be normal in the case of C43 strain (Figure S1). The use of optimized ORF of *HvBT1* along with the C43 strain provided an ideal expression system to sustain cell viability to perform the transport assay procedures.
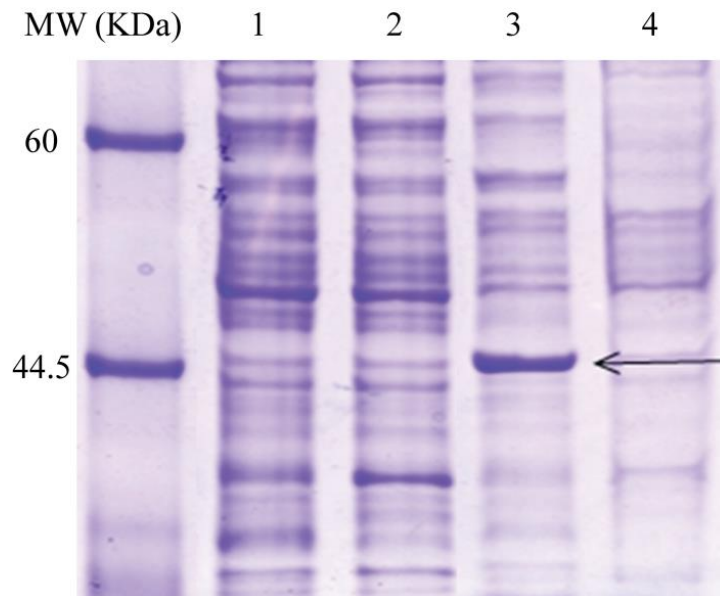
Figure 2.6. SDS-PAGE analysis of HvBT1 protein.

Escherichia coli C43 and rosetta2 strains harboring the original (org) or the optimized (opc) ORF of *HvBT1* were grown in 2xYT liquid media supplied with IPTG (0.5 mM final concentration). His-tagged HvBT1 membrane protein was purified and subjected to 12% SDS-PAGE. Lane 1 and 2 represent Rosetta 2 harboring opc and org ORF of *HvBT1*, respectively. Lane 3 and 4 represent C43 harboring opc and org ORF of *HvBT1*, respectively. Black arrows point to a band size of 45 KDa. Protein standard molecular weight is shown.

2.4.6. [α-^{32}P] ADP-Glucose transport assay

The transport of [α-^{32}P] ADP-Glc was studied using intact *E. coli* cells harboring the expression plasmid containing *HvBT1* or the control plasmid (with no *HvBT1*). The results showed that the import of the α-^{32}P labeled substrate follows a non-linear regression trend for Michaelis-Menten kinetics (Figure 2.7A). The affinity of HvBT1 for ADP- glucose was analyzed with different concentrations of [α-^{32}P] ADP-glucose using the Wolfram *Mathematica* 8.0 software (Wolfram, Champaign, IL, USA). Increasing the substrate concentration led to increased radiolabeled ADP-glucose uptake into the intact *E. coli* cells expressing the *HvBT1*. The K_m value of ADP-Glc was calculated to be 614.5 µM and the V_{max} to be 254.1 nmol of ADP-Glc mg of protein^{-1} h^{-1} (Figure 7A). Uptake for [α-^{32}P] ADP was also analyzed as described for [α-^{32}P] ADP-Glc. Likewise; an increase in the import rate of [α-^{32}P] ADP was observed with increased concentrations of [α-^{32}P] ADP. The K_m and V_{max} values for ADP are 334.7 µM and 74.07 nmol of ADP mg protein^{-1} h^{-1}, respectively (Figure 2.7B).

Efflux of the intracellular [α-^{32}P] ADP-Glc and [α-^{32}P] ADP was monitored using the intact IPTG-induced *E. coli* cells harboring *HvBT1* as described in the materials and methods. Rapid export of [α-^{32}P] ADP-Glc was enhanced by dilution of the assay reaction with a high concentration of ADP or AMP, which caused a 75% or 60% reduction from the initial amount, respectively. Meanwhile, dilution of [α-^{32}P] ADP-Glc with a high concentration of non-labeled ADP-Glc or ATP led to 43% or 36% reduction from the initial amount, respectively, within 8 min of incubation (Figure 8A). Increased efflux of putative [α-^{32}P] ADP was also observed by dilution of the medium with high concentration of non-labeled ADP-Glc at different incubation periods (Figure 8B). No significant difference in efflux was found between dilution with ADP and the control.
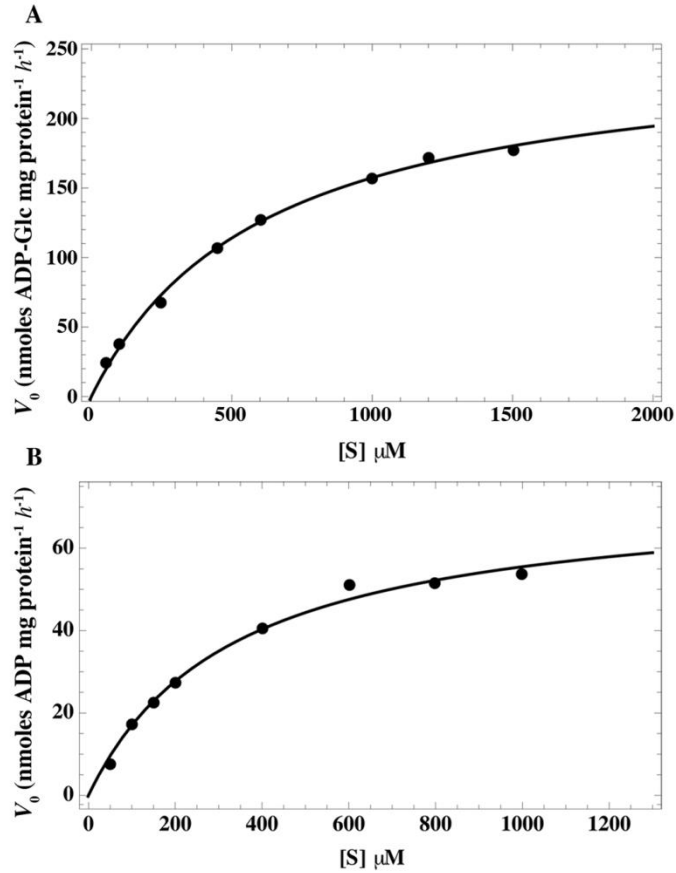
Figure 2.7. Transport activity of *HvBT1* in intact *E. coli* cells.

Escherichia coli C43 cells harboring the recombinant plasmid and the empty one (Control) were incubated with different concentrations of [α-^{32}P] ADP-Glc. The cells were incubated at 30°C for 10 min. The control values have been subtracted. The data is the mean of three independent experiments ± SE with three replicates each. **A:** K_m value of ADP-Glc is 614.5±33.24 μM and V_{max} of 254.14 ±19.45 nmol of ADP-Glc / mg of protein^{-1} h^{-1}. **B:** K_m and V_{max} values of ADP is 334.7±39.3 μM and of 47.07 ±3.51 nmol of ADP-Glc / mg of protein^{-1} h^{-1}, respectively.

To identify the possible counter-exchange substrates of HvBT1, intact *E. coli* cells were preloaded with ATP, ADP or AMP at a concentration of 1 mM for 10 min at 30°C followed by addition of [α-^{32}P] ADP-Glc (final concentration of 1 mM) and incubation for 10 minutes. Our results indicated that preloading with ADP or AMP has a positive impact on [α-^{32}P] ADP-Glc uptake, while preloading with ATP does not have significant effect (Figure 2.8C).

To investigate if the [α-^{32}P] ADP-Glc transport activity of HvBT1 is inhibited or activated by other metabolic intermediates, intact *E. coli* cells harboring *HvBT1* were incubated with 100 μM [α-^{32}P] ADP-Glc combined with the different metabolic intermediates at a final concentration of 1 mM. Our results showed that the uptake rate of [α-^{32}P] ADP-Glc was enhanced by ~ 88% or 70% when co-incubated with D-glucose or glucose-1- phosphate, respectively (Table 1). Co-incubation with non-labeled ADP-Glc reduced the uptake of [α-^{32}P] ADP-Glc by ~50% as compared to the control. Similarly, the uptake of [α-^{32}P] ADP-Glc was negatively affected by co-incubation with the nucleotide ADP, whereas the other nucleotides ATP and AMP did not have effect. The reduction of [α-^{32}P] ADP-Glc uptake due to co-incubation of *E. coli* cells harboring *HvBT1* with ADP-Glc or ADP indicated the substrate specificity of HvBT1.
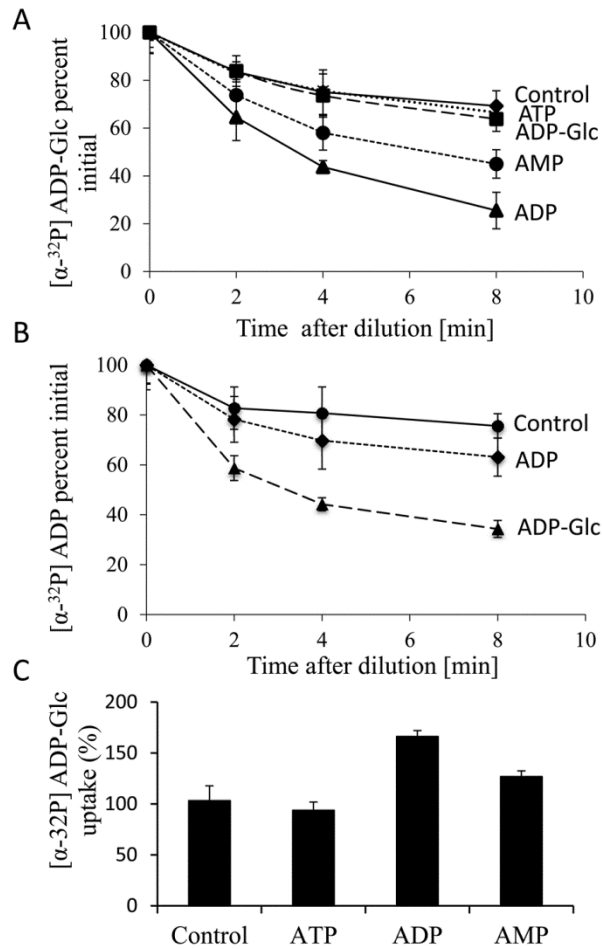
Figure 2.8. Exchange of intracellular radiolabeled substrates.

A: *E. coli* cells harboring *HvBT1* and the given control were incubated with 1 μM [α-^{32}P] ADP-Glc at 30°C in eppendorf tube for 5 min. The assay buffer was diluted with non-labeled ATP, ADP, AMP, and ADP-Glc for indicated time points. The cells were filtered and washed under vacuuming and measured for radioactivity. The data present here is the mean of three independent experiments ±SE with three replicates. **B:** the procedures for ADP efflux assay was performed as described for ADP-Glc in (A) with ADP and ADP-Glc dilutions. **C:** *E. coli* C43 cells harboring *HvBT1* and the given control were preloaded with nucleotides at final concentration of 1 mM, and then the cells were incubated at 30°C for 5 min. The cells were centrifuged and re-suspended in potassium phosphate buffer (50 mM, pH 7.2) with [α-^{32}P] ADP-Glc at concentration of 100 μM at 30°C for 8

min. The data present here is the mean of three independent experiments ±SE with three replicates.

Table 2.1. **Effects of different metabolites on [α-^{32}P] ADP-glucose transport activities of HvBT1**.

Effectors	[α-^{32}P] ADP-Glc transport		
	nmol. mg protein^{-1}	%	% changes
Control[a]	12.99 ± 0.72[b]	100	0
D-glucose	24.5 ± 0.76	188.54	+ 88.54
Glucose 1-P	22.12 ± 0.91	170.17	+70.17
ADP-glucose	6.46 ± 0.35	49.67	- 50.33
ATP	11.98 ± 0.98	95.276	- 4.73
ADP	8.22 ± 0.85	63.18	- 36.82
AMP	11.16 ± 0.78	85.89	- 14.11

[a] Control = [α-^{32}P] ADP-glucose (100 μM)
[b] Data are means ± SE, n=3

Various metabolites at final concentration of 1 mM were tested for their activation or inhibition of ADP-Glc transport. [α-^{32}P] ADP-Glc was present in the uptake buffer at final concentration of 100 μM. Uptake assay was carried out with IPTG-induced *E. coli* C43 cells harboring *HvBT1* (opc) for 10 min and stopped by quick vacuuming. The data present in this table is the mean of three independent experiments ± SE with three replicates each.

2.5. Discussion

In cereal grains, starch is synthesized exclusively in the plastids. ADP-glucose, the precursor of starch, is synthesized mainly in the cytosol of the endospermic cells by the cytosolic AGPase form. The majority of AGPase activity in cereals is reported to be in the cytosol (extra-plastidial) (Denyer et al. 1996; Tetlow et al. 2003). Different mutants from cereals such as maize shrunken 2 (*sh2*) and brittle 2 (*bt2*) mutants (Giroux and Hannah 1994), and barley mutant Risø 16 (Johnson et al. 2003), are characterized by the lack of the activity of cytosolic AGPase, which in turn leads to the deposition of less starch as compared to their control. Under normal conditions, the ADP-glucose synthesized in the cytosol of the endospermic cells has to be transported into the amyloplasts' envelope membrane through a protein carrier. A study conducted on low starch mutants of barley revealed that Risø13 mutant has low starch yield as compared to the parental control. This is attributed to the decrease in the activity of ADP-glucose transporter due to a point mutation in its cDNA sequence that led to the substitution of GLU for VAL at position 273 in helx4 (Patron et al. 2004).

Amino acid sequence-based phylogenetic analysis revealed the clustering of BT1 proteins into two main groups. The first group contained only those isolated from monocotyledonous species including the main cereal crops. HvBT1 (GenBank ID: AAT12275) was assigned to this group, along with proteins from maize, rice, wheat and other grasses. Some of the BT1 proteins in this cluster have been characterized. The ZmBT1 (GenBank ID: ACF78275) is characterized biochemically to function as plastidial ADP-glucose transporter (Kirchberger et al. 2007). ZmBT1 is also reported to have dual function of targeting plastids and mitochondrial envelope membranes (Bahaji et al. 2011), suggesting that it might have a role of transporting some other mitochondrial

energy molecules. The barley ADP-glucose transporter (*HvNST1*) is identified in a mutant that accumulates less starch as compared to the wild type (Patron et al. 2004), while wheat ADP-glucose transporter is identified by reconstituting amyloplasts envelope membranes proteins in liposomes (Bowsher et a. 2007). As opposed to the first cluster, BT1 proteins from both monocotyledonous and dicotyledonous species were assigned to the second cluster. Most of these proteins have not been characterized yet but are predicted to act as adenylate transporters. For example, the BT1 from potato (*Solanum tuberosum*, StBT1) (GenBank ID: CAA67107) is identified as plastidial adenine nucleotide uniporter (Leroch et al. 2005), and the *Arabidopsis thaliana* (AtBT1) (GenBank ID: NP194966) as a plastidial nucleotide uniporter (Kirchberger et al. 2008). The alignment of the deduced amino acid sequence of BT proteins indicates that the BT1 homologues belong to the mitochondrial carrier family (MCF) that possesses membrane spanning domains (Leroch et al. 2005) and conserved motifs designated as mitochondrial energy transfer signature (METS) (Millar and Heazlewood 2003). A signal peptide of 53 amino acids is located at N-terminal of HvBT1 protein was detected.

Southern blot analysis indicated the presence of only one copy of *BT1* in the barley genome (Figure 2.2). However, two copies of *BT1* are detected in maize; *ZmBT1* and *ZmBT1-2*. The *ZmBT1* is found to be expressed exclusively in the endosperm, while *ZmBT1-2* in both autotrophic and heterotrophic tissues. The *ZmBT1-2* might work as an adenine nucleotide transporter that supplies the cells with adenine nucleotides that synthesized in the plastids (Kirchberger et al. 2007). QPCR and RNA in situ hybridization-based gene expression analysis indicated that the HvBT1 is exclusively expressed in the endosperm during grain filling (Figure 2.3 and 2.4). Detecting the

expression of *HvBT1* at low level in autotrophic leaf and stem tissues might suggest its dual function in the chloroplasts and mitochondrial envelope membranes like that of maize plastidial ADP-glucose transporter (*ZmBT1*) (Bahaji et al. 2011). However, localization of HvBT1 to the plastid membrane suggested that it acts as an ADP-glucose transporter across the plastid membrane (Figure 2.5A and B).

This study, using an *E. coli* expression system, characterized the *HvBT1* as ADP-glucose transporter. The first most important step of this study was to identify the proper *E. coli* strain to avoid the possible toxic effect of the expressed membrane protein. Heterologous expression of HvBT1 in two *E. coli* strains showed the inhibitory effect of HvBT1 on the cell growth of Rosetta2 strain harboring either original (org) or optimized (opc) ORFs of *HvBT1* (Appendex 1). However, cells of *E. coli* C43 strain, a mutant of BL21, harboring *HvBT1* were able to grow on both liquid and solid media after induction with IPTG, showing that the suitability of this strain of *E. coli* as a system in studying such membrane localized transporter proteins. At the protein level, Rosetta 2 harboring either org or opc ORFs was able to express the HvBT1 protein at low level as well as C43 cells harboring the original ORF, while C43 cells harboring the optimized ORF was able to produce HvBT1 at high level (Figure 2.6). Heterologous expression and purification of membrane proteins is the bottleneck of understanding their functional and structural prosperities (Bernaudat et al. 2011). Some eukaryotic membrane proteins are toxic to *E. coli* cells. Under normal conditions, membrane biogenesis in newly dividing *E. coli* cells is a multistep process in which the cells can produce adequate amounts of proteins, especially membrane proteins, to meet the cellular demand, mainly by controlling the translation machinery (Valent et al. 1997; Nagamori et al. 2004). However, when foreign

proteins transformed into the *E. coli* cells are expressed at higher rate, the cells are unable to accommodate the large amounts of expressed proteins, thereby affecting natural rhythm of the translation machinery (Narayanan et al. 2001). Another problem associated with the expression of membrane proteins in the *E. coli* system is mis-folding of the expressed proteins and storage of the aggregates in form of inclusion bodies (Bernaudat et al. 2011), which increases toxicity and arrests the cell growth (Akiyama 2009; Wagner et al. 2007). These factors might explain the growth arrest of the Rosetta 2 cells expressing both the original and optimized ORFs in both liquid and solid media. The *lacUV5* promoter in C41 and C43 strains has three mutations, two in the -10 region of the promoter and one in the *lac* operator. These mutations make the *lacUV5* promoter weak as compared to the wild type found in the original strain BL21 (Wagner et al. 2008), leading to low expression of the membrane protein that can help the cells expressing it to proliferate normally. Our data shows that slow expression of HvBT1 in the C43 strain allows the cells to produce soluble and functional proteins and keeps the cells active.

ADP-glucose transporter of barley, *HvBT1,* transports ADP-Glc in counter-exchange with ADP with apparent affinities of 614 μM and 334 μM, respectively (Figure 2.7A and B). Similar results have been reported in maize where *ZmBT1* was able to transport ADP-Glc in counter-exchange with ADP with apparent affinities of 850 μM and 465 μM, respectively (Kirchberger et al. 2007). Wheat endosperm amyloplast ADP-glucose transporter was also analyzed by reconstituting amyloplasts envelope membrane proteins in a proteolosome. Its apparent affinities for ADP-Glc and both ADP and AMP were found to be 430 μM and 200 μM, respectively (Bowsher et al. 2007).

Enhancing the efflux of [α-32p] ADP-Glc by dilution of the medium with high concentration of ADP and AMP revealed the potentials of these nucleotides as counter exchange substrates (Figure 2.8A). This result was supported by the efflux of the putative [α-^{32}P] ADP by dilution with high concentration of nonlabeled ADP-Glc (Figure 2.8B). In agreement with this, efflux study with intact amyloplasts of wheat showed that ADP-glucose transporter protein transports ADP-Glc into the amyloplasts in counter exchange with ADP and AMP (Bowsher et al. 2007). In addition, preloading induced *E. coli* cells harboring *HvBT1* with ADP and AMP resulted in increased ADP-Glc uptake as compared to the control (Figure 8C). Similar results have been reported in maize using *ZmBT1* (Kirchberger et al. 2007).

Testing several effectors on the [α-^{32}P] ADP-Glc uptake in the intact *E. coli* cells expressing *HvBT1* protein showed that the transport rate of [α-^{32}P] ADP-Glc increased when co-incubated with glucose or glucose 1-phosphate (Table 2.1). Interestingly, co-incubation with glucose also increased the uptake rate of [α-^{32}P] ADP-Glc by almost double of the control. Glucose as a sole carbon source plays an important role in the activation of *E. coli* metabolism (Brown et al. 2008), which subsequently increases the ability of the cells to uptake [α-^{32}P] ADP-Glc. Glucose 1-phosphate also had a positive effect on the uptake of [α-^{32}P] ADP-Glc (Table 1). Meanwhile, co-incubation with unlabeled ADP-Glc reduced the uptake of [α-^{32}P] ADP-Glc by ~ 50% as compared to the control due to its competition as a substrate with the labeled ADP-Glc. Reduction in the uptake of [α-^{32}P] ADP-Glc was also observed by co-incubation with ADP, indicating the substrate specificity of HvBT1 for ADP-Glc and ADP.

In summary, the findings of this study show that HvBT1 is able to transport ADP-glucose with high affinity in counter-exchange with ADP and probably with AMP. Its localization to the plastids envelopes and exclusive expression in the endospermic cells of the barley grains indicates its potential significance in determining starch yield in barley.

CHAPTER 3. THE IMPACT OF PLASTIDIAL ADP-GLUCOSE TRANSPORTER (*HvBT1*) EXPRESSION ON STARCH SYNTHESIS IN BARLEY

3.1. Abstract

In the endosperm of cereal grains, ADP-glucose transporter is the main gate for transportation of ADP-glucose from the cytosol into the amyloplasts. We investigated the importance of the barley plastidial ADP-glucose transporter, HvBT1, for starch synthesis using gene expression analysis of *HvBT1* and other starch synthesis-related genes. The expression of *HvBT1* in Harrington was almost 10 times higher than Golden Promise. In the grain composition, starch content was 2.5 % higher in Harrington than Golden Promise while Harrington starch had higher amylopectin amylose ratio than Golden Promise. In Harrington, *AGPL1* and *AGPL2* were expressed at late and early stages of grain filling, respectively. The expression of the large and small subunits of AGPase was significantly higher in Harrington as compared to Golden Promise. Similarly, AGPase activity in Harrington was significantly higher than its activity in Golden Promise. The expression patterns of Granule-Bound Starch Synthases1a and 1b (*GBSS1a & 1b*) followed the same trend, and showed higher expression in Harrington. Oppositely, soluble Starch Synthases (*SS*) showed significantly higher expression in Golden Promise than Harrington, except *SS3b* which showed higher expression in Harrington. Also, Starch Branching Enzyme1 (*SBE1*) showed significantly higher expression in Golden Promise. Protein, β-glucan and lipids were significantly higher in Golden Promise which accumulated less starch. This result is in line with the negative correlation between starch content and other grain components. We speculate that starch content in Harrington was higher as a result of a higher expression of *HvBT1*.

3.2. Introduction

Starch is the main storage polymer in higher plants and has a great impact as a renewable source for human nutrition and a renewable source of industrial end-uses especially biofuel production (Smith, 2008). Starch contains two polymers, amylose and amylopectin, which is synthesised in both photosynthetic and non-photosynthetic organs (Zeeman et al. 2010). Barley grain contains ~50 – 60% starch which is composed of ~ 25% and 75% amylose and amylopectin, respectively (Li et al. 2011). In heterotrophic cells of dicotyledonous species, glucose 6-phosphate is synthesized in the cytosol from sucrose and imported into amyloplasts via glucose 6-phosphate / Pi translocator (Kammerer et al. 1998). Then, glucose 6-phosphate is converted to glucose 1-phosphate by plastidial phosphoglucomutase (PGM). ADP-glucose, the glucosyl donor for starch synthesis, is made through the reaction driven by plastidial ADP-glucose pyrophosphorylase (AGPase) which catalyzes the conversion of glucose 1-phosphate using ATP into ADP-glucose and release inorganic phosphate (PPi) (Gross and apRees, 1986). Starch synthesis in cereal endosperm is a complex process as compared to other species. The starch biosynthesis pathway is divided into two main streams; the first is cytosolic and responsible for ADP-glucose synthesis, and the second one is plastidial and directly involved in the starch synthesis process. The major activity of ADP-glucose pyrophosphorylase (AGPase) was reported as cytosolic, which represents 85-95 % of the total activity (James et al. 2003). Subsequently, the majority of ADP-glucose (80-90%) is made in the cytosol of the endospermic cells (Tiessen et al. 2012) and must be imported into amyloplasts where the starch is made. ADP-glucose is transported into amyloplasts in counter-exchange with ADP via an ADP-glucose transporter (Bowsher et al. 2007;

Kirchberger et al. 2007). Mutation in ADP-glucose transporter impairs starch accumulation in barley mutant RisØ 13 (Patron et al. 2004).

In the plastids, many enzymes are involved in amylose and amylopectin synthesis; granule-bound starch synthases, soluble starch synthases, starch branching and de-branching enzymes. Amylose is synthesized by granule-bound starch synthase (GBSS) in the plastids. The effect of GBSS on amylose synthesis was demonstrated by generating amylose free starch as a result of lacking GBSS activity (Denyer et al. 2001). GBSS is able to form long glucan chains and elongates the side chains forming long chains of amylopectin molecules (Denyer et al. 1999; Fulton et al. 2002; Hanashiro et al. 2008). Amylopectin is a branched molecule which is synthesized by the function of soluble starch synthases by transferring the glucosyl moiety to the existing glucan chains (Zeeman et al. 2010). Different types of starch synthases are involved in amylopectin synthesis. Analysis of different mutants and transgenic plants lacking the activity of one of those enzymes showed negative effect on the amylopectin synthesis and altered the amylose/amylopectin ratio in cereal grains. The high-amylose starch in durum wheat was generated by a mutation in starch synthase 2a (*SS2a*) (Hogg et al. 2013). Also, the barley mutant *sex6* lacking the activity of starch synthase 2a (SS2a) produced high-amylose starch (Morell et al. 2003). In rice, the null mutant of *SS3a* created white-core floury endosperm, characterized by reducing the length of long chain of amylopectin and increased amylose content (Ryoo et al. 2007).

The unique function of ADP-glucose transporter, HvBT1, makes them good candidates as limiting factors in the starch synthesis process. In the present study, we investigated the effect of the expression of the plastidial ADP-glucose transporter *HvBT1*

on the starch synthesis process in two malting barley cultivars. Grain composition analysis and expression of starch-related genes were investigated to determine the unique combination the key factors that involved in this process.

3.3. Materials and methods

3.3.1. Plant materials

Two barley (*Hordeum vulgare L.*) cultivars; Golden Promise and Harrington were used in the present study. Barley plants were grown under greenhouse conditions (16/8 hrs day/ night photoperiod). Spike samples were collected at 2, 4, 6, 8, 10, 12, 14, 16 and 20 days after anthesis (DAA) during grain filling. The tissues were collected and immediately placed in liquid nitrogen. In ceramic mortars, the tissues were ground to fine powder, and stored at – 80°C.

3.3.2. RNA extraction and cDNA synthesis

Total RNA was extracted from collected tissues using RNaesy Plant Mini Prep Kit (Qaigen, Germany). The extraction procedures were performed on 100 mg ground tissues as described in the instructions manual. Genomic DNA contamination was eliminated by in-column DNase digestion using RNase-Free DNase Set (Qiagen, Germany). The RNA integrity was visualized on agarose gel and the concentration measured by a Nanodrop spectrophotometer (Thermo Fisher, USA). The first strand DNA was synthesized from 5 µg total RNA by Revert Aid™ First Strand cDNA Synthesis Kits (Fermentas) using oligo $(dT)_{18}$ primers. Primers were designed by TaqMan (Genescript, USA). The primers were designed with particular criteria as follow; Tm, 59±1°C, primer length 20±1 and amplicon size 80-150 bp with GC content ranging between 45% and 55%.

3.3.2. Quantitative Real-Time RT-PCR analysis

Quantitative Real-Time PCR (qRT-PCR) was conducted on a CFX96 Thermal Cycler (Bio-Rad) with SsoFast EvaGreen Supermix (Bio-Rad) according to the manufacturer's instructions. Actin was used as an internal control to normalize qRT-PCR. The qRT-PCR was assayed on 4 ng cDNA /µL final volume. The selected genes accession numbers and primer sequences are shown in Table1. The qRT-PCR results were analyzed using $2^{-\Delta\Delta}$ Ct method (Livak and Schmittgen, 2001).

3.3.3. ADP-glucose pyrophosphorylase (AGPase) activity

ADP-Glc was enzymatically synthesized using a modified protocol of Ghosh and Preiss (1966) and Rösti et al. (2006) as follows: ADP-glucose pyrophosphorylase (AGPase) was extracted from barley caryopsis 10 DAA (0.5 g) with an extraction buffer containing 50 mM HEPES (pH 7.4), 2 mM $MgCl_2$, 1 mM EDTA and 1mM DTT. The mixture was centrifuged at 10,000 g for 15 min at 4°C. Total protein in the extraction buffer was measured by the Bradford standard protocol and used directly in the assay. The direct ADP-glucose synthesis was conducted in assay buffer (0.2 mL) containing 100 mM HEPES (pH 7.6), 15 mM $MgCl_2$, 0.025 % (w/v) BSA, 0.5 units inorganic pyrophosphatase from baker's yeast (Invitrogen), 0.5 mM glucose 1- phosphate, 1.5 mM ATP, 15 mM 3-PGA. The supernatant containing AGPase (20 µL) was added to the assay buffer and incubated at 37°C for 20 min followed by boiling the mixture for 2 min at 95°C to stop the reaction, and then the mixture was centrifuged at 10,000 rpm for 5 min and filtered.

Table 3.1. Starch biosynthesis-related gene specific primer sequences and accession numbers.

Gene	Primer name	Primer sequence	Accession No. (NCBI)
AGP.L1	AGP L1-F	5'-TCAACAAGTGGCATCAACAA-3'	AL506975.1
	AGP L1-R	5'- GGCCCAATACCTCAACAGAT-3'	
AGP.L2	AGP L2-F	5'- GACCAGGCTCTTCCCTCTC-3'	BQ470624.1
	AGP L2-R	5'- TTGATGCAGTTGCTCATGG-3'	
AGPS1a	AGP S1a-F	5'- CGAGGCACACATCACTCAAT-3'	BU971115.1
	AGP S1a-R	5'- CATTGTTCATGCTTGGAAGG-3'	
AGPS1b	AGP S1b-F	5'- CGTCATCTCTCACGAGCCTA-3'	BQ462814.1
	AGP S1b-R	5'- GCAGCAAGGACTTCAACAAA-3'	
AGPS2	AGP S2-F	5'- ATGGCTGTTTGAGGAACACA-3'	AL503815.1
	AGP S2-R	5'- GCAGCCACAGTAATATCAGCA-3'	
SS 1	SS1-F	5'-TGGTGAAGCTGCTCCTTATG-3'	BQ472054.1
	SS1-R	5'-CTCGGCATTACAACCATCAC-3'	
SS 2a	SS2a-F	5'-AGGACTTCAGCTGGGAACAT-3'	BU966952.1
	SS2a-R	5'-CGTTCACCACTGGTACTTGG-3'	
SS 2b	SS2b-F	5'-CCGGAGTAACCAAGGATCAC-3'	CA011643.1
	SS2b-R	5'-CACGAACCTGACTGAACTGG-3'	
SS 3a	SS3a-F	5'-TTCTTGGAGTGGCACAGAAA-3'	BU970315.1
	SS3a-R	5'-CAAATCTGCGGTCATCATTC-3'	
SS 3b	SS3b-F	5'-CGGAAGAAGGTGGGATGTAT-3'	BU970246.1
	SS3b-R	5'-ACCTTTGCAATAGGAGCCAT-3'	
SS 4	SSIV-F	5'-CTGCATTTGTTGCACCTCTT-3'	FD523091.1
	SSIV-R	5'-TAGGTGCTCAACATCAAGGC-3'	
GBSS 1a	GBSS1a-F	5'-GGTATGAGGACTATCGGAGCA-3'	AL508933.1
	GBSS1a-R	5'-ACGAACACGAGGTTCATGC-3'	
GBSS 1b	GBSS1b-F	5'-GAACAGAAAGGGTCGGACAT-3'	BU997101.1
	GBSS1b-R	5'-GCATCAGTTCCTCCTCCATT-3'	
HvBT1	HvBT1-F	5'-GAGGCAGGTGTACAAGAACG-3'	AY560327.2
	HvBT1-R	5'-TAGCACATGAAGGAGATGCC-3'	
Beta-Actin	HvACTN-F	5'-GCTGATCGTATGAGCAAGGA-3'	AK248710.1
	HvACTN-R	5'-CACATCTGCTGGAAAGTGCT-3'	

ADP-glucose was quantified using High Performance Liquid Chromatography (HPLC) (Waters 2695 Separations Module). The reaction was performed without a protein extract as a blank, while the boiled extract was used in the reaction buffer as a negative control. Ten microliters of the assay mixture was injected in an HPLC equipped with Waters 996 Photodiode Assay Detector and LichroCART 250 x 4 Lichrospher 100 RP-18 (5µm) column (Merck KGaA, Germany). The samples were eluted by gradients of acetonitrile in water as follows: time (min)/flow rate (mL/min)/acetonitrile (%): 0.01/1/0, 0.8/1/5, 1.6/1/20, 2.12/1/75, 4/1/100, 4.8/1/100, 6/1/0, 15/0.2/0.

3.3.4. Grain yield and physical parameters

A hundred grains were counted using a seed counter, and then grain weight was recorded for three replicates from three individual samples from each cultivar. A single grain weight was measured on the counted seeds ± SE. Grain length, width and area were examined by scanning 25 grains in 5 replicates from each cultivar with *Assess 2.0* (Lamari, 2008). Cross-sectioned and intact barley grains were examined by stereoscopic microscopy for external appearance and plumpness.

3.3.5. Grain composition
3.3.5.1. Starch, Amylose and B-glucan contents

Barley whole grains were ground to a fine powder and used for extraction of total starch, amylose and β-glucan. The extraction was performed with AOAC Method 996.11/AACC Method 76.13, K-AMYL 07/11, K-BGLU kits (Megazyme International Ltd., Wicklow, Ireland) for starch, amylose and B-glucan, respectively. The extraction

procedures were achieved according to the manufacturer's procedures. The assay was performed on three biological replicates with two technical replicates from each.

3.3.5.2. Protein content

The total protein content was determined in the barley cultivars mature grains as total nitrogen content using a combustion nitrogen analyzer (Leco FP – 528, Nitrogen/Protein Determinator Corporation, St. Joseph, Mich). The protein values were calculated by multiplying the obtained nitrogen value by a factor of 6.25. The assay was performed on three biological replicates with three technical replicates from each.

3.3.5.3. Lipids content

Lipids were extracted and quantified from barley whole meal (1gm) of the barley cultivars using a gravimetric method after extraction with a chloroform-methanol mixture. The procedures were performed according to Phillips et al. (1997). Thin layer chromatography (TLC) was performed by applying 10 µL of total lipid extracts on silica gel (AL SIL G, plate size 20x20 cm with 0.25 mm thickness, Whatman) according to Mangold and Malins (1960) and Mangold (1961) and separated by petroleum ether :diethyl ether : glacial acidic acid (80:20:1, v:v:v) according to Kates (1972). Lipid fractions were visualized using iodine vapor. The lipid fractions were identified by comparing RF values to published RF values of lipid standards.

3.2.5.4. Water-soluble carbohydrate content

Water-soluble carbohydrates were extracted according to Yemm and Willis (1954) with modifications described in Clarke et al. (2008). In brief, 100 mg of barley whole meal was extracted in 10 mL 80% ethanol by boiling in a water bath for 10 min. The extraction was performed three times and the supernatant pooled and freeze-dried. The carbohydrates were re-suspended in 1 mL milliQ water and carbohydrate sugars were quantified using High Performance Anion Exchange Chromatography (HPAEC) according to Ruuska et al. (2006)

3.3.6. Statistical analysis

Student T-test ($P < 0.05$) was used to analyze the significant differences of single traits between the barley cultivars. The analysis of variance (ANOVA analysis) was performed with Proc GLM SAS 9.2 to assess the interaction of different factors in the traits and cultivars.

3.4. Results

3.4.1. Plastidial ADP-glucose transporter (*HvBT1*)

The expression analysis of *HvBT1* followed the same trend in both cultivars over time (Figure 3.1). *HvBT1* expression started at very low levels from 2-8 DAA, increased drastically during the period 10-16 DAA, and decreased again at 20 DAA. The expression level of *HvBT1* in Harrington was significantly higher (10 folds) than in Golden Promise at all tested time points. The expression of *HvBT1* reached a peak in both

cultivars between 14-16 DAA, and then decreased after 20 DAA in Golden Promise, while it was sustained in Harrington.
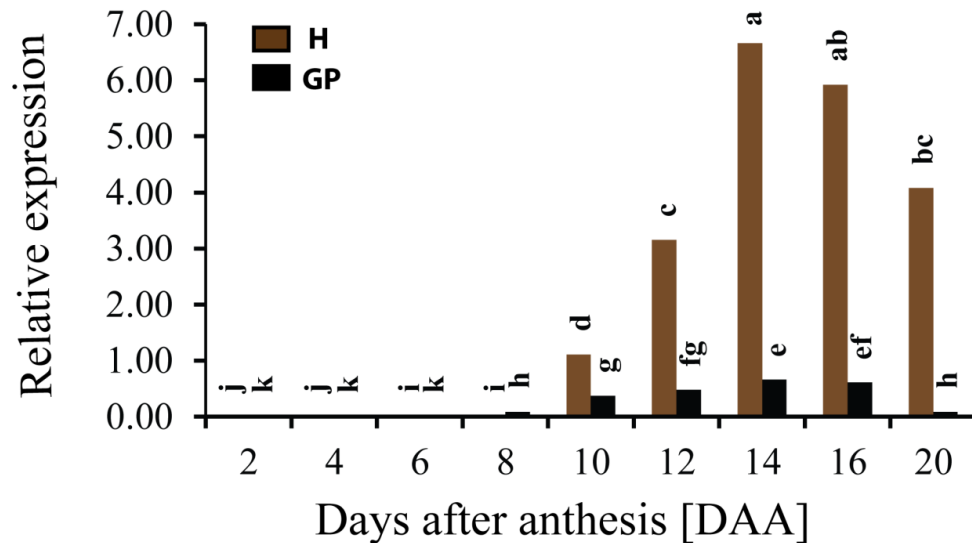
Figure 3.1. Expression analysis of the plastidial ADP-glucose transporter (*HvBT1*).

The expression of *HvBT1* in Harrington (H) is shown by brown bars, while Golden Promise (GP) by black bars. The letters show the significance of the expression of *HvBT1* among time points and cultivars. The bars which have the same letter are not significantly different, while the bars with different letters are significantly different at *P < 0.05*.

ADP-glucose pyrophosphorylase (AGPase)

3.4.2.1.AGPase Large Subunits (LSUs).

Cultivars, Golden Promise and Harrington, showed differential expression patterns of AGPase large subunits (LSU) genes (Figure 3.2). The expression of *AGPL1* and *AGPL2* showed different trends, where the expression of *AGPL1* started at early stages at very low levels, but the expression reached a peak from 14 to 20 DAA in both cultivars. The expression of *AGPL1* in Harrington was aproximatley 10 times higher than in Golden Promise (Figure 3.2A). Meanwhile, the expression of *AGPL2* was lower than *AGPL1*, and showed different trends in the tested cultivars. Its expression in Harrington was detected at early stages from 2 to 10 DAA, while in Golden Promise was detected at late stages from 8 to 20 DAA. Generally, the expression of *AGPL1* and *AGPL2* was higher in Harrington than Golden Promise (Figure 3.2B).

3.4.2.2. ADP-glucose pyrophosphorylase small subunits (SSU).

The small subunits represent the catalytic activity of AGPase which are responsible for converting glucose 1- phosphate into ADP-glucose using ATP. The expression of *AGPS1a* was detected at very low levels at early stages of grain filling from 2 to 10 DAA in both barley cultivars. The expression significantly increased from 12 to 20 DAA, and was significantly higher in Harrington than in Golden Promise. The expression in Harrington remained at higher levels at late stages of grain filling, while the expression in Golden Promise was significantly lower at the entire time points, and reached a peak at 14 DAA, thereafter decreased from 16 to 20 DAA (Figure 3.2C). No significant differences were detected at early stages for *AGPS1b* expression in either cultivar (Figure

3.2D). In Harrington, the expression of *AGPS1b* at 12 to 20 DAA was significantly higher by aproximatley double of Golden Promise. *AGPS1b* showed higher expression level in Golden Promise at 12 DAA as compared to Harrington. Generally, the expression of *S1b* was significantly higher in Harrington than in Golden Promise. The expression of *AGPS2* was detected at very low levels at early stages of grain filling until 10 DAA, and followed the same trend in both cultivars. At 12 DAA, it increased dramatically and continued over the tested times in both cultivars. A significantly higher expression occurred in Harrington at 14-16 DAA as compared to Golden Promise. Interestingly, the expression of *AGPS2* remained almost stable at late stages of grain filling in Golden Promise (Figure 3.2E).

3.4.2.3.Granule-bound starch synthase (GBSS)

Granule-bound starch synthases (GBSS) are responsible for amylose biosynthesis. Also they are involved in synthesis of long chains in amylopectin molecules. In this research, we investigated the expression of GBSS-encoded genes (*GBSS1a* and *1b*) in barley cultivars. The expression of *GBSS1a* was not detected at early stages of grain filling from 2 to 6 DAA in either cultivar, and then increased drastically from 12 to 20 DAA in both cultivars. The expression of *GBSS1a* was significantly higher in Harrington as compared to Golden Promise from 14 to 20 DAA. In contrast, *GBSS1b* expression was higher at early stages from 2 to 10 DAA in both cultivars, with significantly more in Harrington, and a maximum expression at 8 and 10 DAA. Generally, the expression of both *GBSS1a* and *GBSS1b* was significantly higher in Harrington as compared to Golden Promise (Figure 3.3).
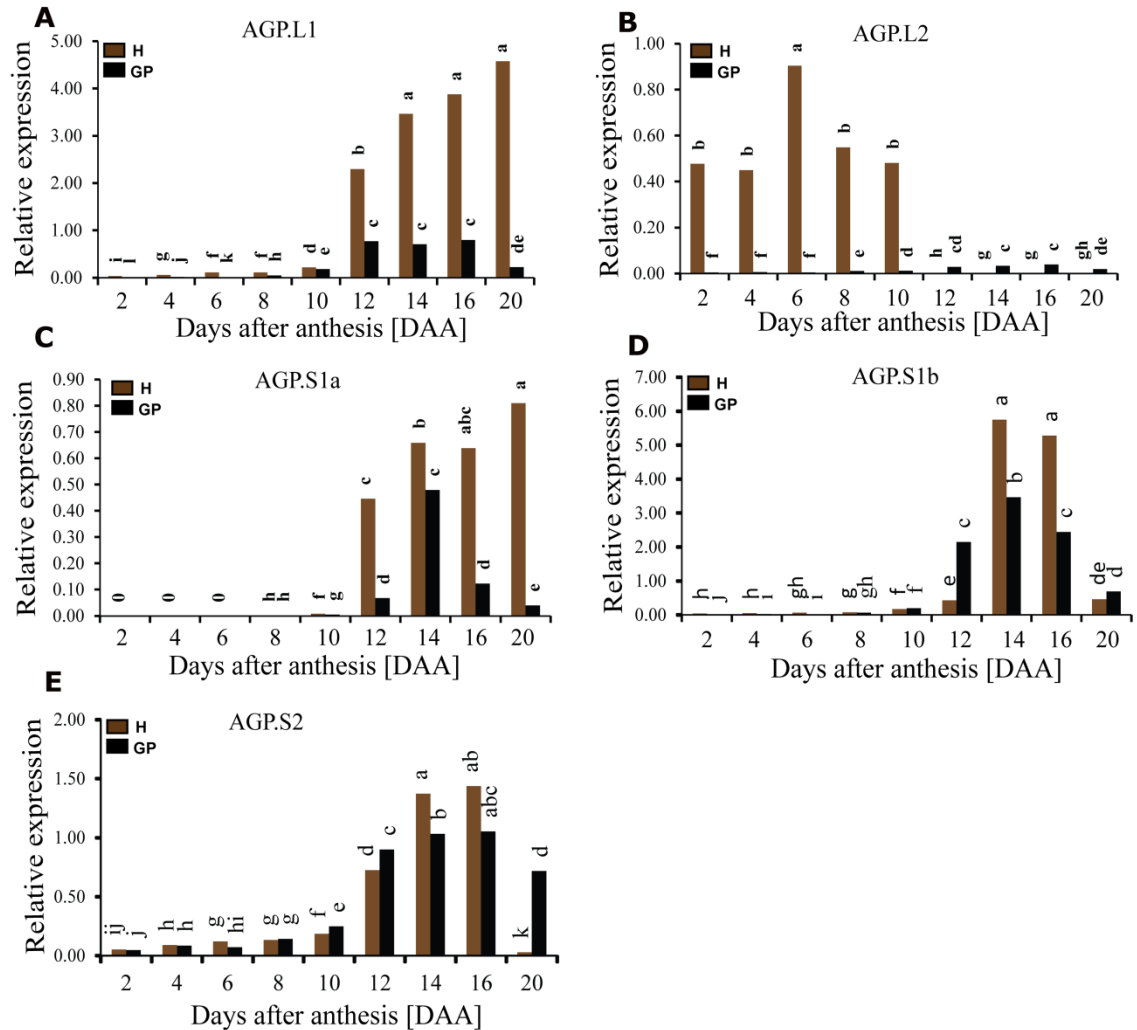
Figure 3.2. Expression of AGPase-encoding genes (*AGP.*)

The expression *AGPase* in cv. Harrington (H) is shown by brown bars, while cv. Golden Promise (GP) by black bars. The expression of the large subunits; (**A**) *AGPL1* and (**B**) *AGPL2*. AGPase small subunit genes (*AGPS*); (**C**) *AGPS1a*, (**D**) *AGPS1b* and (**E**) *AGPS2*. The bars which have the same letter are not significantly different, while the bars with different letters are significantly different at P < 0.05.
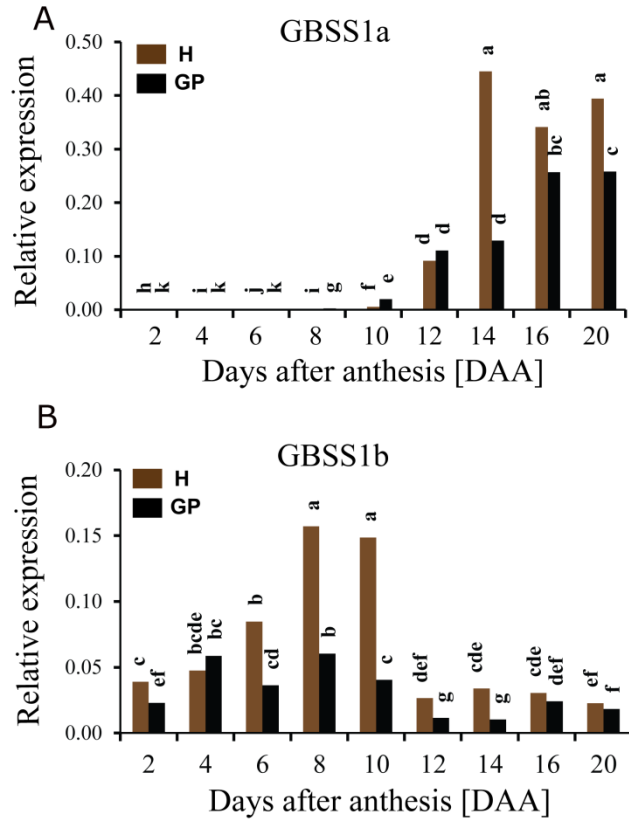
Figure 3.3. Expression of granule-bound starch synthase-encoding genes (*GBSS*).

The expression of *GBSSs* in cv. Harrington (H) is shown by brown bars, while cv. Golden Promise (GP) by black bars. The expression of *GBSS1a* is shown in (**A**), while the expression of *GBSS1b* is shown in (B) .The bars which have the same letter are not significantly different, while the bars with different letters are significantly different at P < 0.05.

3.4.2.4.Soluble-starch synthase (SS)

The expression of starch synthase1 (*SS1*) was detected at all stages during grain filling in both cultivars. It started at low levels from 2 to 10 DAA, and then increased considerably over time (Figure 3.4A). The maximum expression was recorded at 16 DAA in Golden Promise, and at 14 and 16 DAA in Harrington, and then decreased in both cultivars. At 8 to 12 DAA, the expression of *SS1* was significantly higher in Golden Promise as compared to Harrington. The expression of starch synthase 2a (*SS2a*) was detected at early stages during grain filling in both cultivars, but was at very low levels in both cultivars at 2 to 6 DAA (Figure 3.4B). The expression was drastically increased from 10 to 16 DAA and decreased thereafter at 20 DAA. The expression was significantly higher in Golden Promise starting at 8 DAA and reached a peak at 12 to 16 DAA, then decreased at 20 DAA. In Harrington, it was at very low levels until 10 DAA and then increased over time to reach a peak at 14 DAA, then decreased gradually. Generally, the expression of *SS2a* was significantly higher in Golden Promise than Harrington between 8 to 20 DAA, while the expression of *SS2b* was stable over time from early to late stages in both cultivars. There was little difference in the expression patterns of *SS2b* between the two cultivars. In Harrington, the expression of *SS2b* was higher at early stages of grain filling from 2 to 6 DAA and reached a peak at 6 DAA (Figure 3.4C). In Golden Promise, the expression of *SS2a* was higher at late stages of grain filling as compared to Harrington.

The expression of Starch synthase 3a (*SS3a*) was detected at very low levels during early stages up to 8 DAA in both cultivars (Figure 3.4D). The expression drastically increased in Golden Promise from 10-16 DAA, while in Harrington, the expression of

SS3a increased at a later stage (12 DAA) and continued until 20 DAA. Generally, the expression of *SS3a* was significantly higher in Golden Promise as compared to Harrington, except at 20 DAA. The expression analysis of *SS3b* indicated continuous expression through the tested time points (Figure 3.4E). In Harrington, the expression of *SS3b* was significantly higher in all time points as compared to Golden Promise. The expression of *SS3b* reached a maximum level between 14-16, and at 16 DAA for Harrington and Golden Promise, respectively. Starch synthase 4 gene (*SS4*) showed stable expression over time in both cultivars (Figure 3.4F). The expression of *SS4* started at very early stages of grain filling from 2 DAA and extended until 20 DAA. In Golden Promise, the expression of *SS4* was significantly higher at 8-12 DAA as compared to Harrington, where it reached a peak at 12 DAA.

3.4.2.5. Starch branching enzyme 1 (SBE1)

Starch branching enzymes1 (*SBE1*) is responsible for initiation of amylopectin branches. The expression of *SBE1* was detected at all-time points in both cultivars. It started at low levels at early stages from 2 to12 DAA and increased at late stages from 14 to 20 DAA. Although, the expression of *SBE1* followed the same trend in both cultivars, it was significantly higher in Golden Promise than in Harrington, and reached a peak at 14-20 DAA (Figure 3.5).
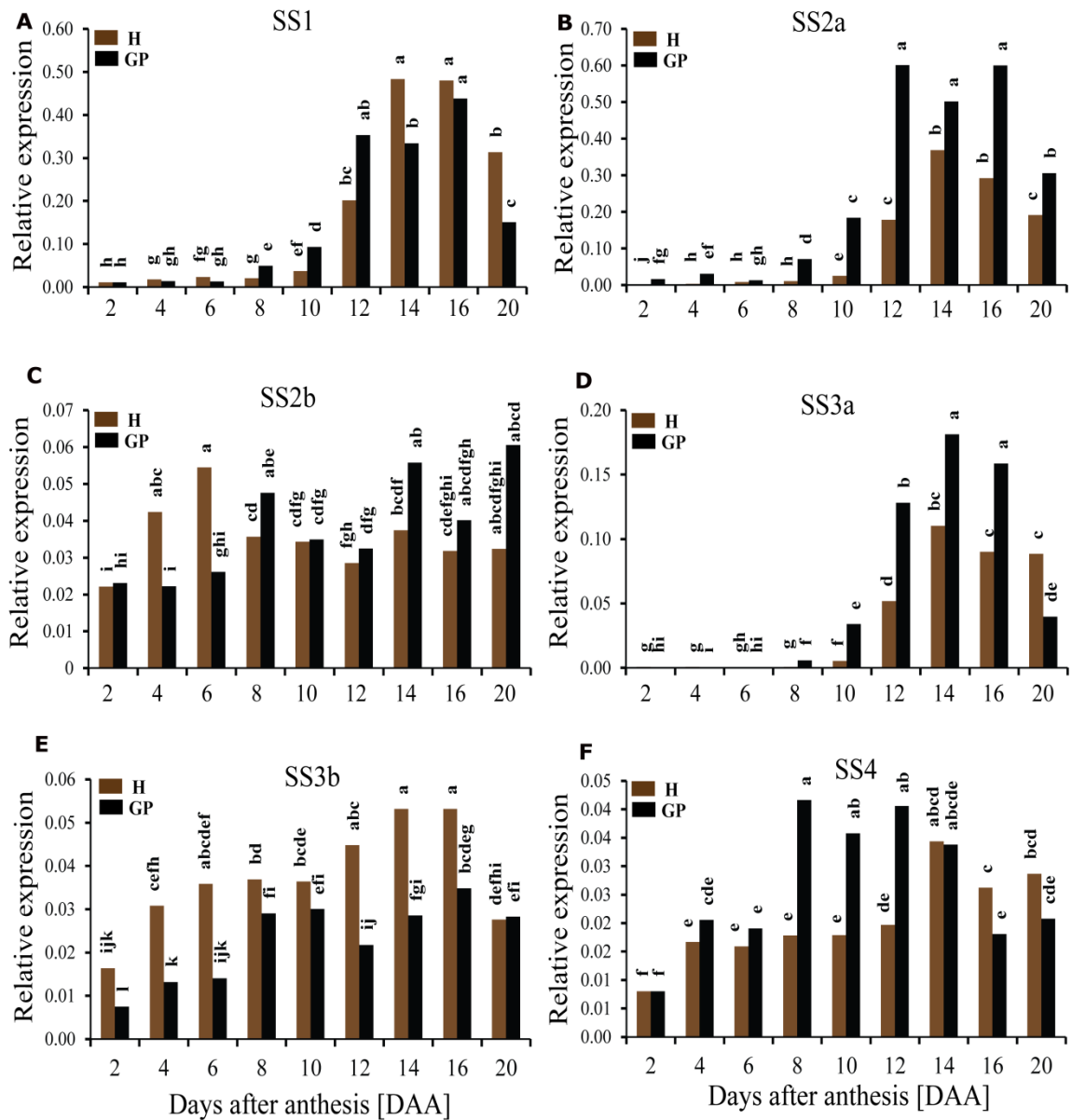
Figure 3.4. Expression of soluble starch synthase-encoding genes (*SSs*).

The expression of *GBSSs* in cv. Harrington (H) is shown by brown bars, while cv. Golden Promise (GP) by black bars. The expression of starch synthase-encoded genes shown in the panel is ; (**A**) *SS1,* (**B**) *SS2a,* (**C**) *SS2b*, (**D**) *SS3a*, (**E**) *SS3b* , and (**F**) *SS4*. The bars which have the same letters are not significantly different, while the bars with different letters are significantly different at P < 0.05.
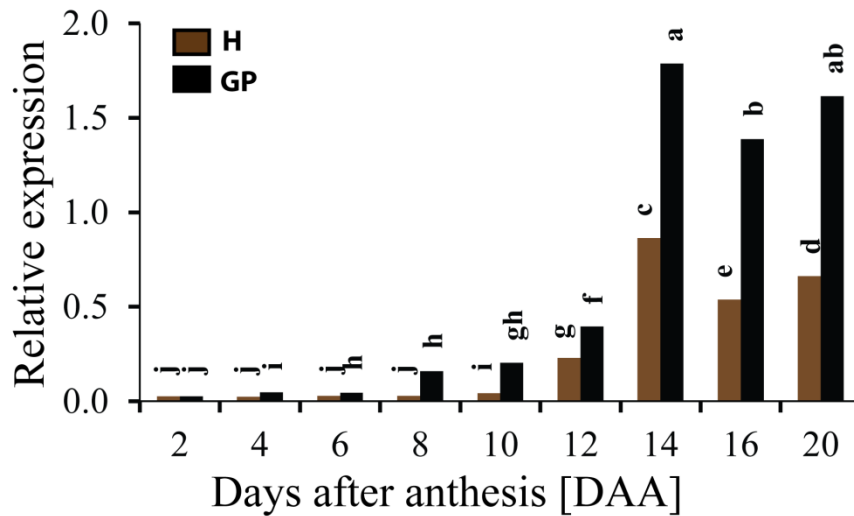
Figure 3.5. Expression of starch branching enzyme 1 (*SBE1*).

The expression of starch branching enzyme1 gene (*SBE1*) was detected at the indicated time points from 2 to 20 DAA. The expression of *SBE1* in cv. Harrington is shown by white bars, while cv. Golden Promise by black bars. The bars which have the same letter are not significantly different, while the bars with different letters are significantly different at P < 0.05.

3.4.3. ADP-glucose pyrophosphorylase (AGPase) activity

ADP-glucose pyrophosphorylase activity was assayed on barley spike tissues. The AGPase activity was determined by measuring ADP-glucose with HPLC by converting glucose 1-phosphate into ADP-glucose in the presence of ATP (Figure 3.6). ADP-glucose synthesis increased significantly in the assay that was conducted with Harrington protein extract as compared to Golden Promise ($P < 0.05$). There was no ADP-glucose detected when boiled protein extracts were used.
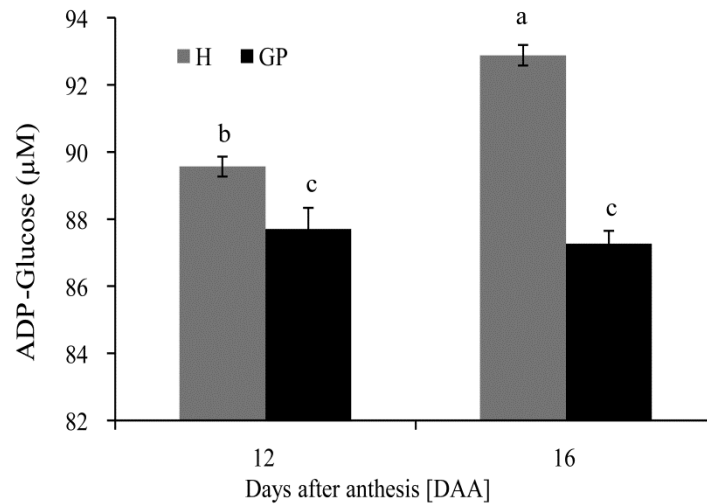
Figure 3.6. ADP-glucose pyrophosphorylase (AGPase) activity.

AGPase activity was detected in the endosperm of barley cultivars at 12 and 16 DAA. The activity of AGPase was measures by the conversion of glucose 1-phosphate into ADG-glucose, and then ADP-glucose concentration was measured by HPLC. The data represented the peak height ±SE bars. The bars which have the same letter are not significantly different, while the bars with different letters are significantly different at $P < 0.05$.

Grain yield and physical parameters

A single grain weight in Harrington was significantly higher than in Golden Promise. Consequently, a hundred grain weight also was significantly higher in Harrington. Grain length and area in Harrington were higher in values than in Golden Promise, while grain width showed no difference between the two cultivars (Table 2). The stereoscopic examination of the cross-sectioned and the whole grains showed differences in grain size and plumpness, where Harrington has bigger grains as compared to Golden Promise (Figure 3.7).

Table 3.2. Grain yield-related traits

Genotype[a]	Single grain weight (mg)	100 grain weight (g)[b]	Grain length (mm)[c]	Grain width (mm)[c]	Grain area (mm)[c]
G. Promise	48.184 ± 0.62	4.825 ± 0.1	8.9472 ± 0.088	3.9132 ± 0.19	23.6508 ± 0.37
Harrington	53.412 ± 0.66*	5.118 ± 0.18*	10.406 ± 0.088*	3.9012 ± 0.043	27.9704 ± 0.27*

[a] Moisture content ~ 9-10 %
[b] Seed counter was used for counting 100 grains
[c] Grain physical parameters were assessed using *Assess 2.0*

3.4.4. Grain composition

3.4.4.1. Starch and amylose contents

Total starch content in Harrington (55.84%) was higher than in Golden Promise (53.35%), representing ~ 2.5% higher starch content. In contrast to starch, amylose content is lower in Harrington cultivar as compared to Golden Promise), with 26.8% and 27.65 %, respectively. Amylopectin was higher in Harrington than in Golden Promise with 73.2% and 72.35%, respectively (Table 3).
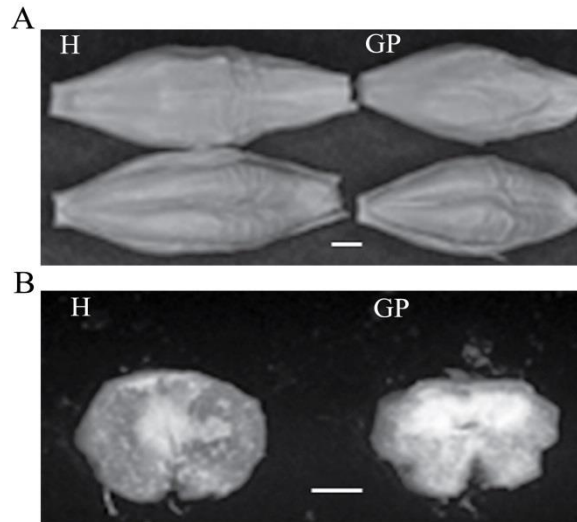
Figure 3.7. Stereoscopic analysis of the whole and cross-sectioned grains.

Stereoscopic analysis of whole grain (A) and cross section (B) showed differences in the grain length (A) and plumpness (B). The image size is indicated by the bar of 1mm in length.

3.4.4.2. β- glucan and protein contents

β-glucan, a non-starch polysaccharide, was quantified in the whole meal of barley cultivars. β-glucan content was 5.49% and 4.77 % in the whole meal of Golden Promise and Harrington, respectively, representing 0.8% difference (Table 3). Protein content was 14.25% and 16.11 % in the whole meal of Harrington and Golden Promise, respectively, representing ~1.8% higher protein in Golden Promise than in Harrington.

Table 3.3. Grain composition

Genotype [a]	Total starch (%)[b]	Amylose (%)	Amylopectin (%)	Protein (%)[c]	β-glucan (%)[d]
G. Promise	53.35 ± 0.872	27.65± 0.25*	72.35 ± 0.25	16.115 ± 0.95*	5.40 ± 0.037*
Harrington	55.8 ± 1.195*	26.8± 0.2	73.2 ± 0.2*	13.25 ± 1.026	4.77 ± 0.18

[a] Moisture content ~ 9-10% and the percentage of the components based on the total weight used for the assay (100 mg).
[b] Total starch, amylose and amylopectin were measured in the whole meal.
[c] Protein values were obtained by multiplying nitrogen value by a factor of 6.25.
*Asterisk star indicates significance at $P < 0.05$.

3.4.4.3. Lipids content

Total lipids were extracted from the whole meal of Harrington and Golden Promise. The lipid content was significantly higher in Golden Promise than in Harrington with 65.7 mg/g DW and 53.1 mg/g DW, respectively (Figure 3.8A). The gravimetric method used for this quantification seems to overestimate lipid contents in the dry matter. Thin-layer chromatography of extracted lipids did not discern changes in the lipids' profiles of the two cultivars (Figure 3.8B).

3.4.4.4. Waster-soluble carbohydrates

Water-soluble carbohydrates in grains of the two cultivars were measured by HPAEC. Glucose, fructose, sucrose, and maltotriose contents were higher in Harrington than in Golden Promise. Sucrose and fructose represented the highest soluble carbohydrates in the grains (Figure 3.9).
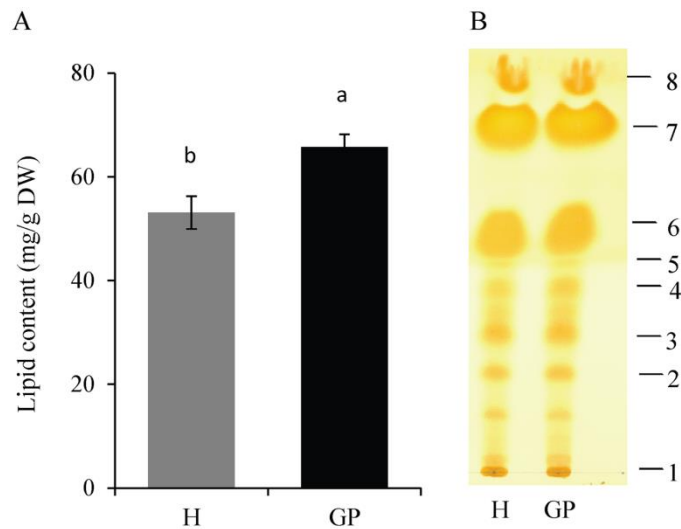
Figure 3.8. Total lipids content and thin layer chromatography (TLC).

Total lipids content was assayed from barley cv. Harrington (H) and cv. Golden Promise (GP) whole milled grains using the gravimetric method (A). A volume of 10 µL different lines was separated on silica gel plate and visualized by iodine vapor (B). Spots are marked with number on the left side of the gel. 1, Polar lipids; 2, Mono-glycerides; 3, 1,2 & 2,3 Di-glycerides; 4, Sterols; 5, 1,3 Di-glycerides; 6, Free fatty acids; 7, Triglycerides; 8, Sterol esters.
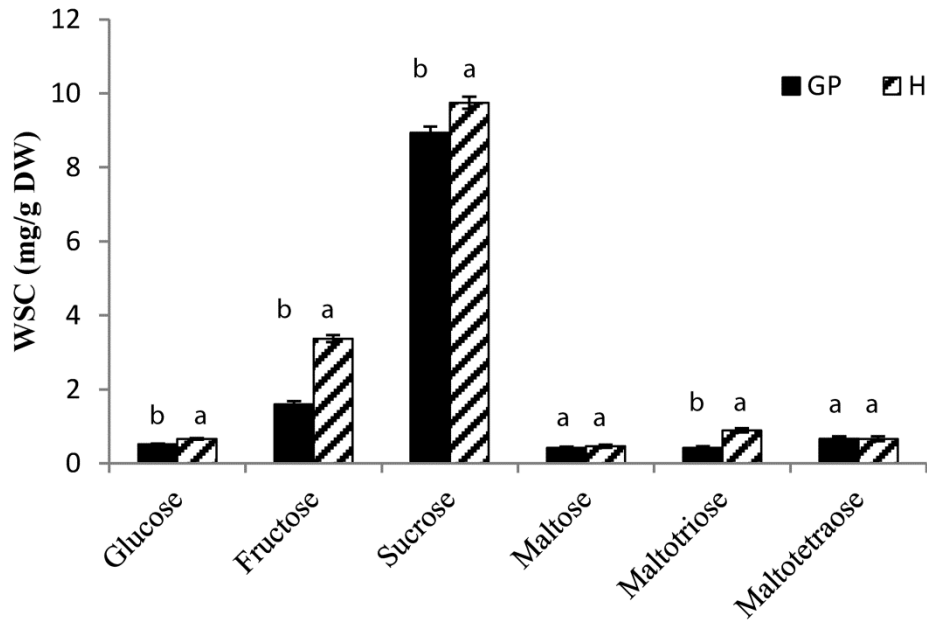
Figure 3.9. Water-soluble carbohydrates of barley grains

Y-axis represents the contents in mg/g DW, while X-axis showed the assayed components. The mean values which marked by the same letter are not significantly different at $P < 0.05$. Barley cv. Harrington is indicated with black box and cv. Golden Promise with box with upward slanting diagonal lines.

3.5. Discussion

Identifying key elements or ideal combinations of different factors in the starch synthesis process is essential for improving starch yield and quality. Many factors are involved in the starch synthesis, including various enzymes and carrier proteins that contribute to producing intermediate precursors and transporting the corresponding substrates to be used for starch biosynthesis. ADP-glucose transporter is considered a key factor in starch synthesis because of its unique function and localization. In this study, we investigated the impact of *HvBT1* and other starch synthesis-related genes on the grain yield and composition in two malting barley cultivars.

Changes in starch content of cereal grains contribute to grain weight and grain yield components (Table 1 and 2). Similar results were obtained from maize, where increasing starch content led to an increase of grain weight (Li et al. 2011). Barley grain contains ~50-60% starch that is composed of ~25% and 75% amylose and amylopectin, respectively (Li et al. 2011). Changes in starch content of cereal grains contribute to grain weight and grain yield components. Variations in the grain composition and grain yield-related traits resulted in a 2.5% higher starch in Harrington (Table 3.3), similar to increased seed weight in maize (Li et al. 2011).

A negative correlation between starch and protein was clearly observed in the present study, where Harrington accumulated higher starch and significantly lower protein content as compared to Golden Promise (Table 3.3). Such negative correlation between starch and protein content was previously reported in maize (Seebauer et al. 2010) and in barley *SS2a* mutants (Clarke et al. 2008). Decreasing amylopectin content has a great negative impact on starch yield (Morell et al. 2003). Therefore, the higher amylopectin

and low amylose content observed in Harrington was a determinant factor in increasing starch yield in this cultivar. Starch yield mainly relies on amylopectin content which represents around 70-80% of starch dry weight (Regina et al. 2010). High levels of β-glucan in Golden Promise were accompanied with high amylose content, which suggested a correlation between those two components in cereal grains (Table 3.3). Izydorczyk *et al.* (2000) reported that a positive correlation between β- glucan and amylose content was found in barley. Similar results have been reported by Caciofi et al. (2012) by suppression of all SBE genes in barley. Hang et al. (2006) reported that amylose was negatively correlated with proteins and β- glucan contents. β-glucan content in barley grains varies from 3-20% of the dry matter and depends on the genotype and environmental conditions (Aastrup and Munck, 1985; Munck et al. 2004; Aastrup, 1979; Fincher and Stone, 1986). Lipids represent 1-3% of the cereal grain and are distributed in different compartments; aleurone layer, scutella, embryo and endosperm, mainly depending on the genetic background (Morrison, 1978; Jacobsen et al. 2005). Crude lipids were significantly higher in Golden Promise, along with high amylose and lower starch content (Figure 3.8). Oppositely, sucrose and fructose were higher in Harrington than Golden Promise (Figure 3.9). The differences in grain size and plumpness, as indicated by stereoscopic analysis of barley intact and cross sectioned grains, respectively (Figure 3.7), which showed higher values in Harrington are controlled genetically (Bednarek et al. 2012) and / or environmentally (Chen et al. 2012).

Changing grain composition was genetically indicated by analysis of starch synthesis-related genes. ADP-glucose pyrophosphorylase (AGPase) is one of the limiting factors in this process, which is responsible for ADP-glucose synthesis. Higher expression of

AGPase-encoding genes for large and small subunits in Harrington (Figure 3.2) can give an indication of the efficiency of intermediate precursor's conversion. The AGPase activity in Harrington was higher at both indicated time points (Figure 3.6). Increasing the activity of AGPase helps to enhance starch accumulation and increase seed weight (Li et al,. 2001). The AGPase activity result coincides with the results obtained from the gene expression analysis. Another indicator for the efficiency of starch synthesis process in Harrington came from a higher expression level of ADP-glucose transporter *HvBT1* than in Golden Promise (Figure 3.1). HvBT1 is located in amyloplasts` membrane and mediates ADP-glucose transport from the cytosol into amyloplasts (Bowsher et al. 2007; Kirchberger et al. 2007). The position of HvBT1 and its unique function make it another possible limiting factor in starch synthesis process along with AGPase. Increasing the expression of *GBSS1a* and *b* (Figure 3.3) in Harrington may contribute to amylopectin synthesis along with the main function of amylose synthesis, which may explain the high ratio of amylopectin/amylose in Harrington. Granule-bound starch synthase (GBSS) isoforms are responsible for amylose synthesis and producing long chains of amylopectin (Shure et al. 1983; Denyer et al. 1999a; Denyer et al. 1999b). *GBSS1a* is normally expressed in the endosperm, while *GBSS1b* is expressed in the pericarp (Radchuk et al. 2009). GBSSs are exclusively located inside starch granules and act on amylopectin side-chains forming long chains (Fulton et al. 2002; Hanashiro et al. 2008). Amylopectin is synthesized by starch synthase isoforms in the plastids. Generally, starch synthases (*SSs*) in both cultivars followed the same trends and there were not many differences between these cultivars (Figure 3.4). Soluble starch synthases (*SS*) were grouped into three distinct classes; early, late and steady expressers (Hirose and Terao, 2004). Late expressed genes

include *SS1*, *SS2a* and *SS3a*, while steady expressed genes include *SS2b*, *SS3b* and *SS4*. Starch synthase genes showed differential expression patterns in both cultivars. Higher expression of AGPase genes for large and small subunits genes in Harrington, supported by the higher AGPase activity as well as the high expression of *HvBT1,* can explain increased starch content in comparison to Golden Promise.

3.6. Conclusion

The expression of the plastidial ADP-glucose transporter (*HvBT1*) in Harrington was significantly higher (almost 10 times) than in Golden Promise. The combined activities of AGPase and *HvBT1*, which generate ADP-glucose in the cytosol and transport it into amyloplasts, respectively, can help improve starch accumulation in cereal grains. Interestingly, the expression of starch synthase-encoding genes was significantly lower in Harrington, but starch content was significantly higher by 2.5% as compared to Golden Promise. This result provided a positive sign about the importance of the combination of AGPase and HvBT1 in starch synthesis. As a result of changes in starch content in barley grains, other grain components changed accordingly. β-glucan, protein and lipids showed significantly lower content in Harrington which correlate negatively with starch content. Genetic manipulation of HvBT1 by changing its expression may provide amenable opportunities to increase starch accumulation in cereal grains.

CHAPTER 4. DOWN-REGULATION OF THE PLASTIDIAL ADP-GLUCOSE TRANSPORTER (HvBT1) IMPAIRS STARCH ACCUMULATION AND ALTERS GRAIN COMPOSITION IN BARLEY.

4.1. Abstract

Down-regulation of barley plastidial ADP-glucose transporter HvBT1 resulted in negative effects on starch accumulation and composition, and concurrent changes in the grain size and grain weight. Starch decreased by 9.5% in transgenic grains as compared to those of the wild type. Also, starch composition was altered, with amylose decreased by 3.5%, and amylopectin decreased by 6%. Wild type grains were plump and well-filled, whereas transgenic grains were incompletely filled. On the other hand, protein and lipid content increased significantly in the transgenic grains. Grain yield-related traits were negatively affected by increased grain size, which led to a decreased number of grains per spike, and decreased spike length and number of spikes per plant. *HvBT1* seems to have pleotropic effects on starch synthesis-related genes such as the large and small subunits of ADP-glucose pyrophosphorylase (*AGPLs* and *AGP.Ss*), granule-bound starch synthases (*GBSSs*) and soluble Starch Synthases (*SSs*). Interestingly, *AGPLs* were down-regulated while small subunit genes, *S1b* and *S2* were up-regulated in the transgenic plants. Soluble starch synthases (*SS*) expressed differentially in the transgenic plants. *SS2a* and *SS3a* were down-regulated while, plastidial *AGPS2b* was up-regulated in the transgenic plant. HvBT1 is a key factor in starch biosynthesis process. It has negative effects on starch accumulation and composition and other grain components.

4.2. Introduction

Barley (*Hordeum vulgare L.*) is one of the oldest grain crops. Globally, it stands after maize, wheat, rice, and soybean in term of importance (Dahleen et al. 2007). In ancient times, barley was mainly used as a human food source. After the domestication of wheat and rice, its use is shifted mainly for feeding live-stocks and malting and brewing (Newman and Newman 2006). Barley products have much potential for human health. For example, β-glucan reduces blood cholesterol and glycemic index (Baik et al. 2008), and many other useful compounds found in barley grains work as antioxidants such as tocopherols and tocotrienols which reduce serum LDL cholesterol (Qureshi et al. 1991). The starch content of barley ranges between ~ 50 and ~ 60% and contains two main components, amylose (~25%) and amylopectin (~75%) (Li et al. 2011). Amylose is a linear molecule composed of α-D-glucopyranosyl units connected by (1-4) linkage, whereas, amylopectin is a branched molecule of (1-4) linked D-glucopyranosyl units connected by (1-6) linkage (Whister and Daniel, 1984). The synthesis of starch in higher plants takes place in the plastids and is catalyzed by several enzymes. ADP-glucose, the main substrate for starch synthesis, is synthesized by ADP-glucose pyrophosphorylase (EC 2.7.7.27) via catalyzing the conversion of glucose 1-phosphate using ATP to ADP-glucose. Amylose and amylopectin are formed from ADP-glucose by starch synthases (EC 2.4.1.21), starch branching (SBE, EC 2.4.1.18) and de-branching enzymes (EC 3.2.1.41 and 3.2.1.68). Multiple isoforms of these enzymes are present in the plastids of photosynthetic and non- photosynthetic tissues of higher plants (Li et al. 2011). In heterotrophic tissues of mono-cotyledonous plants, starch is synthesized via catalyzing hexose phosphate via plastidial form of AGPase in amyloplasts. Glucose 6-phosphate is

transported across the amyloplast envelops via glucose 6-phosphate/phosphate translocator (GTP) in counter-exchange with inorganic phosphate and can be used either for starch biosynthesis or for triose phosphate production (Kammerer et al. 1998).

The extra-plastidial activity of AGPase has been reported in several cereal crops and other graminaceous grasses (Beckles et al. 2001). The majority of AGPase activity in cereal crops is extra-plastidial in the endosperm (Denyer et al. 1996; Thorbjørnsen et al. 1996; Tetlow et al. 2003), in which the majority of ADP-glucose is synthesized in the cytosol and transported into the amyloplasts, where starch synthesis takes place. It has been shown, for example, the isolated amyloplasts of wheat and barley transported the exogenous ADP-glucose in and formed starch (Tetlow et al. 1994; Patron et al. 2004). As a result of the extra-plastidial activity of AGPase in the endosperm of cereal plants, the majority of ADP-glucose is synthesized in the cytosol and should be transported into amyloplasts where starch biosynthesis takes place.

In different plant species, *Brittle1* (*BT1*) homologues are members of the mitochondrial carrier family (MCF), which transport different metabolite precursors. ADP-glucose transporters have been characterized in different cereal crops and are shown to be capable of transporting ADP-glucose in counter exchange with ADP and AMP (Krishberger et al. 2007; Bowsher et al. 2007). Mutation in the *lys5* locus led to defect in ADP-glucose transport, and reduced starch accumulation. Expression analysis of the maize *BT1* gene showed that its expression exclusively localized in the endosperm (Krishberger et al. 2007). In dicotyledonous species, several BT1 homologues were characterized as nucleotide transporters including *Solanum tuberosum StBT1* and *Arabidopsis thaliana AtBT1* (Loerch et al. 2005; Kirchberger et al. 2008). The dual

function of BT1 homologues was reported, where maize ADP-glucose transporter *ZmBT1* and Arabidopsis adenine nucleotides transporter *AtBT1* were localized in chloroplasts and mitochondrial envelops (Bahaji et al. 2011).

Different techniques have been successfully implemented for barley transformation including; particle bombardment (Lemaux et al. 1994), electroporation (Gurel et al. 2000), and *Agrobacterium*-mediated transformation (Tingay et al. 1997) have been successfully used for stable barley transformation. *Agrobacterium*-mediated transformation in many crops is preferable due to the low copy number of T-DNA integrations in the genome of transgenic lines that increase the stability over generations (Shou et al. 2004). Transformation of cereal plants is a genotype-dependent, which is still a big challenge to improve traits through gene transfer in commercial cultivars (Shrawat et al. 2007). Most of the biolistic and *Agrobacterium*-mediated transformations of barley have used the model cultivars such as Golden Promise and Igri for their high callus induction and regeneration characteristics (Dahleen et al. 2007). The immature embryo has been considered as the most relevant explant that is highly responsive to tissue culture conditions. However, mature embryos axis-based explants and shoot meristematic cultures have been used for successful stable transformation in model and commercial barley cultivars (Zang et al. 1999; Sharma et al. 2005).

In cereals, improving starch yield and quality is the target of many researchers, which can be achieved by manipulating genes that are involved in ADP-glucose synthesis and transport in the endospermic cells during grain filling. Our goals in this research are investigating the impact of knocking down the barley plastidial ADP-glucose transporter HvBT1 on starch accumulation and grain composition, and investigating the impact of

the *HvBT1* expression on some genes that are involved in the starch biosynthesis pathway.

4.3. Materials and methods

4.3.1. Plant material and immature embryo isolation

Barley cv: Golden Promise was grown in the greenhouse under controlled conditions with photoperiod 16/8 and temperature 22/18 C day and night with humidity 80%. Immature barley spikes were collected after 12-14 days after anthesis (DAA) whereas; immature embryos were 1.5-2 mm in diameter. The grains were surface sterilized using 1.2% sodium hypochlorite and few drops of tween 20. The immature embryos were dissected using fine forceps (5- Inex, Invitorgen, CA, USA), to removed or disrupt embryonic axis which prevented embryo germination and increased callus induction. The extracted embryos were placed on callus induction medium (CIM) containing 4.3 g l^{-1} Murashige & Skoog salt base (Phytotechnology Lab.), 30 g/L Maltose, 1 g/L Casein hydrolysate, 350 mg/L myo-inositol, 690 mg/L proline, 1 mg/L thiamine HCl, 2.5 mg/L dicamba (Sigma-Aldrich) and 3.5 g/L phytagel (Bartlett et al. 2008) with additional 1.25 mg/L CuSO$_4$.5H2O (Cho et al. 1998).

4.3.2. Cloning of antisense HvBT1 and binary plasmid construct

Spike tissue from different time points after anthesis were collected and immediately frozen in liquid nitrogen. RNA was extracted using RNeasy Plant Mini Kit (Qiagen, Hilden, Germany). The genomic DNA was digested in column and eliminated using RNase-Free DNase I Kit (Qiagen). The purity and concentration of the RNA was

determined by visualizing on agarose gel and measuring absorbance on a Nanodrop spectrophotometer (Thermo Fisher, MA, USA). The cDNA was synthesized using Revert Aid First Strand cDNA Synthesis Kits (Fermentas). The open reading frame (ORF) was amplified using gene specific primers, which were designed based on the reported DNA sequence (NCBI: AY560327.2). The ORF was cloned in the pGEM-T-Easy plasmid and verified by sequencing (Macrogen, USA). *HvBT1* coding sequence was amplified from pGEM-T-easy plasmid using gene specific primers flanked by restriction sites for EcoR1 (Foreword, 5'-TAgaattcTCATGGTCGATCACCG-3') and Xho1 (Reverse, 5'-CGctcgagATGGCGGCGGCAAT-3'). Lowercase letters indicate restriction enzymes cutting sites. After PCR purification and digestion, the digested PCR product was cloned into the entry plasmid pENTR1A (Invitrogen, CA, USA), where the HvBT1 ORF was cloned in the opposite orientation. LR clonase reaction (Invitrogen) was performed to clone pBract 214 (John Inns Centre, UK). The LR clonase ligation procedure was performed based on the manufacturer instructions (Figure 4.1).
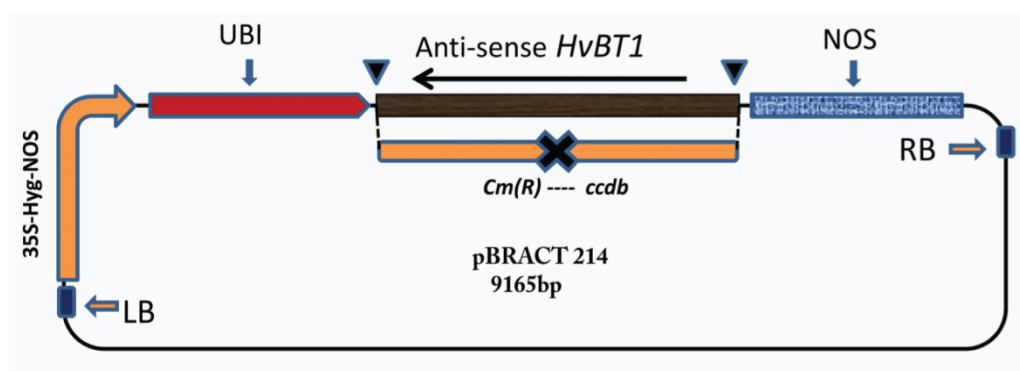
Figure 4.1. Map of pBract214::HvBT1 antisense construct

4.3.3. Agrobacterium strain and binary plasmid transformation

Agrobacterium tumefaciens AGL1 cells harboring pBract 214 vector were used in this experiment. This vector contains a hygromycin resistant gene (*hpt* gene) controlled by CaMv 35S promoter. Also, it has a negative selection marker (*ccdB*) flanked by the Gateway recombination sites to facilitate the cloning of the gene of interest. *HvBT1* is driven by maize ubiquitin promoter *Ubi1*. Bract vectors are based on pGreen and needs a helper plasmid (pSoup) to be propagated in *Agrobacterium* cells. The helper plasmid was electroporated into *Agrobacterium* cells along with the pBract vector. The two plasmids are required for successful transformation in *Agrobacterium*. One microliter from each plasmid was added to 100 µL *Agrobacterium* cells for co-electroporation using Bio-Rad Gene Pulser (2.5 kV, 25u FD, 400 ohms). The cells were transferred into new eppendorf tubes containing LB media and shaken gently at 28°C and 180 rpm for 2 hrs and then 100 µL of pre-culture was spread on LB media plates containing 50 µg/mL kanamycin and 25µg/ml rifampicin and incubated for 2-3 days at 28 C. One colony was selected and inoculated in fresh LB media to make standard culture.

4.3.4. Agrobacterium inoculation and co-cultivation

The extracted immature embryos were placed on callus induction media (CIM) scutella side up (25 embryos/plate). *Agrobacterium* cells were resuspended in diluted CIM (1:10) and used to inoculate the embryos for 2-3 hours at room temperature. Acetosyringone at final concentration of 200 µM and Silwet L77 detergent at final concentration of 0.04% were added to the *Agrobacterium* diluted culture before inoculation. Acetosyringone enhances the *vir* genes and Silwet L77 increases Ti-DNA

delivery. The embryos were co-cultivated and placed scutella side down into fresh callus induction media CIM without antibiotics for 2-3 days at 23-24°C in dark.

4.3.5. Selection of transgenic plants

After co-cultivation with *Agrobacterium* AGL1 strain, 25 immature barley embryos were plated scutella side down on callus induction media (CIM) supplemented by 50 mg/L hygromycin B and 300 mg/L timentin as *Agrobacterium* killer. The discected embryos were incubated in CIM for 3-6 weeks and the induced calli were transferred onto fresh CIM every 15 days (2 – 3 rounds). After callus induction, the embryonic callus was transferred into shoot initiation media supplemented with plant growth hormones. The shoot initiation (transition) medium contained 2.7 g/L Murashige & Skoog modified plant salt base (without NH4NO3) (PhytoTechnology Lab., USA), 20 g/L maltose, 165 mg/L NH4NO3, 750 mg/L glutamine, 100 mg/L myo-inositol, 0.4 mg/L thiamine HCl, 1.25 mg/L CuSO4.5H2O, 2.5 mg/L 2, 4 Dichlorophenoxy acetic acid (2,4-D) (Sigma-Aldrich), 0.1 mg/L 6-Benzylaminopurine (BAP), 3.5 g/L Phytagel (Sigma-Aldrich), 50 mg/L hygromycin (PhytoTechnology Lab, USA) and 160 mg/L timentin (PhytoTechnology Lab, USA). The embryonic calli were incubated in dim light on the transition media for 3-4 weeks to form shoots. After shoot formation, plantlets were transferred into regeneration media. Regeneration media is CIM media including 50 mg/L hygromycin B and 200 mg/L timentin but without growth regulators. The regenerated plants were incubated in full light at 24°C until the plants reached 2-3 cm in length and had good root systems, then transferred to the soil and grown under the same condition as the parent plants (Harwood et al. 2009).

4.3.6. PCR analysis of transgenic lines

Genomic DNA of transgenic barley lines was extracted using CTAB method (Murray and Thompson, 1980) and used for PCR amplification. Two sets of primers were used to examine the transgenic lines. The *hpt* gene (*aphIV*) primers (forward: 5'-ACTCACCGCGACGTCTGTCG-3'; reverse: 5'-GCGCGTCTGCTGCTCCATA-3') were used for PCR amplification of a 927 bp to confirm the integration of the *hpt* gene in the regenerated lines. A second PCR reaction was conducted with primers to examine the *HvBT1* (HvBT1 R-5' TCATGGTCGATCACCGTTG-3') and the vector backbone (Nos-Term R 5'-TGATATCAGCTTGCATGCCGGTC-3') presence in the genome. The amplicon size is ~ 1800 bp. Phusion High-Fidelity DNA Polymerase (Fermentas) was used for this assay. The polymerase chain reaction was performed according to the manufacturer procedures. Genomic DNA samples from barley wild type and transformed lines were used at a concentration of 50-100 ng/50 μL PCR reaction volume.

4.3.7. Northern blot analysis

Northern blot analysis was performed on total RNA from immature barley grains at 10 DAA. Total RNA (10 μg) was separated on 1% agarose formaldehyde gel and transferred by capillary system onto Hybond-NI membranes (Amersham Bio-sciences) and fixed by UV cross-linking according to the standard protocol. The probe was prepared using DIG-labeling Kit (Roche). Briefly, 400 bp fragment of *HvBT1* cDNA was amplified and cloned in pGEM-T-Easy plasmid (Promega), then amplified using M13 forward and reverse primers which are located in the upstream and downstream of T7 and SP6 promoter regions, respectively. The PCR products were used as templates for T7 RNA polymerase reaction to produce antisense RNA probe. The procedures were performed

according to DIG Northern Starter Kit (Roche Applied Science, Mannheim, Germany). After hybridization with RNA probe, the chemiluminescent signal of alkaline phosphatase was generated and detected using CDP-Star reagent and developed on X-ray film.

4.3.8. Grain morphology and cross section

Immature caryopsis harvested at 14 DAA, mature whole grains, mature grain cross sections and dissected mature embryos were examined by stereoscopic microscope and photographed (Li et al. 2011). Mature grains from individual transgenic lines and wild type were assayed for seed area, seed length and seed width using *Assess 2.0* Image Analysis Software (Lamari, 2008). Thirty five grains from three transgenic lines and wild type seed area, seed length and seed width were analyzed using *Assess 2.0*. The measurement was replicated three times.

4.3.9. Analysis of grain composition

Analysis of starch and grain composition was performed on T2 grains from different individual transgenic lines and the wild type control. Three biological sets of grains from each line including the wild type was used for total starch analysis, amylose / amylopectin, β-glucan and total protein content.

4.3.9.1. Starch content

Barley grains were ground in a mill grinder (Retsch 0.5 mm at 14,000 rpm). Total starch content was assayed using AOAC Method 996.11/AACC Method 76.13 kit (Megazyme International Ltd., Wicklow, Ireland). The assay was performed with 100 mg

whole meal and extraction procedures were performed according to the manufacturer's instructions.

4.3.9.2. Amylose content

Amylose content was assayed using K-AMYL 07/11 kit (Megazyme International Ltd., Wicklow, Ireland). The assay was performed with 20 − 25 mg sample weight. Three biological samples from each line and three technical replicates for each were used in this assay.

4.3.9.3. Protein content

The total protein content was determined in different transgenic lines along with wild type mature grains based on total nitrogen content using a combustion nitrogen analyzer (Leco FP − 528, Nitrogen/Protein Determinator Corporation, St. Joseph, Mich). The nitrogen was converted to protein by multiplying the obtained nitrogen values by a factor of 6.25.

4.3.9.4. β-glucan content

β-glucan content was determined with whole meal using K-BGLU kit (Megazyme International Ltd., Wicklow, Ireland). The assay was performed on three biological samples from each line with three technical replicates.

4.3.9.5. Lipids extraction and thin layer chromatography

Lipids were extracted and quantified from barley whole meal (1 g) of wild type and transgenic lines using gravimetric method after extraction with chloroform-methanol

mixture. The procedures were performed according to Phillips et al. (1997). Thin layer chromatography (TLC) was performed by applying 10 µL of total lipid extracts on silica gel (AL SIL G, plate size 20x20 cm with 0.25 mm thickness, Whatman) according to Mangold and Malins, (1960) and Mangold, (1961) and separated by petroleum ether :diethyl ether : glacial acidic acid (80:20:1, v:v:v) according to Kates, (1972). Lipid fractions were visualized using iodine vapor. The lipid fractions were identified by comparing RF values to published RF values of lipid standards.

4.3.9.6. Water-soluble carbohydrate content

Water-soluble carbohydrates were extracted according to Yemm and Willis, (1954) with some modification made by Clarke et al. (2008). In brief, 100 mg of barley whole meal was extracted in 10 mL 80% ethanol by boiling in water bath for 10 min. The extraction was performed three times and the supernatant pooled and freeze dried. The carbohydrates were re-suspended in 1 mL milliQ water and carbohydrate sugars were quantified using HPAEC according to Ruuska et al. (2006).

4.3.10. Analysis of grain yield parameters

Number of spikes per plant, single grain weight, number of grains per spike, spike length, hundred grains weight and total grain weight per plant were assayed in wild type and transgenic lines to assess yield component parameters.

4.3.11. Quantitative qRT-PCR of starch synthesis related genes

Total RNA was extracted from barley heads at 8 and 12 DAA as previously described. The first strand DNA was synthesized using Revert Aid First Strand cDNA Synthesis

Kits (Fermentas). Quantitative Real-Time PCR was conducted using a CFX96 Thermal Cycler (Bio-Rad) and Sso Fast Eva Green Supermix (Bio-Rad) according to the manufacturer's instructions. Actin was used as an internal control to normalize qRT-PCR. The qRT-PCR was assayed on cDNA with 4 ng/μL final volume. The selected genes accession numbers and primer sequences are shown in (Chapter 2 Table 2.1). The qRT-PCR results were analyzed using $2^{-\Delta\Delta C_t}$ method (Livak and Schmittgen, 2001).

4.3.12. Starch granule morphology

The morphology of starch granules was tested by Scanning Electron Microscope (SEM). Barley flour was sprinkled onto double sided sticky tape on circular aluminum stubs and coated by gold. Starch granules were photographed by SEM (Cambridge S120).

4.3.13. Statistical analysis

Analysis of variance was performed using Proc GLM SAS 9.2 (SAS Institute Inc., USA) to determine the significance between wild type and transgenic lines parameters

4.4. Results

4.4.1. Generation and characterization of transgenic barley plants

To investigate the impact of down-regulation of HvBT1 on starch accumulation and composition, an antisense approach was implemented using the maize ubiquitin promoter to drive the expression of the antisense *HvBT1* in barley. The transgenic plants were selected on hygromycin selective media (50μg/mL). Seven individual transgenic lines

were generated successfully and assayed for transgene integration with PCR and northern blot analysis. Our PCR analysis with the hygromycin specific primers generated amplicon size of 920 bp in the transgenic lines and no amplification was detected in the wild type (Figure 4.2A).

A subsequent PCR reaction was further performed using primers specific to the vector backbone (NOS terminator region) and the transgene, resulting in a specific band with amplicon size of ~ 1800 bp in the transgenic lines but not in the wild type. In addition, the northern blot analysis showed the presence of strong signals in the wild type (Figure 4.1B), while weak signals were detected in the transgenic lines (Lane 1-7). The signal intensity in the transgenic lines was ~ 10 % of the signal intensity detected in wild type RNA (Figure 4.2B).
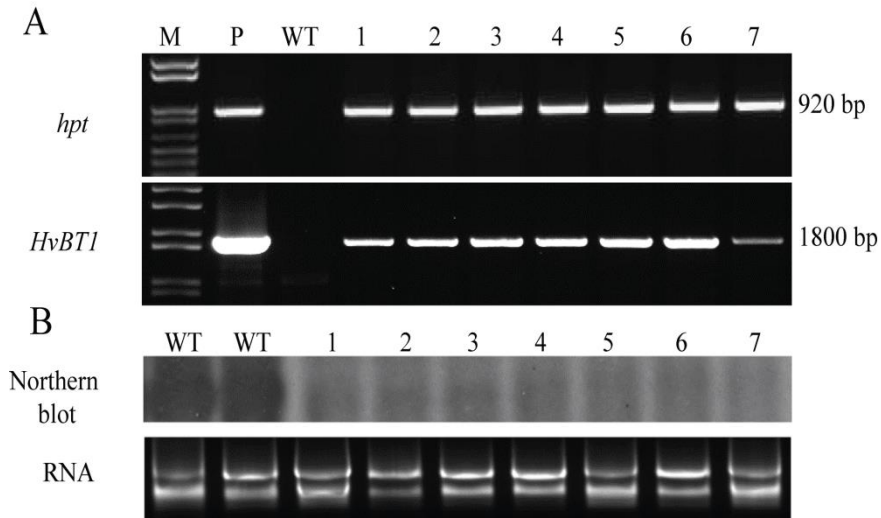
Figure 4.2. PCR and northern blot analysis of barley lines.

PCR was performed on barley genomic DNA from different transgenic lines and wild type control using hygromycin resistant gene *hpt* specific primers which produced 920 bp, while amplicon of 1800 bp was produced using NOS terminator primer with *HvBT1* specific primer (**A**), M, DNA marker; P, plasmid; WT, wild type; 1-7, transgenic lines. Northern blot analysis was performed on total RNA from different transgenic and wild type lines. The antisense *HvBT1* RNA probe was used for hybridization (**B**). Barley transgenic lines produced a weak signal ~ 10% of the wild type control. Almost equal total RNA quantities were run on the gel.

4.4.2. Grain morphology and cross- section

Length, width and area of three transgenic lines and wild type control mature grains were assessed by *Assess 2.0* (Lamari, 2008). Transgenic grains showed significant increase in length and subsequently in grain area as compared to wild type grains (Figure 4.3A1). Mature grains from transgenic and wild type plants were examined by stereoscopic microscopy for both dorsal and crease sides, as well as the whole caryopsis

(Figure 4.3B1 and 7). Both mature and immature grains showed differences in the grain length and area during grain filling and after maturity. The wild type produced short, plump and well-filled grains, while transgenic lines produced long and incomplete grains (Figure 4.3 B1 and 3). This result coincides with the cross-section of the grains (Figure 4.3 B2 and 4) which showed well-filled endosperm in the wild type grains as compared to incomplete endosperm in the transgenic grains. The dissected mature embryos from transgenic grains were bigger in size than wild type control (Figure 4.3 B 5 and 6).
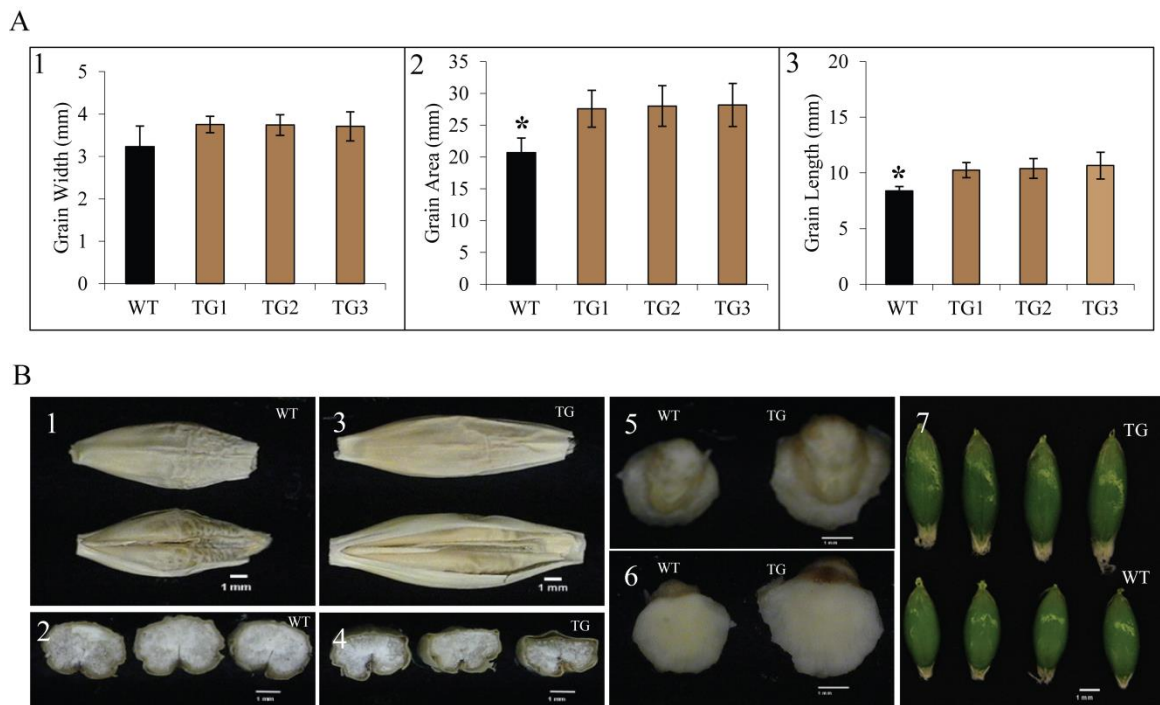
Figure 4.3. Grain morphology and cross-section.

Barley grain morphology was assessed by *Assess 2.0* for grain width for Golden Promise (WT) and transgenic (TG) lines. **A1**, area; **A2**, and length (**A3**). Stereoscopic examination of mature and immature grains is shown in **B1**, **B3** and **B7**. Plumpness of wild type and transgenic grains is shown in **B2** and **B4**, respectively. Embryo size variation is shown in the dissected embryos (**B5** and **B6**).

4.4.3. Grain composition

4.4.3.1. Starch content

Starch content was measured as a percentage of seed dry weight in three transgenic lines as well as in the wild type. Our results show that the total starch content in the seeds of the three transgenic lines averaged 44.28% of the seed dry weight, while in the wild type, it accounted for 53.27%. Starch content was significantly lower by ~ 9% DW, which represents 17% less starch in the transgenic grains as compared to the wild type control. There were no significant differences among the transgenic lines in terms of total starch content (Table 4.1).

4.4.3.2. Amylose/amyloplectin content

Comparison of the amylose content between the seeds of the transgenic lines and wild type showed significant difference. The transgenic lines contained 5.3% less amylose than the wild type (Table 4.1). Amylopectin content in the grains of the transgenic lines averaged ~ 2% lower than the wild type grains. No significant difference in amylose content was detected among the three transgenic lines.

4.4.3.3. β-glucan content

The transgenic lines accumulated significantly lower amounts of β-glucan (~ 3.48% of grain dry weight) than the wild type (~5.56% of the seed dry weight), resulting in about 2% reduction in the transgenic grains, which represents 37% less β-glucan in transgenic lines compared to the wild type (Table 4.1). There were no significant differences in β-glucan among the three different transgenic lines.

Table 4.1. Grain composition

	Total starch (%)[b]	Amylose (%)	Amylopectin (%)	Protein (%)[c]	β- glucan (%)[d]
Wild type	53.27± 1.3[a]	27.6±0.14[a]	72.4±0.15[a]	15.29±0.21[a]	5.56±0.28[a]
TG1	44.31± 0.83[b]	26±0.15[b]	74±0.15[b]	19.93±0.52[b]	3.43±0.18[b]
TG2	43.85± 0.7[b]	25.9±0.14[b]	74.1±0.15[b]	19.44±0.37[b]	3.52±0.05[b]
TG3	44.7± 1.3[b]	26.5±0.12[b]	73.5±0.12[b]	18.44±0.36[c]	3.48±0.14[b]

[a]Moisture content ~ 9-10% and the percentage of the components based on the total weight used for the assay (100 mg). Wild type control is cultivar Golden Promise, TG represents the transgenic line.
[b]Total starch, amylose and amylopectin were measured in the whole meal and are represented as %, which represents the amount in mg per 100 mg dry weight.
[c]Protein values were obtained by multiplying the obtained nitrogen value by a factor of 6.25.

4.4.3.4. Protein content

Comparison of the protein content of three transgenic lines and wild type grains showed that the protein level in the transgenic lines accounted for 19.27% of the seed dry weight, compared to 15.29% in the wild type, resulting in a statistically significant difference in protein content between transgenic and wild type lines. Total protein content was on average 4-5% higher in the transgenic grains than the wild type control (Table 4.1).

4.4.3.5. Lipids content

Quantification of total lipids in the grains of transgenic and wild type plants showed that the transgenic grains accumulated significantly higher quantities of lipids than the wild type control. The transgenic grains contained ~ 88 mg/g DW, while the wild type control contained 65 mg/g DW (Figure 4.4A), which represents ~35% higher lipids in transgenic grains. The gravimetric method used for this quantification seems to overestimate lipid content in the dry matter. Analysis of the lipid extracts with Thin Layer Chromatography (TLC) indicated that the seeds of the transgenic lines

accumulated more free fatty acid (spot 6), while the seeds of the wild type contained slightly more triglycerides (Figure 4.4B).
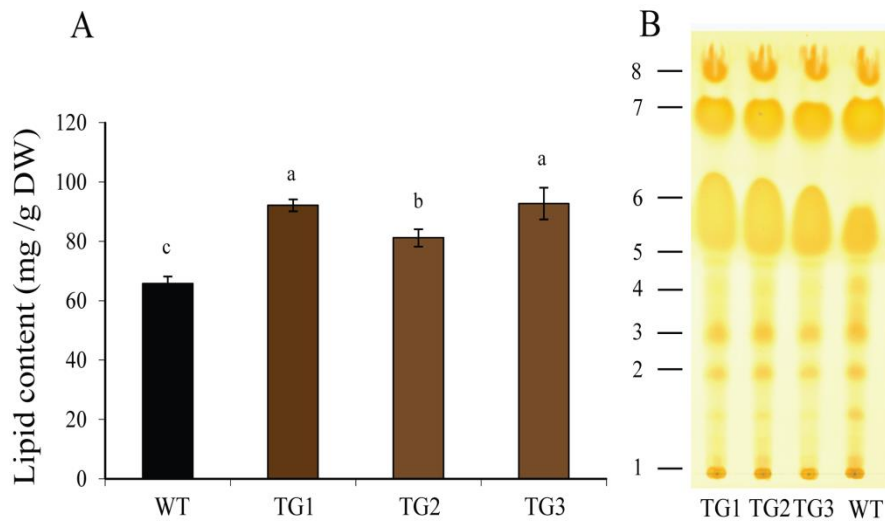
Figure 4.4. Total lipids content and thin layer chromatography (TLC).

Total lipid content was assayed from barley wild type (WT) and transgenic lines (TG) using the gravimetric method (**A**). A volume of 10 μL from different lines was separated on silica gel plate and visualized by iodine vapor (**B**). Spots are marked with number on the left side of the gel. 1, Polar lipids; 2, Mono-glycerides; 3, 1,2 & 2,3 Di-glycerides; 4, Sterols; 5, 1,3 Di-glycerides; 6, Free fatty acids; 7, Triglycerides; 8, Sterol esters.

4.4.3.6. Water soluble carbohydrate (WSC)

Water soluble carbohydrate composition of the mature grains of wild type and transgenic lines were measured by High Performance Anion Exchange Chromatography (HPAEC). Glucose and fructose were significantly higher in the transgenic lines than in the wild type, while there was no significant difference in maltose content between the

two samples. The content of sucrose decreased significantly in the seeds of the transgenic lines to wild type control. Oligosaccharides also showed significant differences, for example, maltotetraose was lower in the transgenic lines than that found in the wild type (Figure 4.5).
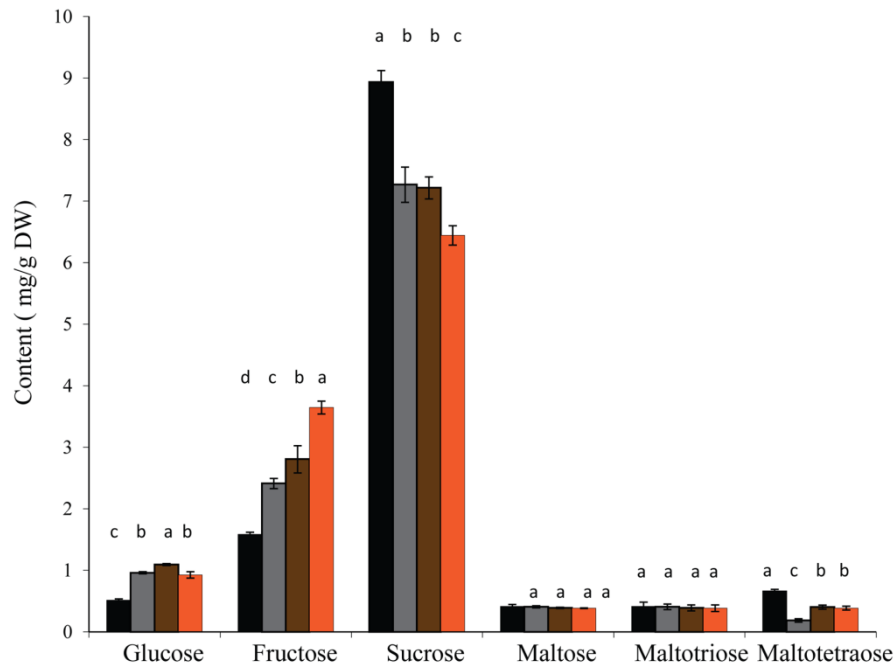
Figure 4.5. Quantification of water-soluble carbohydrates in barley grain.

Y-axis represents the contents in mg/g DW, while X-axis showed the assayed components. The letters on standard error bars are based on the LSD. The mean values which marked by the same letter are not statistically significant, while the mean values which marked by different letters are significantly different at $P < 0.05$. Barley lines assayed are; wild type (black bars), TG1 (Gray bars), TG2 (Brown bars), TG3 (Orange bars).

4.4.4. Starch granule morphology

Starch granule morphology was examined by Scanning Electron Microscope (SEM) in transgenic and wild type cross-sectioned grains (Figure 4.6). Variations in the size of starch granules were detected between transgenic and wild type starch. Wild type starch granules are smaller in size than those obtained from the transgenic lines. Granule sizes in the starch of the transgenic lines were variable in size (Figure 4.6 C,D), while in the wild type, starch granules were similar (Figure 4.6 A,B). There was no difference in the shapes of starch granules observed between the two lines.
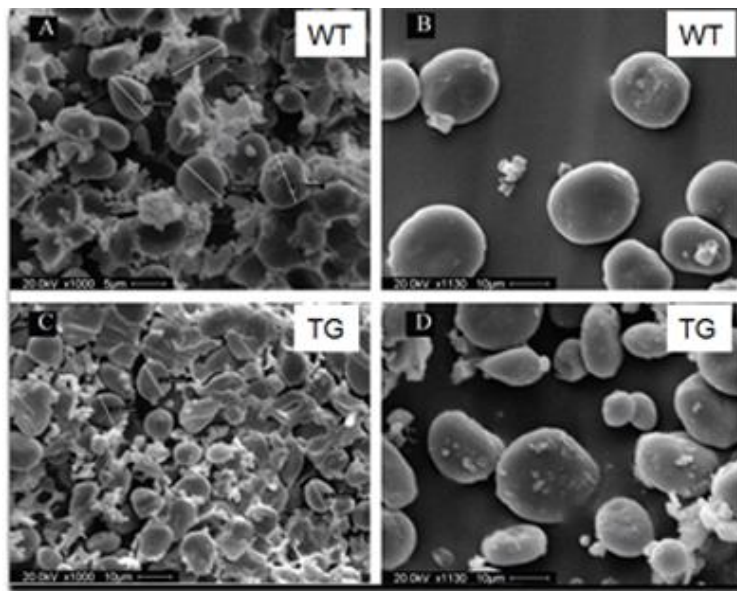
Figure 4.6. Starch granule morphology.

Barley grain cross-sections and purified starch of wild type (WT) and transgenic lines (TG) were subjected to SEM. **A**, wild type grain cross section; **B**, wild type purified starch; **C**, transgenic grain cross-section; **D**, transgenic purified starch. Starch granule diameter is shown with straight lines across starch granules with values. Scale bars are shown at the bottom of the images.

4.4.5. Grain yield parameters

Different grain yield related traits were assayed in the present study. Single grain weight was significantly increased in transgenic lines as compared to wild type. As a result of increasing the average single grain weight, a hundred grain weight significantly increased in transgenic lines. Compared to wild type, the number of spikes per plant, spike length and number of grains per spike decreased significantly in the transgenic lines. Subsequently, total grain yield per plant also significantly lower by ~ 30% in the transgenic lines as compared to the wild type control (Figure 4.7).

4.4.6. Expression of starch biosynthesis-related genes

Expression of starch biosynthesis related genes was analyzed by qRT-PCR in both wild type and transgenic plants at 8 and 12 DAA. Our results showed that AGPase large subunits genes (*AGPL*) were down-regulated in the transgenic lines as compared to the wild type at both stages analyzed (Figure 4.8A, B). The AGPase small subunits genes (*AGPS*) showed different expression pattern. *AGPS1b* and *S2* were up-regulated in the transgenic lines (Figure 4.8D, E), while *AGPS1a* gene showed no significant changes in its expression between the wild type and transgenic samples (Figure 4.8C).

Granule-bound starch synthase genes (*GBSS*) expressed differently in the wild type and transgenic plants (Figure 9). The expression of *GBSS1a* was significantly down-regulated in the transgenic samples as compared to the wild type (Figure 4.9A). *GBSS1b* was significantly up-regulated in the transgenic lines when compared to wild type samples in both stages (Figure 4.9B).
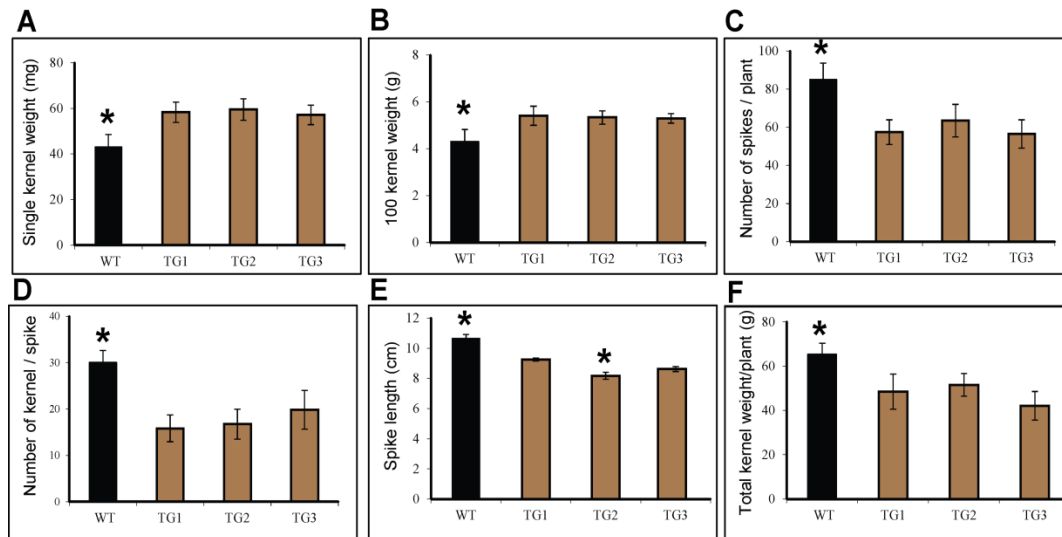
Figure 4.7. Grain yield-related traits of barley wild type and transgenic lines.

The mean values of the tested traits are shown in columns with standard error bars. The mean values which marked by asterisk star is statistically significant at $P < 0.05$. The Y-axes represented the tested parameters, while the X-axes represented the barley lines. The wild type (WT) was shown by black bars and transgenic lines (TG) by brown bars.

Soluble starch synthase genes (*SS*) showed variation in their expression patterns (Figure 4.10). The transgenic line showed stable expression of SS1 in both time points, but significantly higher at 8 DAA, while no significant difference was observed at 12 DAA. Interestingly, *SS2a* and *SS2b* were expressed differently in both stages as compared to wild type. In the transgenic plant, the expression of *SS2a* was significantly lower, while *SS2b* was significantly higher as compared to the wild type. In addition, transcripts of *SS3a* in the transgenic line were hardly detected at both stages, while *SS3b* showed no significant differences with the wild type at both stages. *SS4* showed stable expression at both stages, and showed lower expression at 8 DAA in the transgenic line than the wild type, while the expression at 12 DAA remained at the same level (Figure 4.10).
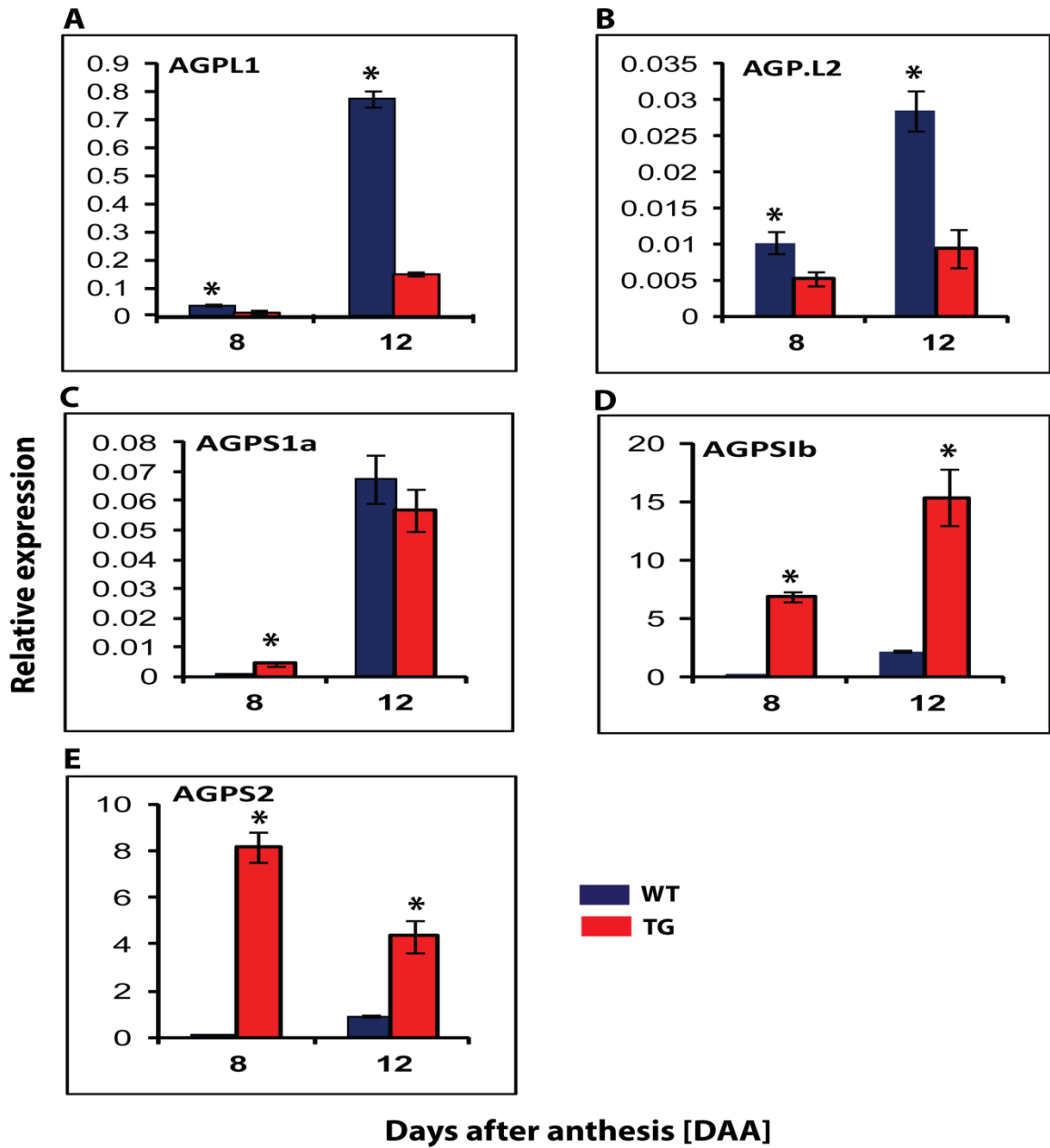
Figure 4.8.. Expression analysis of ADP-glucose pyrophosphorylase genes.

Barley wild type expression is represented in the graphs by blue bars with standard error bars, while expression of transgenic line is presented by red bars with standard error bars. **A**, *AGPL1*; **B**, *AGPL2*; **C**, *AGPS1a*; **D,** *AGPS1b*, and **E**, *AGPS2*. The mean of the fold change values which marked asterisk star is significant at $P < 0.05$.
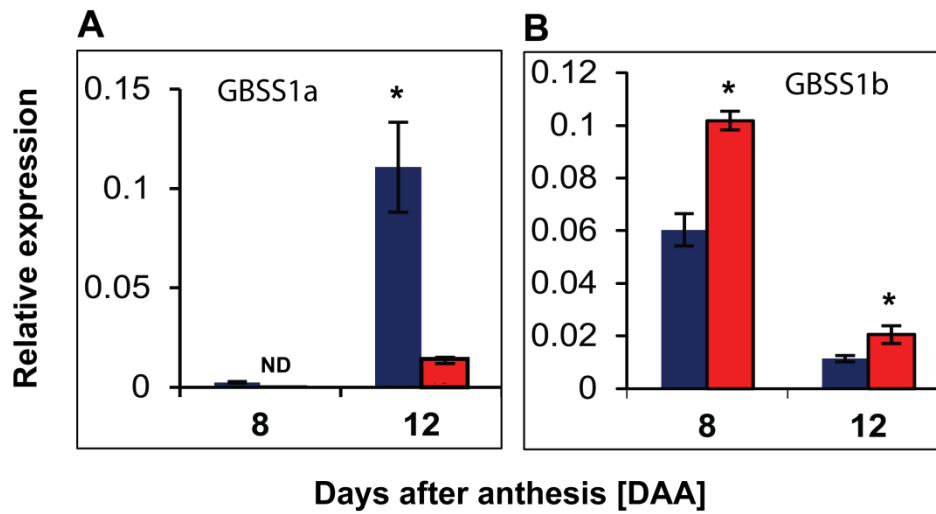
Figure 4.9. Expression analysis of granule-bound starch synthase genes.

The mean values of the fold change are presented with standard error bars. Blue bars represent wild type, while red bars represent transgenic lines. The mean values which marked by asterisk star is statistically significant at $P < 0.05$. **A**, *GBSS1a*; **B**, *GBSS1b*.
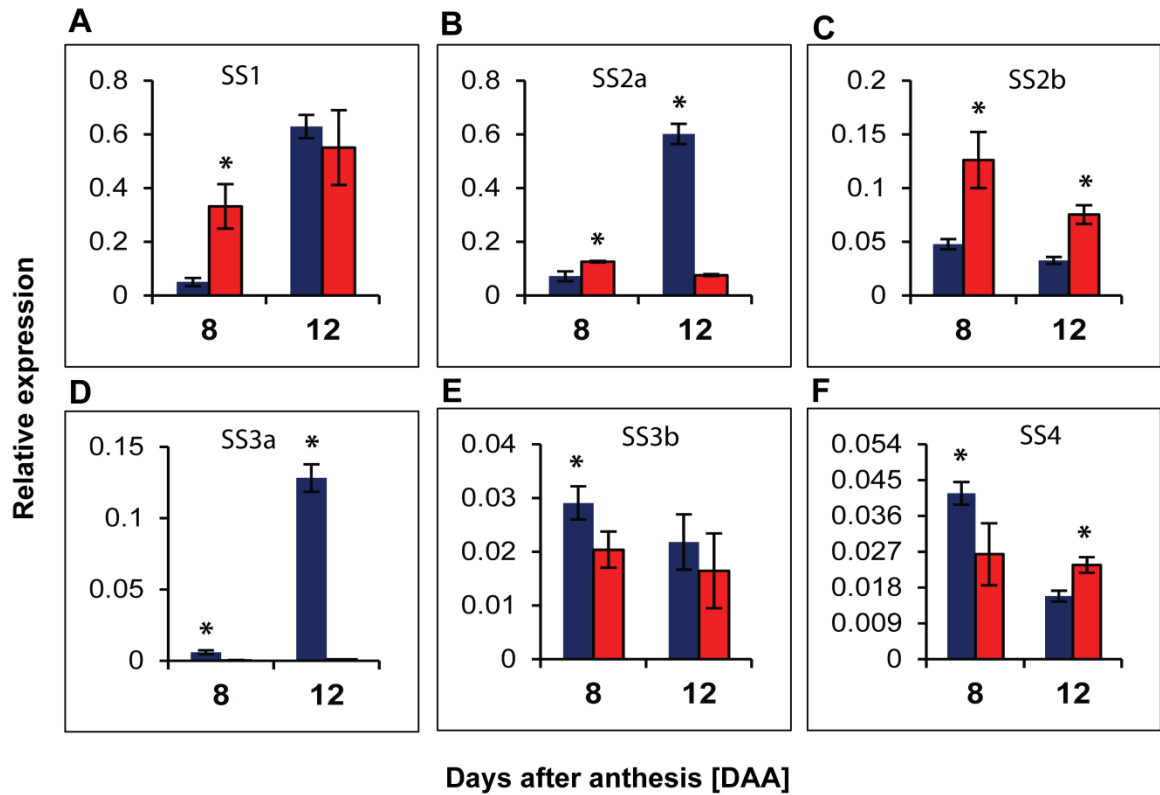
Figure 4.10. Expression analysis of soluble starch synthase (SS) genes.

Barley wild type expression is represented in the graph by blue bars with standard error bars, while expression of transgenic line is represented by red bars with standard error bars. **A**, *SS1*; **B**, *SS2a*; **C**, *SS2b*; **D,** *SS3a*; **E**, *SS3b* and **F**, *SS4*. The mean values of the fold change which marked by asterisk star is significant at $P < 0.05$.

4.5. Discussion

The barley plastidial ADP-glucose transporter HvBT1 is encoded by a single gene forming one polypeptide chain. This gives the gene an advantage for further manipulation, such as plant transformation, in comparison to complex proteins that are encoded by multi-genes such as ADP-glucose pyrophosphorylase (AGPase). Identifying such key elements in the starch synthesis process as HvBT1, is essential for understanding the rhythm of starch accumulation, and provides clues about possible ways to improve the yield and quality of the starch for particular end uses.

Down-regulation of HvBT1 results in changes in the barley grain's physical and yield parameters. Changes in the grain size, represented by the alterations in the grain length and area (Figure 4.2 A2,3) were observed in the transgenic lines, while the grain width for both mature and immature grains remains similar to those of the wild type lines (Figure 4.2 B1, 2 and 7). Cross-sectioned grains (Figure 4.2 B2 and 4) also provided inside view of the changes of the endospermic portion in the grains, where showed the well-filled plump of wild type grains and incomplete grains in the transgenic lines. The level of water-soluble carbohydrates, especially glucose and fructose, was elevated in the transgenic grains, while that of sucrose decreased (Figure 4.4). This alteration in grain carbohydrates composition might explain the increase in grain size in the transgenic lines. Metabolic sugars play an important role in expanding the endospermic cells during grain filling, where sugar alcohol and monosaccharaides have a major effect on the osmotic pressure in the cell (Wang and Stuutte, 1992; Boldingh et al. 2000). It has been shown previously that a high hexose to sucrose ratio promotes cell division and expansion through glucose signalling, while high sucrose to hexose ratio promotes differentiation

and storage (Wobus and Weber 1999). This might explain the negative effect of HvBT1 suppression on the number of grains per spike and overall yield. In addition, increasing starch granule size might be a result of decreasing starch content in the transgenic lines (Figure 4.5). Similar results were reported on Arabidopsis mutant lacking the activity of starch synthase IV (SSIV) type that showed decrease numbers of starch granules per plastid, and oppositely, increasing starch granule size (Roldán et al. 2007).

In contrast to that observed with grain size, the suppression of HvBT1 had a negative effect on the number of spikes per plant, number of grains per spike and total grain yield per plant (Figure 4.6), leading to a negative correlation between grain size and number of grains per spike. Negative correlations between grain size and number of grains per ear have been also shown in other cereals such as sorghum and maize (Kiniry 1988; Kiniry et al. 1990). Alteration of the storage reserve in the grain of the transgenic lines is associated with changes in grain weight. The level of lipids showed an increase in the transgenic lines, and this may contribute to an increase the grain weight (Figure 4.3). As the major amount of lipids is present in the embryo (Price and Parsons, 1979), the increase of lipids in the transgenic grains might be due to an increase in embryo size (Figure 4.2 B 5 and6). On the other hand, the endosperm is the major part of the cereal grain, which contains mainly starch. Expressing the antisense of *HvBT1* led to 17% lower starch yield in the transgenic mature grains (Table 4.1). This could be a result of reducing the activity of HvBT1, subsequently reduced loading of ADP-glucose to the amyloplasts. HvBT1 has a crucial role in starch synthesis process as demonstrated by the reduction of starch accumulation in the barley mutant RisØ13 which carried mutated *HvBT1* (Patron

et al. 2004). This mutation is caused by a base substitution that led to substitution of GLU for VAL. The majority of AGPase activity was reported as cytosolic in storage organs of different cereal plants, including wheat, maize, rice and barley (Tetlow et al. 2003; Hylton and Smith 1992; Denyer et al. 1996). As a result of this activity, the majority of ADP-glucose is synthesized in the cytosol of the endosperm and must be transferred to amyloplasts where starch is synthesized. Down-regulation of HvBT1 decreased loading of ADP-glucose to amyloplasts. As a result of down-regulation of HvBT1, amylose content decreased by approximately 5.3%, while amylopectin increased by 2% in transgenic grains (Table 4.1). At a low level of loading ADP-glucose, the starch biosynthesis process was negatively affected which appeared as low starch yield and altered starch composition.

β- glucan, a soluble non-starch polysaccharide, is found in cereal grains such as oats and barley (Talati et al. 2009). Endospermic cell walls contain 75% of total β- glucan content in the grains of barley (Fincher and Stone 1986). Down-regulation of HvBT1 resulted in 37% lower in β-glucan content (Table 4.1), which normally represents 3-7% of total grain dry weight (Aman and Graham, 1987; Bhatty et al. 1990). β-glucan content is positively correlated to amylose content. Significant differences in β-glucan content were observed in different barley genotypes that showed differences in their amylose content. High β-glucan content was accompanied with high amylose content (Izydorczyk et al. 2000). Similar results have been reported by Carciofi et al. (2012), where all SBE genes in barley were suppressed and knockdown grains showed higher in β-glucan

content than the wild type control. Changes in β-glucan content might contribute to grain weight.

The higher protein content (Table 4.1) of the transgenic grains indicates the effect of HvBT1 suppression on starch level in the endospermic cells. This demonstrates a negative correlation between starch and protein content which has been reported in other cereals. For example, a study on two inbred lines of maize showed the association of high protein content with low starch and high kernel weight (Seebauer et al. 2010). A mutation in starch synthase 2a (*SS2a*) in barley decreased starch content, and consequently protein content was increased (Clarke et al. 2008). In our study, the high protein content in the transgenic lines was accompanied with low starch content that demonstrates the negative correlation between starch and protein content in barley grains.

ADP-glucose transporter had pleotropic effects on starch synthesis-related genes. Changes were observed in the expression patterns of these genes in the wild type and transgenic lines. AGPLSU regulates the response to inducers (3-PGA) and inhibitors (Pi) as regulatory subunits, while AGPSSUs are responsible for the enzymatic catalytic activity (Tetlow et al. 2004; Ballicora et al. 2005; Geigenberger et al. 2005). Reduction of the expression of *AGPLs* (Figure 4.7A and B) might indicate the decrease of AGP-glucose synthesis. Increasing the expression of the plastidial *AGPS1b* and *AGPS2* (Figure 4.7D and E) might compensate the reduction of ADP-glucose synthesis in the cytosol. Previous studies reported that *AGPS1a* encodes for the cytosolic AGPSSU, while *AGPS1b* and *AGPS2* encode for the plastidial AGPSSU (Johnson et al. 2003;

Thorbjørnsen et al. 1996; Rösti et al. 2006). Enhancing the expression of both plastidial *AGPS1b* and *AGPS2* may be correlated to the reduction of cytosolic AGPase activity. The cytosolic AGPase activity in cereal plants represents around 85-95% of the total activity in the endosperm, while a small portion of the activity is plastidial (Tetlow et al. 2003).Then, increasing the expression levels of the plastidial *AGPS1b* and *AGPS2* gave an indication of increasing the activity of plastidial AGPase form, which is an alternative way to synthesize ADP-glucose in the plastids.

Changes in the expression of *GBSSs* (Figure 4.8) provided an indication about amylose synthesis and content in grains. Decreasing the expression of *GBSS1a* (hardly detected) which mainly expressed in the endosperm at late stages of grain filling might contribute to decrease the amylose content in the transgenic grains (Figure 4.8 A). Up-regulation of *GBSS1b* (Figure 4.8 B), mainly expressed in the pericarp only at early stages of grain filling (Radchuk et al. 2009), might compensate some loss of the *GBSS1a* expression. Down-regulation of *GBSS1a* might contribute to the reduction in amylose content in the transgenic lines and consequently on starch yield.

Decreasing the expression levels of *SS2a* and *SS3a* (Figure 4.9 B and D) in the transgenic plant might contribute to the reduction in total starch content in the transgenic lines by reducing long and very long chains of amylopectin, respectively. *SS2a* mutant in barley accumulate less starch and high amylose, while amylopectin deceased by 20% of wild type control (Morell et al. 2003; Clarke et al. 2008; Li et al. 2011). Down regulation of *SS2a* led to decrease levels of longer glucan chains of DP 12-35 (Yamamori et al.

2000; Konik-Rose et al. 2007). *SS3a* mutants of barley and rice showed reduction in amylopectin content by reducing the proportion of very long glucan chains and increased amylose content (Fujita et al. 2007; Clarke et al. 2008).

4.6. Conclusion

In this research, we showed that down-regulation of barley plastidial ADP-glucose transporter (HvBT1) has a significant negative impact on starch yield and composition. This was observed by analysis of total starch and amylose content in different transgenic lines compared to wild type. Also, down-regulation of HvBT1 has a negative impact on β-glucan content, which may be correlated to a reduction in amylose content. A negative correlation between starch and protein content was confirmed by 4-5 % increased protein content in transgenic lines, which accumulated ~ 9% less starch. Increased lipid content and water-soluble carbohydrates in the transgenic grains also gave an indication of deficiency in the conversion of sugar metabolites during starch synthesis. We investigated changes in the expression profile of starch biosynthesis genes, especially those involved in amylose and amylopectin synthesis. Phenotypic data also revealed the negative impact on spike characteristics and overall the grain yield.

CHAPTER 5: SUMMARY AND CONCLUSIONS

Barley is one of the oldest grain crops and globally stands after maize, wheat, rice, and soybean in term of importance (Dahleen et al. 2007). In ancient times, barley was mainly used as a human food source. After the domestication of wheat and rice, its use has shifted to mainly feeding live-stocks, malting, and brewing (Newman and Newman, 2006), although barley products have much potential for human health. For example, β-glucan reduces blood cholesterol and the glycemic index (Baik et al. 2008), and many compounds found in barley grains work as antioxidants, i.e., tocopherols and tocotrienols, which reduce serum LDL cholesterol (Qureshi et al. 1991).

We investigated the role of the plastidial ADP-glucose transporter in barley for its impact on the starch biosynthesis process. The study started by characterization of the ADP-glucose transporter HvBT1 using an *E. coli* expression system, and investigated its expression profile and localization in barley grains. The second objective in our study was to investigate the impact of *HvBT1* expression on starch accumulation in two barley cultivars; Harrington and Golden Promise, by evaluating the grain yield and composition, along with the expression analysis of some starch biosynthesis-related genes. The third objective was to investigate the impact of down-regulation of HvBT1 on starch accumulation in Golden Promise using the antisense approach. Our findings are summarized as follows:

We have successfully characterized the barley plastidial ADP-glucose transporter (HvBT1) biochemically using an *E. coli* expression system, and we explored its relationship to other brittle 1 (BT1) homologues from mono and dicotyledonous species. Using molecular and biochemical techniques, we have shed some light on the functional properties of barley plastidial ADP-glucose transporter (HvBT1). Phylogenetic analysis of several BT1 homologues indicated that HvBT1 was assigned to the group which representing BT homologues from monocotyledonous species. Some members of this group, such as maize ZmBT1, mainly work as nucleotide sugar transporters. Gene expression analysis indicated that HvBT1 is mainly expressed in endospermic cells during grain filling. However, *HvBT1*expression was also slightly detected in the autotrophic tissues. These results were supported by southern blot analysis, which showed a single copy of *HvBT1* homolog in the barley genome, providing evidence of a possible alternative biochemical function of HvBT1 in autotrophic tissues. The cellular and subcellular localization of HvBT1 provided evidence that this gene targets the amyloplasts membranes of the endospermic cells. Barley HvBT1 was successfully characterized biochemically using an *E. coli* system. HvBT1 was able to transport ADP-glucose into *E. coli* cells with an affinity of 614.5 μM and in counter-exchange with ADP, with an affinity of 334.7 μM. We also found AMP to be another candidate exchange substrate. The negative effect of nonlabeled ADP-glucose and ADP on the uptake rate of $[\alpha\text{-}^{32}\text{P}]$ ADP-glucose provided evidence for substrate specificity of HvBT1 for ADP-glucose and ADP.

The second objective of our research aimed to investigate the impact of the barley plastidial ADP-glucose transporter HvBT1 on starch synthesis using gene expression analysis of *HvBT1* and other starch synthesis-related genes. To achieve this objective, two barley cultivars, Harrington and Golden Promise, was used to have inside look into the endosperm during grain filling through the expression of *HvBT1* and some starch biosynthesis-related genes in the cytosol and the amyloplasts of endospermic cells, and eventually their impact on the grain composition. Higher expression of AGPase encoding genes reflects on the AGPase activity, where AGPase activity was higher in Harrington. AGPase activity reflects on ADP-glucose synthesis efficiency. The expression of *HvBT1* in Harrington was almost 10 times higher than Golden Promise. The expression of starch synthesis genes reflected on the grain composition analysis, where starch content in Harrington was 2.5 % higher than Golden Promise with high amylopectin /amylose ratio. The expression patterns of granule-bound starch synthases1a and 1b (*GBSS1a & 1b*) followed the same trend, and showed higher expression in Harrington. Oppositely, soluble starch synthases (*SS*) showed significantly higher expression in Golden Promise than Harrington, except *SS3b*. Also, starch branching enzyme1 (*SBE1*) showed higher expression in Golden Promise than Harrington. Protein, β-glucan and lipids were significantly higher in Golden Promise, which accumulated less starch. This result is in line with the negative correlation between starch content and other grain components. We presumed that starch content in Harrington was higher as a result of the high expression of *HvBT1*, which facilitates the loading of ADP-glucose into amyloplasts, where starch is made, combined with the activity of AGPase.

The biochemical characterization of HvBT1 indicated its substrate specificity to ADP-glucose and localization, as well as the possible impact of HvBT1 on starch synthesis process. Down-regulation of HvBT1 approach was important to make a clear picture of its impact on starch yield and overall grain components. We demonstrated that down-regulation of barley ADP-glucose transporter (HvBT1) has negative effects on starch accumulation and composition. Changes in the grain size and grain weight were also investigated in the current study. As a result of down-regulation of HvBT1, starch decreased by 17 % in the transgenic grains as compared to its content in wild type. Also, altering starch composition was observed whereas amylose decreased by 5.3 % compared to the wild type, while amylopectin decreased by 2%. Wild type grain is plump and well-filled, while transgenic grain is incompletely-filled as shown in the grain cross-section. On the other hand, protein and lipid contents increased significantly in the transgenic grains. Increasing water-soluble carbohydrates in transgenic grains might contribute to increasing the grain size. Grain yield related traits were negatively affected by increasing the grain size which led to decreasing the number of grains per spike, decreasing spike length and number of spikes per plant. Also, HvBT1 has pleotropic effects on starch synthesis-related genes such as the large and small subunits of ADP-glucose pyrophosphorylase (*AGPLs* and *AGPSs*), granule-bound starch synthases (*GBSSs*) and soluble starch synthases (*SSs*). Interestingly, *AGPLs* genes were down-regulated while small subunit genes, *S1b* and *S2* were up-regulated in the transgenic plants. Soluble starch synthases (*SS*) expressed differentially in the transgenic plants. *SS2a* and *SS3a* were down-regulated while, plastidial *AGPS2b* was up-regulated in the transgenic plant.

HvBT1 is a key factor in the starch biosynthesis process. It has negative effects on starch accumulation and composition and other grain components.

In conclusion, the barley ADP-glucose transporter (HvBT1) has been successfully characterized as plastidial antiporter capable to transport ADP-glucose in counter-exchange with ADP with high affinities of 614.5 µM and 334.7 µM, respectively. AMP can be another possible counter-exchange substrate for HvBT1, along with ADP. The expression analysis and the cellular and subcellular localization of HvBT1 provided further evidence that HvBT1 targets the amyloplasts of the endospermic cells. The expression of *HvBT1* has effects on starch accumulation in the cereal grains. The expression of starch biosynthesis-related genes in barley cultivars, Harrington and Golden Promise indicated the importance of the HvBT1 for starch accumulation process. The higher expression of AGPase-encoded genes and its activity along with higher expression of *HvBT1* in Harrington provided an ideal combination for improving starch accumulation. This combination might increase the efficiency of synthesizing and transporting ADP-glucose from the cytosol into amyloplasts. Down-regulation of HvBT1 using antisense approach led to a decrease in starch accumulation in the transgenic lines by 9 % and alters starch composition in grains of the transgenic lines. Also, down-regulation of HvBT1 altered the accumulation of other grain components such as protein, lipids and β-glucan. Also, down-regulation of HvBT1 had pleotropic effects on the starch synthesis-related genes.

Future work

- Over expressing of HvBT1 in barley might lead to significant increases in starch yield and might alter starch composition.

- The co-expressing of *HvBT1* and AGPase (*SH2*) in cereal plants might enhance starch accumulation, once they are the two key elements in the starch synthesis process.

REFERENCES

Aastrup S (1979) Effect of rain on β-glucan content in barley grains. *Carlsberg Res. Comm*. 44,381-393

Aastrup S, Munck L (1985) A β-glucan mutant in barley with thin cell walls. Pages 291-296 in: New Approaches to Research on Cereal Carbohydrates. R. D. Hill and L. Munck, eds. Elsevier Science Publishers: Amsterdam.

Adel GJW, Springer F, Willmitzer L, Kossmann J (1996) Cloning and functional analysis of a cDNA encoding a novel 139 kDa starch synthase from potato (*Solanum tuberosum L.*). *Plant J*. **10**, 981-991

Agarwal S, Loar S, Steber C, Zale J (2009) Floral transformation of wheat. *Methods in Molecular Biology, Transgenic wheat, barley and oats* **478**, 105- 113

Altschul SF, Madden TL, Schäffer AA, Zhang J, Zhang Z, Miller W, Lipman DJ (1997) Gapped BLAST and PSI-BLAST: a new generation of protein database search programs. *Nucleic Acids Res*. **25**, 3389-3402

Akiyama Y (2009) Quality control of cytoplasmic membrane proteins in *Escherichia coli. J. Biochem.* **146**, 449–454

Aoki N, Hirose T, Scofield GN, Whitfeld PR, Furbank RT (2003) The Sucrose Transporter Gene Family in Rice. *Plant Cell Physiol* **44**, 223-232

Aman P, Graham H (1987) Analysis of total and insoluble mixed-linked (1-3) (1-4) β-glucans in barley and malt. *J. Agric. Food Chem.* **35**, 704-709

Badr A, Müller K, Schäfer-Pregl R, El Rabey H, Effgen S, Ibrahim H, Pozzi C, Rohde W, Salamini F (2000) On the origin and domestication history of barley (*Hordeum vulgare L.*). *Mol. Biol. Evol*. **17**, 499-510.

Bae JM, Giroux M, Hannah L (1990) Cloning and characterization of the Brittle-2 gene of maize. *Maydica* **35**, 317–322

Bahaji A, Ovecka M, Barany I, Risueno MC, Munoz FJ, Baroja-Fernandez E, Montero M, Li J, Hidalgo M, Sesma MT, Ezquer I, Testillano PS, Pozueta-Romero J (2011) Dual targeting to mitochondria and plastids of *AtBT1* and *ZmBT1*, two members of the mitochondrial carrier family. *Plant Cell Physiol.* **52**, 97-609

Baik Y K, Ullrich SE (2008) Barley for food: Characteristics, improvement, and renewed interest. *J. Cereal Sci.* **48**, 233–242

Ballicora MA, Dubay JR, Devillers CH, Preiss J (2005) Resurrecting the ancestral enzymatic role of a modulatory subunit. *J. Biol. Chem*. **280**, 10189-10195.

Ballicora MA, Laughlin MJ, Fu Y, Okita TW, Barry GF, Preiss J (1995) Adenosine 5-diphosphate-glucose pyrophosphorylase from potato tuber. (Significance of the N terminus of the small subunit for catalytic properties and heat stability). *Plant Physiol*. **109**, 245–251.

Barkat A, Carels N, Bernardi G (1997) The distribution of genes in the genome of Gramineae. *Proc. Natl. Acad. Sci. U.S.A*. **94**, 6857–6861.

Baroja-Ferna´ndez E, Munóz FJ, Zandueta-Criado A,Mora´n-Zorzano MT, Viale AM, Alonso-Casaju´s N, Pozueta-Romero J (2004) Most of ADP-glucose linked to starch biosynthesis occurs outside the chloroplast in source leaves. *Proc. Natl. Acad. Sci. U.S.A* **101**, 13080–13085.

Beatty MK, Rahman A, Cao H, Woodman W, Lee M, Myers AM, James MG (1999) Purification and molecular genetic characterization of *ZPU1*, a pullulanase-type starch-debranching enzyme from maize *Plant Physiol.* **119**, 255–266

Beckles DM, Smith AM, Rees T (2001) A cytosolic ADP-glucose pyrophosphorylase is a feature of graminaceous endosperms, but not of other starch storing organs. *Plant Physiol.* **125**, 818–827.

Bednarek J, Boulaflous A, Girousse C, Ravel C, Tassy C, Barret P, Bouzidi MF, Mouzeyar S (2012) Down-regulation of the TaGW2 gene by RNA interference results in decreased grain size and weight in wheat. *J. Exp. Bot.* **63**, 5945-5955

Bhatty RS, MacGrwgor AW, Rossnagel BG (1990) Total and acid soluble β-glucan content of hulless barley and its relationship to acid-extract viscosity. *Cereal Chem.* **68**, 221-227

Belmonte M, Donald G, Reid D, Yeung E, Stasolla C (2006) Alternations of the glutathione redox state improves apical meristem structure and somatic embryo quality on white spruce (*Picea glauca*). *J. Exp. Bot.* **56**, 23-55

Bernstein AM, Titgemeier B, Kirkpatrick K, Golubic M, RoizenMF (2013) Major Cereal Grain Fibers and Psyllium in Relation to Cardiovascular Health. *Nutrients* **5**, 1471-1487

Bernaudat F, Frelet-Barrand A, Pochon N, Dementin S, Hivin P, Boutigny S, rioux J, Salvi D, Seigneurin-Berny D, Richaud P, Joyard j, Pignol D, Sabaty M, Desnos T, Pebay-Peyroula E, Darrouzet E, Vernet T, Rolland N (2011) Heterologous Expression of Membrane Proteins: Choosing the Appropriate Host. *PLoS ONE* **6**, 1-17

Binns AN, Thomashow MF (1988) Cell biology of *Agrobacterium* infection and transformation of plants. *Ann. Rev. Microbiol.* **42**, 575-606.

Boldingh H, Smith GS, Klages K (2000) Seasonal concentrations of non-structural carbohydrates of five Actinidia species in fruit, leaf and fine root tissue. *Annals of Botany* **85**, 469-476

Bowsher CG, Scrase-Field EFAL, Esposito S, Emes MJ, Tetlow IJ (2007) Characterization of ADP-glucose transport across the cereal endosperm amyloplast envelope. *J. Exp. Bot*. **58**, 1321–1332

Boyko A, Matsouka A, Kovalchuk I. (2009) High frequency Agrobacterium tumefaciens-mediated plant transformation induced by ammonium nitrate. *Plant Cell Rep*. **28**, 737-757

Braun DM, Slewinski TL (2009) Genetic control of carbon partitioning in grasses: Roles of *Sucrose Transporters* and *Tiedyed* loci in phloem loading. *Plant Physiol*. **149**, 71–81

Brettschneider R, Becker D, Lorz H (1997) Efficient Transformation of Scutellar Tissue of Maize Embryos, *Theor. Appl. Gen*et. **94**, 737–748

Brencic A, Winans S (2005) Detection and response to signals involved in host-microbe interactions by plant-associated bacteria. *Microbiol. Mol. Biol. Rev*. **69**, 155–94

Brown W, Ralston A, Shaw K (2008) Positive transcription control: The glucose effect. *Nature Education* 1(1)

Buléon A, Colonna P, Planchot V, Ball S (1998) Starch granules: structure and biosynthesis. *Int. J. Biol. Macromol.* **23**, 85–112

Burton RA, Jenner H, Carrangis L, Fahy B, Fincher GB, Hylton C, Laurie DA, Parker M, Waite D, van Wegen S, Verhoeven T, Denyer K (2002) Starch granule

initiation and growth are altered in barley mutants that lack isoamylase activity. *Plant J.* **31**, 97–112

Cao H, Sullivan TD, Boyer CD, Shannon JC (1995) BT1, a structural gene of the major 39–44 kDa amyloplast membrane polypeptides. *Physiol. Plant*. **95**, 176–186

Cao H, Shannon JC (1996) BT1, a protein critical for in vivo starch accumulation in maize endosperm, is not detected in maize endosperm suspension cultures. *Physiol. Plant*. **97**, 665–673

Cao H, Impari-Radosevich J, Guan H (1999) Identification of soluble starch synthase activities of maize endosperm. *Plant Physiol*. **120**, 205-215

Canton F, Suarez M, Jose-Estanyol M, Canovas F (1999) Expression analysis of cytosolic glutamine synthase gene in cotyledons of Scots pine seedlings: developmental, light regulation and septial distribution of specific transcripts. *Plant Mol. Biol.* **40**, 623-634

Carciofi M, Blennow A, Jensen SL, Shaik SS, Henriksen A, Bulèon A, Holm PB, Hebelstrup KH (2012) Concerted suppression of all starch branching enzymes genes in barley produces amylose-only starch granules. *BMC Plant Biol.* **12**: 1-16

Cho M-J, Jiang W, Lemaux PG (1998) Transformation of recalcitrant barley cultivars through improvement of regenerability and decreased albinism. *Plant Sci.***138**, 229-244

Chen D, Texada DE (2006) Low-usage codons and rare codons of Escherichia coli. *Gene Therapy and Molecular Biology* **10**, 1-12

Cheng M, Lowe BA, Spencer TM, Ye X, Armstrong CL (2004) Factors influencing Agrobacterium-mediated transformation of monocotyledonous species. *In Vitro Cell. Dev. Biol. Plant* **40**, 31–45

Clarke BR, Denyer K, Jenner CF, Smith AM (1999) The relationship between the rate of starch synthesis, the sdenosine 5'-diphosphoglucose concentration and the amylose contentof the starch in developing pea embryos. *Planta* **209**, 324-329

Clarke B, Liang R, Morell MK, Bird AR, Jenkins CLD, Li Z (2008) Gene expression in a starch synthase IIa mutant of barley: changes in the level of gene transcription and grain composition. *Funct. Integr. Genomics* **8**, 211–221

Comparot-Moss S, Denyer K (2009) The evolution of the starch biosynthetic pathway in cereals and other grasses. *J. Exp. Bot.* **60**, 2481-92

Commuri PD, Keeling PL (2001) Chain-length specificities of maize starch synthase I enzyme: studies of glucan affinity and catalytic properties. *Plant J.* **25**, 475- 486

Curá JA, Jansson P-E, Krisman CR (1995) Amylose is not strictly linear. *Starch/Staerke* 47:207-209

Dahleen LS, Manoharan M (2007) Recent advances in barley transformation. *In Vitro Cel. Dev. Biol. – Plants* **43**, 493-506

Danilova SA (2007) The technologies for genetic transformation of cereals. *Russian Journal of Plant Physiol.* **54**, 569-581

Delvallé D, Dumez S, Wattebleb F, Roldán I, Planchot V, Berbezy P, Colonna P, Vyas D, Chatterjee M, Ball S, Mérida A, D'Hulst C (2005). Soluble starch synthase I: A major determinant of the synthesis of amylopectin in *Arabidopsis thaliana* leaves. *Plant J.* **43**, 398 – 412

Denyer K, Clarke B, Hylton C, Tatge H, Smith AM (1996) The elongation of amylase and amylopectin chains in isolated granules. *Plant J.* **10**, 1135-1143

Denyer K, Dunlap F, Thorbjørnsen T, Keeling P, Smith AM (1996) The major form of ADP-glucose pyrophosphorylase in maize endosperm is extraplastidial. *Plant Physiol.* **112**, 779–783

Denyer K, Waite D, Motawia S, Moller B-L, Smith AM (1999a) Granule-bound starch synthase I in isolated starch granules elongates malto-oligosaccharides processively. *Biochem. J.* 340, 183−191

Denyer K, Waite D, Edwards A, Martin C, Smith AM (1999b) Interaction with amylopectin influences the ability of granule-bound starch synthase I to elongate malto-oligosaccharides. *Biochem. J.* **342**, 647−653

Denyer K, Johnson P, Zeeman SC, Smith AM (2001) The control of amylose synthesis. J. *Plant Physiol.* **158**,479–87

Dian W, Jiang H, Wu P (2005) Evolution and expression analysis of starch synthase III and IV in rice. *J. Exp. Bot.* **56**, 623-632

Dinges R, Colleoni C, James MG, Myers AM (2003) Mutational analysis of the pullulanase-type debranching enzyme of maize indicates multiple functions in starch metabolism. *Plant Cell* **15**, 666–680

Emes MJ, Neuhaus HE (1997). Metabolism and transport in non-photosynthetic plastids. *J. Exp. Bot.* **48**, 1995-2005

Emes MJ, Tetlow IJ, Bowsher CG (2001) Transport of metabolites into amyloplastids during starch synthesis. In: Barsby TL, Donald AM, Frazier PJ, eds. Starch advances in structure and function. *Royal Society of Chemistry* 138-143

Emes MJ, Borwsher CG, Hedley C, Burrell MM, Scrase-Field ESF, Tetlow IJ (2003). Starch synthesis and carbon partitioning in developing endosperm. *J. Exp. Bot.* **54**, 569-575

Fincher GB, Stone BA (1986) Cell walls and their components in cereal grain technology. Pages 207-295 in: Advances in Cereal Science and Technology. Y. Pomeranz, ed. AACC International: St. Paul, MN

Fulton DC, Edwards A, Pilling E, Robinson HL, Fahy B et al. (2002) Role of granule-bound starch synthase in determination of amylopectin structure and starch granule morphology in potato. *J. Biol. Chem.* **277**, 10834–10841

Fullner KJ, Nester EW (1996) Temperature Affects the T-DNA Transfer Machinery of *Agrobacterium tumefaciens. J. Bacteriol.* **178**, 1498–1504

Fujita N, Hasegawa H, Taira T (2001) The isolation and characterization of a waxy mutant of diploid wheat (*Triticum monococcum* L.). *Plant Sci.* **160**, 595 – 602

Fujita N, Kubo A, Suh DS, Wong KS, Jane JL, Ozawa K, Takaiwa F, Inaba Y, Nakamura Y (2003) Antisense inhibition of isoamylase alters the structure of amylopectin and the physicochemical properties of starch in rice endosperm. *Plant Cell Physiol.* **44**,607–618

Fujita N, Yoshida M, Asakura N, Ohdan T, Miyao A, Hirochika H, Nakamura Y (2006) Function and characterization of starch synthase I using mutants in rice. *Plant Physiol.* **140**, 1070 – 1084

Fujita N, Yoshida M, Kondo T, Saito K, Utsumi Y, Tokunaga T, Nishi A, Satoh H, Park JH, Jane JL, Miyao A, Hirochika H, Nakamura Y (2007). Characterization of

SSIIIa-deficient mutants of rice: the function of SSIIIa and pleiotropic effects by *SSIIIa* deficiency in the rice endosperm. *Plant Physiol*. **144**, 2009-2023

Fujita N, Toyosawa Y, Utsumi Y, Higuchi T, Hanashiro I, Ikegami A, Akuzawa S, Yoshida M, Mori A, Inomata K, Itoh R, Miyao A, Hirochika H, Satoh H, Nakamura Y (2009) Characterization of pullulanase (*PUL*)-deficient mutants of rice (*Oryza sativa* L.) and the function of PUL on starch biosynthesis in the developing rice endosperm. *J. Exp. Bot.* **60**,1009–1023

Furbank RT, Scofield GN, Hirose T, Wang X-D, Patrick JW, Offler CE (2001) Cellular localisation and function of a sucrose transporter *OsSUT1* in developing rice grains. *Aust. J. Plant Physiol*. **28**, 1187–1196

Gao M, Wanat J, Stinard PS, James MG, Myers AM (1998) Characterization of dull1, a maize gene coding for a novel starch synthase. *Plant Cell* **10**, 399 - 412

Gelvin S (2003) *Agrobacterium*-mediated plant transformation: The biology behind the ' Gene-Jockeying' tool. *Microbiol. Mol. Biol. Rev*. **67**, 16-37

Geigenberger P, Kolbe A, Tiessen A (2005) Redox regulation of carbon storage and partitioning in response to light and sugars. *J. Exp. Bot*. **56**, 1469-1479

Geirger DR, Servaites JC, Fuchs MA (2000) Role of starch in carbon translocation and partitioning at the plant level. *Aust. J. Plant Physiol*. **27**, 571-582

Ghosh HP, Preiss J (1966) Adenosine diphosphate glucose pyrophosphorylase: a regulatory enzyme in biosynthesis of starch in spinach leaf chloroplasts. *J. Biol. Chem*. **241**, 4491–4504

Giroux MJ, Hannah LC (1994) ADP- glucose pyrophosphorylase in shrunken-2 and brittle-2 mutants of maize. *Mol. Gen. Genet*. **243**, 400-408

Gross P, ap Rees T. (1986) Alkaline inorganic pyrophosphatase and starch synthesis in amyloplasts. *Planta* **167**, 140–145

Guan HP, Preiss J (1993) Differentiation of the properties of the branching isozymes from maize *(Zea mays L.). Plant Physiol*. **102**, 12691273

Guan HP, Keeling PL (1998) Starch biosynthesis: understanding the functions and interactions of multiple isozymes of starch synthase and branching enzyme. *Trends Glycosci. Glycotechnol*. **10**, 307 - 319

Gürel F, Gözükirmizi N (2000) Optimization of gene transfer into barley (*Hordeum vulage L)* marure embryos by tissue electroporation. *Plant Cell Rep*. **19**, 787-791

Hanashiro I, Itoh K, Kuratomi Y, Yamazaki M, Igarashi T, Matsugasako J, Takeda Y (2008) Granule-bound starch synthase I is responsible for biosynthesis of extra-long unit chains of amylopectin in rice. *Plant Cell Physiol*. **49**, 925-933

Harlan JR (1978) On the origin of barley. Pages 10-36 in: Barley: Origin, Botany Culture, Winter Hardiness, Genetics, Utilization, Pests. Agriculture Handbook 338. US. Department of Agriculture, Washington, DC.

Harn C, Knight M, Ramakrishan A, Guan HP, Keeling PL,Wasserman BP (1998) isolation and characterization of the SS2 starch synthase cDNA clones from maize endosperm. *Plant Mol. Biol*. **37**, 629-637

Harwood WA, **Bartlett J, Alves S, Perry M**, **Smedley M**, **Leyland N, Snape JW** (2009) Barley transformation using Agrobacterium-mediated techniques. In: Huw D Jones and Peter R Shewry (eds), *Methods in Molecular Biology, Transgenic Wheat, Barley and Oats,* Vol 478, Chapter 9, pp137-147

Hayashimoto A, Li Z, Murai N (1990) A polyethylene glycol-mediated protoplast transformation system for production of fertile transgenic rice plants. *Plant Physiol*. **93**, 857-863

He GY, Lazzeri PA (1998) Analysis and optimization of DNA delivery into wheat scutellum and tritordeum inflorescence explants by tissue electroporation. *Plant Cell Rep*. **18**, 64–70

Hirose T, Terao T (2004) A comprehensive expression analysis of the starch synthase gene family in rice (*Oryza sativa L.*). *Planta* **220**, 9–16

Hogg AC, Gause K, Hofer P, Martin JM, Graybosch Robert A, Hansen LE, Giroux MJ (2013) Creation of a high-amylose durum wheat through mutagenesis of starch synthase II (*SSIIa*). *J. Cereal Sci*. **57**, 377-383

Hood LF (1982) Current concepts of starch structure. Pages 218-224 in: *Food Carbohydrates*. D. R. Lineback and G. E. Inglett, Eds. AVI, Westport, CT.

Imparl-Radosevich JM, Gameon JR, Mckean A, Wetterberg D**,** Keeling P L **,** Guan H. (2003) Understanding catalytic properties and functions of maize starch synthase isozymes. *J. Appl. Glycoscience* **50**, 117-182

Ishimaru K, Hirose T, Aoki N, Takahashi S, Ono K, Yamamoto S, Wu J, Saji S, Baba T, Ugaki M, Matsumoto T, Ohsugi R (2001) Antisense expression of a rice sucrose transporter *OsSUT1* in rice (*Oryza sativa L.*). *Plant Cell Physiol*. **42**, 1181–1185

Izydorczyk MS, Storsley J, Labossiere D, MacGregor AW, Rossnagel BG (2000) Variation in total and soluble β-glucan content in hulless barley: Effects of thermal, physical, and enzymatic treatments. *J. Agric. Food Chem.* **48**, 982–989

James MG, Robertson DS, Myers AM (1995) Characterization of the maize gene *sugary1*, a determinant of starch composition in kernels. *Plant Cell* **7**, 417–429

James MG, Denyer K, Myers AM (2003) Starch synthesis in the cereal endosperm. *Curr. Op Plant Biol*. **6**, 215–222

Jarchow E, Grimsley NH, Hohn B (1991) *virF*, the host-range determining virulence gene of *Agrobacterium tumefaciens*, affects T-DNA transfer to *Zea mays. Proc. Natl. Acad. Sci. USA* **88**, 10426–10430

Jacobsen, S, Søndergaard I, Møller B, Desler T, Munck L (2005) A chemometric evaluation of the underlying physical and chemical patterns that support near infrared spectroscopy of barley seeds as a tool for explorative classification of endosperm genes and gene combinations. *J. Cereal Sci*. **42**,281-299

Jespersen HM, MacGregor AE, Henrissat B, Sierks MR, Svensson B (1993) Starch- and glycogen-debranching and branching enzymes: prediction of structural features of the catalytic (P/u)a-barrel domain and evolutionary relationship to other amylolytic enzymes. *J. Protein Cherm.* **12**, 791-805

Jeon JS, Ryoo N, Hahn T, Walia H, Nakamura Y (2010) Starch biosynthesis in cereal endosperm. *Plant Physiol. Biochem*. **48**, 383-392

Johnson PE, Patron NJ, Bottrill AR, Dinges JR, Fahy BF, Parker ML, Waite DN, Denyer K (2003)A low-starch barley mutant, Riso16, lacks the cytosolic small subunit of ADP-glucose pyrophosphorylase, reveals the importance of the cytosolic isoform and the identity of the plastidial small subunit. *Plant Physiol.* **131**, 684–696

Kalra S, Joad S (2000) Effect of dietary barley β- glucan on cholesterol and lipoprotein fractions in rates. *J. Cereal Sci*. **31**: 141-145

Kammerer B, Fisher K, Hilpert B, Schuber S, Gutensohn M, Weber A, Flügge U-I (1998) Molecular characterization of a carbon transporter in plastids from heterotrophic tissues: the glucose 6-phosphate antiporter. *Plant Cell* **10**, 105-117

Kampfenkel K, Mohlmann T, Batz O, van Montagu M, Inze D, Neuhaus HE (1995) Molecular characterization of an Arabidopsis thahana cDNA encoding for a novel putative adenylate transporter of higher plants. *FEBS Letters* **374**, 351-5

Kates M (1972) Techniques of lipiology isolation. Analysis and identification of lipids. *North Holland Publishing Co. Amesterdam, London*

Kiniry JR (1988) Kernel weight increase in response to decreased kernel number in sorghum. *Agron. J.* **80**, 221-226

Kiniry JR, Wood CA, Spanel DA, Bockholt AJ (1990) Seed weight response to decreased seed number in maize. *Agron. J.* **82**, 98-102

Kirchberger S, Leroch M, Huynen MA, Wahl M, Neuhaus HE, Tjaden J (2007) Molecular and biochemical analysis of the plastidic ADP-glucose transporter (*ZmBT1*) from *Zea mays*. *J. Biol. Chem.* **282**, 22481–22491

Kirchberger S, Tjaden J, Neuhaus HE (2008) Characterization of the Arabidopsis Brittle1 transport protein and impact of reduced activity on plant metabolism. *Plant J.* **56**, 51–63

Kloti A, Iglesias VA, Wunn J, Burkhardt PK, Datta SK, Potrykus I (1993) Gene transfer by electroporation into intact scutellum cells of wheat embryos. *Plant Cell Rep.* **12**, 671-675

Konik-Rose C, Thistleton J, Chanvrier H, et al. (2007) Effects of starch synthase IIa gene dosage on grain, protein and starch in endosperm of wheat. *Theor. Appl. Genet.* **115**, 1053–1065

Kubo A, Rahman S, Utsumi Y, Li Z, Mukai Y, Yamamoto M, Ugaki M, Harada K, Satoh H, Konik-Rose C, Morell M, Nakamura Y (2005) Complementation of *sugary-1* phenotype in rice endosperm with the wheat isoamylase1 gene supports a direct role for isoamylase1 in amylopectin biosynthesis. *Plant Physiol.* **137**, 43–56

Kühn C (2010) Sucrose transporters and plant development. In: Signalling and Communication in Plants: Transporters and pumps in plant signalling. Eds. K. Venema, Springer Verlag, Heidelberg, pp. 225-251

Laemmli UK, Molber E, Showe M, Kelenberger E (1970) Form-determining function of genes required for the assembly of the head of bacteriophage T4. *J. Mol. Biol.***49**, 99-113

Lamari L (2008) ASSESS 2.0: Image Analysis Software for Plant Disease Quantification. St Paul, MN: *Amer Phytopathological Society*

Lazzeri PA, Brettschneider R, Luhrs R, Lorz H (1991) Stable transformation of barley via PEG-induced direct DNA uptake into protoplasts. *Theor. Appl. Genet.* **81**, 437–444

Leedell PJ, Zhany G, Cass DD (1997) Transient GFP expression in sperm cells and zygotes of *Zea mays L. Plant Physiol.* **114**, 297–298

Léon J, Silz S, Harloff HJ (2000) β-glucan content during grain filling in spring barley and its wild progenitor *H. vulgare* ssp. *spontaneum. J. Agron. Crop Sci.* **185**: 1-8

Leroch M, Kirchberger S, Haferkamp I, Wahl M, Neuhaus HE, Tjaden J (2005) Identification and characterization of a novel plastidic adenine nucleotide uniporter from *Solanum tuberosum. J. Biol. Chem.* **280**, 17992–18000

Li Z, Mouille G, Kosar-Hashemi B, Rahman S, Clarke B, Gale KR, Appels R, Morell MK (2000) The structure and expression of the wheat starch synthase III gene. Motifs in the expressed gene define the lineage of the starch synthase III gene family. *Plant Physiol*. **123**, 613 – 624

Li Z, Li D, Du X, Wang H, Larroque O, LenkinsCLD, Jobling SA, Morell MK (2011) The barley *amo1* locus is tightly linked to the starch synthase *IIIa* gene and negatively regulates expression of granule-bound starch synthetic genes. *J. Exp. Bot*. **62**, 5217–5231

Linka N, Hurka H, Lang BF, Burger G, Winkler HH, Stamme C, Urbany C, Seil I, Kusch J, Neuhaus HE (2003) Phylogenetic relationship of non-mitochondrial nucleotide transport proteins in bacteria and eukaryotes. *Gene* **306**, 27–35

Lioyd JR, Landschütze V, Kossmann J (1999) Simultaneous antisense inhibition of two starch synthase isoforms in potato tubers leads to accumulation of grossly modified amylopectin. *Biochem. J.* **338**, 515-521

Lorz H, Lazzeri PA (1992) In vitro regeneration and genetic transformation of barley. *Barley Genet VI II* 807-815

Livak, KJ, Schmittgen TD. (2001) Analysis of relative gene expression data using real-time quantitative PCR and the $2^{-\Delta\Delta C_T}$ method. *Methods* **25**, 402–408

Mangold HK, Malins DC (1960) Fractionation of fats, oils and waxes on thin-layer of silica acid. *J. Am. Oil Chem. Soc*. **37**, 383-387

Mangold HK (1961) Thin-layer chromatography of lipids. *J. Am. Oil Chem. Soc*. **38**, 708-727

Martin T, Ludewig F (2007)   Transporters in starch synthesis. *Funct. Plant Biol*. **34**, 474-479

Matthews PR, Wang MB, Waterhouse PM, Thornton S, Fieg SJ, Gubler F, Jacobsen JV (2001) Marker gene elimination from transgenic barley using co-transformation with adjacent 'twin T-DNAs' on standard Agrobacterium transformation vector. *Mol. Breed.* **7**, 195–202

Messens E, Dekeyser R, Stachel SE (1990) A non-transformable *Triticum monococcum* monocotyledonous culture produces the potent Agrobacterium vir-inducing compound ethyl ferulate. *PNAS* **87**, 4368-4372

Miller M, Tagliani L, Wang N, Berka B, Bidney D, Zhao ZY (2002) High efficiency transgene segregation in co-transformed maize plants using an *Agrobacterium tumefaciens* 2 T-DNA binary system. *Transgenic Res*. **11**, 381–396

Millar AH, Heazlewood JL (2003) Genomic and proteomic analysis of mitochondrial carrier proteins in Arabidopsis. *Plant Physiol*. **131**, 443–453

Möhlmann T, Tjaden J, Henrichs G, Quick WP, Ha¨usler R, Neuhaus HE (1997) ADP-glucose drives starch synthesis in isolated maize endosperm amyloplasts: characterisation of starch synthesis and transport properties across the amyloplast envelope. *Biochem. J.* **324**, 503–509

Morell MK, Blennow A, Kosar-Hashemi B, Samuel MS (1997) Differential expression and properties of starch branching enzyme isoforms in developing wheat endosperm. *Plant Physiol.* **113**, 201–208

Morell MK, Kosar-Hashemi B, Cmiel M, Samuel MS, Chandler P, Rahman S, Buleon A, Batey IL, Li ZY (2003) Barley sex6 mutants lack starch synthase IIa activity and contain a starch with novel properties. *Plant J*. **34**, 172-184

Morell MK, Myers A (2005) Towards the rational design of cereal starches. *Curr. Opin. Plant Biol.* **8**, 204- 210

Morrison W R (1978) Wheat lipid composition. *Cereal Chem*. **55**, 548- 558

Morrison W R (1993) Cereal starch granule development and composition. Pages 179-209 in: Proceedings of the Phytochemical Society of Europe. P.R. Shewry and K. Stobart, eds. Clarendon Press: Oxford

Munck L, Møller B, Jacobsen S, Søndergaard I (2004) Near infrared spectra indicate specific mutant endosperm genes and reveal a new mechanism for substituting starch with (1-3,1-4) beta glucan in barley. *J. Cereal Sci*. **40**, 213–222

Murray AA, Thompson WF (1980) Rapid isolation of high molecular weight plant DNA. *Nuc. Acid Res*. **8**, 4321-4325

Nakamura Y, Sakurai A, Inaba Y, Kimura K, Iwasawa N, Nagamine T (2002) The fine structure of amylopectin in endosperm from Asian cultivated rice can be largely classified into two classes. *Starch* **54**, 117–131

Nakamura Y, Umemoto T, Ogata N, Kuboki Y, Yano M, Sasaki T (1996) Starch debranching enzyme (R-enzyme or pullulanase) from developing rice endosperm: purification, cDNA and chromosomal localization of the gene. *Planta* **199**, 209–218

Nagamori S et al. (2004) Role of YidC in folding of polytopic membrane proteins. *J. Cell Biol*. **165**, 53–62

Narayanan A, Ridilla M, Yernool DA (2001) Restrained expression, a method to overproduce toxic membrane proteins by exploiting operator–repressor interactions. *Protein Sci.* **20**, 51-61

Neuhaus EH, Wagner R (2000) Solute pores, ion channels, and metabolite transporters in the outer and inner envelope membranes of higher plant plastids. *Biochim. Biophys. Acta* **1465**, 307–323

Newman CW, Newman RK (2006) A brief history of barley foods. *Cereal Foods World* **51**, 4–7

Nobre J, Davey MR, Lazzeri PA, Cannell ME (2000) Transformation of barley scutellum protoplasts: regeneration of fertile transgenic plants. *Plant Cell Rep*. **19**, 1000–1005

Ohdan T, Francisco PB Jr, Sawada T, Hirose T, Terao T, Satoh H, Nakamura Y (2005) Expression profiling of genes involved in starch synthesis in sink and source organs of rice. *J. Exp. Bot.* **56**, 3229 - 3244

Orzaez D, Mirabel S, Wieland WH, Granell A (2006) Agroinjection of tomato fruits: A tool for rapid functional analysis of transgenes directly in fruit. *Plant Physiol.* **140**, 3-11

Otten L, DeGreve H, Leemans J, Hain R, Hooykaas P, Schell J (1984) Restoration of virulence of *vir* region mutants of *Agrobacterium tumefaciens* strain B6S3 by coinfection with normal and mutant *Agrobacterium* strains. *Mol. Gen. Genet*. **195**, 159–163

Patron NJ, Smith AM, Fahy BF, Hylton CM, Naldrett MJ, Rossnagel BG, Denyer K (2002) The altered pattern of amylose accumulation in the endosperm of low-amylose

barley cultivars is attributable to a single mutant allele of granule-bound starch synthase I with a deletion in the 5'-non-coding region. *Plant Physiol*. **130**, 190 – 198

Patron NJ, Greber B, Fahy BF, Laurie DA, Parker ML, Denyer K (2004) The *lys5* mutations of barley reveal thenature and importance of plastidial ADP-glucose transporters for starch synthesis in cereal endosperm. *Plant Physiol*. **135**, 2088–2097

Pein FM, Shannon JC (1996) Plant Physiology 111 (suppl.) S100

Peng M, Hucl P, Chibbar RN (2001) Isolation, characterization and expression analysis of starch synthase I from wheat (*Triticum aestivum L.*). *Plant Sci*. **161**, 1055-1062

Phillips KM, Tarrangó -Trani MT, Grove TM, Grün I, Lugogo R, Harris RF, Stewart KK (1997) Simplified gravimetric determination of total fat in food composites after chloroform-methanol extyraction. *JAOCS* 74, 1-6

Picault N, Hodges M, Palmieri L, Palmieri F (2004) The growing family of mitochondrial carriers in Arabidopsis. *Trends Plant Sci.* **9**, 138–146

Prasanna GL, Panda T (1997) Electroporation basic principles, practical considerations, applications in molecular biology. *Biopress Engineering* **16**, 261-264

Price PB, Parsons J (1979) Distribution of lipids in embryonic axis, bran-endosperm, and full fractions of hulless barley and hulless oat grains. *J. Agric. Chem*. **27**, 813-815

Purohit SD, Raghuvanshi S, Tyagi A (2007) Biolistic-mediated DNA delivery and transient expression of GUS in hypocotyles of Feronia limonia L- A fruit tree. *Indian J. Biotech*. **6**, 504-507

Qureshi AA, Qureshi N, Wright JJK, Shen Z, Kramer G, Gapor A, Chong YH, Dewitt G, Ong ASH, Peterson DM, Bradlow BA (1991) Lowering serum cholesterol in

hypercholesterolemic humans by tocotrienols (palmvitee). *Am. J. Clin. Nutr.* **53**, 1021–1026

Radchuk VV, Borisjuk L, Sreenivasulu N, Merx K, Mock H-P, Rolletschek H, Wobus U, WeschkeW (2009) Spatiotemporal profiling of starch biosynthesis and degradation in the developing barley grain. *Plant Physiol*. **150**,190–204

Regina A, Kosar-Hashemi B, Li Z, Pedler A, Mukai Y, Yamamoto M, Gale K, Sharp PJ, Morell MK, Rahman S (2005) Starch branching enzyme *IIb* in wheat is expressed at low levels in the endosperm compared to other cereals and encoded at a non-syntenic locus. *Planta* **222**, 899-909

Regina A, Kosar-Hashemi B, Ling S, Li Z, Rahman S,Morell M (2010) Control of starch branching in barley defined through differential RNAi suppression of starch branching enzyme IIa and IIb. *J. Exp. Bot*. **61**, 1469–1482

Reinders A, Sivitz AB, Hsi A, Grof CP, Perroux JM, Ward JM (2006) Sugarcane *ShSUT1*: analysis of sucrose transporter activity and inhibition by sucralose. *Plant Cell Environ*. **29**, 1871-1880

Reiser J, Linka N, Lemke L, Jeblick W, Neuhaus HE (2004) Molecular physiological analysis of the two plastidic ATP/ADP transporters from Arabidopsis. *Plant Physiol*. **136**, 3524–3536

Repellin A, Baga M, Jauhar PP, Chibbar RN (2001) Genetic enrichment of cereal crops via alien gene transfer: new challenges. *Plant Cell, Tissue and Organ Culture* **64**, 159–183

Rieder B, and Neuhaus HE (2011) Identification of an Arabidopsis plasma membrane–located ATP transporter important for anther development. *Plant Cell* **23**, 1932–1944

Register JC, Peterson DJ, Bell PJ, Bullock WP, Evans IJ, Frame B, Greenland AJ, Higgs NS, Jepson I, Jiao S, Lewnau CJ, Sillick JM, Wilson M (1994) Structure and Function of Selectable and Non- Selectable Transgenes in Maize after Introduction by Particle Bombardment. *Plant Mol. Biol*. **25**, 951–961

Risacher T, Craze M, Bowden S, Paul W, Barsby T (2009) High efficient Agrobacterium-mediated transformation of wheat via in planta inoculation. *Methods in Molecular Biology, Transgenic wheat, barley and oats* **478**, 115- 124

Roldán I, Wattebled F, Mercedes Lucas M, Delvallé D, Planchot V, Jiménez S, Pérez R, Ball S, D'Hulst C, Mérida A (2007) The phenotype of soluble starch synthase IV defective mutants of *Arabidopsis thaliana* suggests a novel function of elongation enzymes in the control of starch granule formation. *Plant J*. **49**, 492 – 504

Rösti S, Rudi H, Rudi K, Opsahl-Sorteberg H., Fahy B, Denyer K (2006) The gene encoding the cytosolic small subunit of ADP-glucose pyrophosphorylase in barley endosperm also encodes the major plastidial small subunit in the leaves. *J. Exp. Bot*. **57**, 3619–3626

Ruuska S, Rebetzke G, van Herwaarden A, Richards RA, Fettell N, Tabe L, Jenkins CLD. (2006). Genotypic variation in water-soluble carbohydrate accumulation in wheat. *Funct. Plant Biol.* **33**, 799–809

Ryoo N, Yu C, Park CS, Baik MY, Park IM, Cho MH, Bhoo SH, An G, Hahn TR, Jeon JS (2007) Knockout of a starch synthase gene *OsSSIIIa/Flo5* causes white-core floury endosperm in rice (*Oryza sativa L*.). *Plant Cell Rep* **26**, 1083–1095

Sambrook J, Fritsch EF, Maniatis T (1989) *Molecular Cloning: A Laboratory Manual*, Cold Spring Harbor Laboratory, Cold Spring Harbor, NY

Satoh H, Nishi A, Yamashita K, Takemoto Y, Tanaka Y, Hosaka Y, Sakurai A, Fujita N, Nakamura Y (2003) Starch branching enzyme 1–deficent mutant specifically affects the structure and properties of starch in rice endosperm. *Plant Physiol*. **133**, 1111-1121

Satoh H, Shibahara K, Tokunaga T, Nishi A, Tasaki M, Hwang SK, Okita TW, Kaneko N, Fujita N, Yoshida M, Hosaka Y, Sato A, Utsumi Y, Ohdan T, Nakamura Y (2008) Mutation of the plastidial alpha-glucan phosphorylase gene in rice affects the synthesis and structure of starch in the endosperm. *Plant Cell* **20**,1833–1849

Sauer N. (2007) Molecular physiology of higher plant sucrose transporters. *FEBS letter* **581**, 2309-2317

Scofield GN, Hirose T, Aoki N, Furbank RT (2007) Involvement of the sucrose transporter, *OsSUT1*, in the long distance pathway for assimilate transport in rice. *J. Exp Bot*. **58**, 3155-3169

Seebauer JR, Singletary GW, KrumpelmanPM,Ruffo ML, Below FE (2010) Relationship of source and sink in determining kernel composition of maize. *J. Exp. Bot.* **61**, 511–519

Shannon JC, Pien FM, Liu KC (1996) Nucleotides and nucleotide sugars in developing maize endosperms: Synthesis of ADP-glucose in brittle 1. *Plant Physiol*. **110**, 835–843

Shannon JC, Pien FM, Cao H, Liu KC (1998) Brittle-1, an adenylate translocator, facilitates transfer of extraplastidial synthesized ADP-glucose into amyloplasts of maize endosperms. *Plant Physiol*. **117**, 1235-1252

Sharma VK, Hansch R, Mendel RR, Schuize J (2005) Mature embryo axis-based high frequency somatic embryogenesis and plant regeneration from multiple cultivars of barley (*Hordeum vulgare L.*). *J. Exp. Bot.* **417**, 1913-1922

Shrawat AK, Horst Lörz (2006) *Agrobacterium*-mediated transformation in cereals: a promising approach crossing barriers. *Plant Biotech. J.* **4**, 575-603

Shrawat AK, Decker D, Lorz H (2007) *Agrobacterium tumefaciens*-mediated genetic transformation of barley (*Hordeum vulgare L.*). *Plant Sci.* **172**, 281-290

Shou H, Frame BR, Whitham SA, Wang K (2004) Assessment of transgenic maize events produced by particle bombardment or *Agrobacterium*-mediated transformation. *Mol. Breed.* **13**, 201–208

Shure M, Wessler S, Fedoroff N (1983) Molecular identification and isolation of the waxy locus in maize. *Cell* **35**, 225−233

Sikka VK, Choi SB, Kavakli IH, Sakulsingharoj C, Gupta S,Ito H, Okita TW (2001) Subcellular compartmentation and allosteric regulation of the rice endosperm ADP-glucose pyrophosphorylase. *Plant Sci.* **161**, 461–468

Sivitz AB, Reinders A, Johnson ME, Krenz AD, Grof CP, Perroux JM, Ward JM (2007) Arabidopsis sucrose transporter *AtSUC9*. High affinity transport activity, intragenic control of expression, and early flowering mutant genotype. *Plant Physiol.* **143**, 188-198

Smith AM (2008) Prospects for increasing starch and sucrose yields for bioethanol production. *Plant J.* **54**, 546–58

Songstad DD, Halaka FG, DeBoer DL, Armstrong CL, Hinchee MAW, Ford-Santino CG, Brown SM, Fromm ME, Horsch R.B (1993) Transient Expression of

GUS and Anthocyanin Constructs in Intact Maize Immature Embryos Following Electroporation. *Plant Cell, Tissue Organ Cult.* **33**, 195–201

Sorokin AP, Ke XY, Chen D, Elliott MC (2000) Production of fertile transgenic wheat plants via tissue electroporation. *Plant Sci*. **156**, 227-233

Stachel SE, Nester EW (1986) The genetic and transcriptional organization of the *vir* region of the A6 Ti plasmid of *Agrobacterium tumefaciens. EMBO J.* **5**, 1445–1454

Stark DM, Timmerman KP, Barry GF, Preiss J, Kishore GM (1992) Regulation of the amount of starch in plant tissues by ADP-glucose pyrophosphorylase. *Science* **258**, 287–292

Steup M (1988) Starch degradation. *In:* Stumpf PK, Conn EE (Eds), The Biochemistry of Plants. Academic Press, NY. vol.14, pp.255-296.

Streb S, Delatte T, Umhang M, Eicke S, Schorderet M, Reinhardt D, Zeeman SC (2008) Starch granule biosynthesis in *Arabidopsis* is abolished by removal of all debrancing enzymes but restored by the subsequent removal of an endoamylase. *Plant Cell* **20**, 3448–3466

Sullivan TD, Kaneko Y (1995). The maize *Brittle1* gene encodes amyloplast membrane polypeptides. *Planta* **196**, 477-484

Szydlowski N, Ragel P, Raynaud S, Lucas MM, Roldan I, Montero M, Muñoz FJ, Ovecka M, Bahaji A, Planchot V, Pozueta-Romero J, D'Hulst C, Mérida A (2009) Starch granule initiation in Arabidopsis requires the presence of either class IV or class III starch synthases. *Plant Cell* **21**, 2443 – 2457

Tada Y, Sakamoto M, Fujmura T (1990) Efficient Gene Introduction into Rice by Electroporation and Analysis of Transgenic Plants: Use of Electroporation Buffer Lacking Chloride Ions. *Theor. Appl. Genet*. **80**, 475–480

Tahir M, Law D, Stasolla C (2006) Molecular characterization of PgAGO, a novel conifer gene of the ARGONAUTE family expressed in apical cells and required for somatic embryo development in spruce. *Tree Physiol.* **26**, 12-57

Talati R, Baker WL, Pabilonia MS, White CM, Coleman CI (2009) The effects of barley-derived soluble fiber on serum lipids. *Ann. Fam. Med.* **7**, 157–163

Tamura K, Peterson D, Peterson N, Stecher G, Nei M, Kumar S (2011) MEGA5: molecular evolutionary genetics analysis using maximum likelihood, evolutionary distance, and maximum parsimony methods. *Mol. Biol. Evol.* **28**, 2731-2739

Tang K, Wu A, Yao J, Qi H, Lu X (2000) Development Mediated Transformation and Genetic Analysis − Based Selection. *Acta Biotech*. **20**, 175–183

Tetlow IJ, Blissett KJ, Emes MJ (1994) Starch synthesis and carbohydrate oxidation in amyloplasts from developing wheat endosperm. *Planta* **194**, 454–460

Tetlow IJ, Davies EJ, Vardy KA, Bowsher CG, Burrell MM, Emes MJ (2003) Subcellular localization of ADP-glucose pyrophosphorylase in developing wheat endosperm and analysis of a plastidial isoform. *J. Exp. Bot.* **54**, 715–725

Tetlow IJ, Morell MK, Emes MJ (2004) Recent developments in understanding the regulation of starch metabolism in higher plants. *J. Exp. Bot*. **55**, 2131-2145

Tetlow IJ, Morell MK, Emes MJ (2009) Recent developments in understanding the regulation of starch metabolism in higher plants. *J. Exp. Bot.* **55**, 2131–2145

Tetlow IJ, Emes MJ (2011) Plant Systems. Starch Biosynthesis in Higher Plants: The Starch Granule. In: Murray Moo-Young (ed.), *Comprehensive Biotechnology*, Second Edition, Vol 4, pp 37-45.

Thompson JD, Gibson TJ, Plewniak F, Jeanmougin F, Higgins DG (1997) The CLUSTAL_X windows interface: flexible strategies for multiple sequence alignment aided by quality analysis tools. *Nucleic Acids Res.* **25**, 4876-82

Thomashow MF, Panagopoulos CG, Gordon MP, Nester EW (1980) Host range of *Agrobacterium tumefaciens* is determined by the Ti plasmid. *Nature* **283**, 794–796

Thorbjørnsen T, Villand P, Denyer K, Olsen OA, Smith AM (1996a) Distinct isoforms of ADP-glucose pyrophosphorylase occur inside and outside the amyloplasts in barley endosperm. *Plant J.* **10**, 243–250

Thorbjørnsen T, Villand P, Kleczkowski LA, Olsen OA (1996b) A single gene encodes two different transcripts for the ADP-glucose pyrophosphorylase small subunit from barley (*Hordeum vulgare L.*). *Biochem. J.* **313**, 149–154

Tiessen A, Nerlich A, Faix B, Hümmer C, Fox S, Trafford K, Weber H, Weschke W, Geigenberger P (2012) Subcellular analysis of starch metabolism in developing barley seeds using a non-aqueous fractionation method. *J. Exp. Bot.* **63**, 2071-87

Tickle P, Burrell MM, Coates SA, Emes MJ, Tetlow IJ, Bowsher CG (2009) Characterization of plastidial starch phosphorylase in *Triticum aestivum* L. endosperm. *J. Plant Physiol.* **166**,1465–1478

Tingay S, McElroy D, Kalla R, FiegS, Wang M, Thornton S, Brettell R (1997) *Agrobacterium tumefaciens*-mediated barley transformation. *Plant J.* **11**, 1369–1376

Tjaden J, Schwöppe C, Möhlmann T, Quick PW, Neuhaus HE. (1998). Expression of the plastidic ATP/ADP transporter gene in Escherichia coli leads to the presence of a functional adenine nucleotide transport system in the bacterial cytosolic membrane. *J. Biol. Chem.* **273**, 9630–9636

Tjaden JI, Haferkamp B, Boxma AGM, Tielens M, Huynen M, Hackstein JHP (2004) A divergent ADP/ATP carrier in the hydrogenosomes of Trichomonas gallinae argues for an independent origin of these organelles. *Mol. Microbiol*. **51**: 1439–1446

Tomlinson K, Denyer K (2003) Starch synthesis in creal grains. *Adv. Bot. Res*. **40**, 1-61

Topping DL, Clifton PM (2001) Short Chain Fatty Acids and Human Colonic Function: Roles of Resistant Starch and Non Starch Polysaccharides. *Physiol Rev*.**81**, 1031-1064

Toriyama KF, Arimoto Y, Uchimiya H, Hinata K (1988) Transgenic rice plants after direct gene transfer into protoplasts. *Biotechnol* **6**, 1072-1074

Tsai C-Y, Nelson OE (1966) Starch-deficient maize mutants lacking adenosine diphosphate glucose pyrophosphorylase activity. *Science* **151**, 341–343

Vain P, De Buyser J, Trang VB, Haicour R, Henry Y (1995) Foreign gene delivery into monocotyledonous species. *Biotechnol. Adv.* **13**, 653-671

Vain P, Afolabi AS, Worland B, Snape JW. (2003) Transgene behavior in populations of rice plants transformed using a new dual binary vector system: pGreen/pSoup. *Theor. Appl. Genet*.**107**, 210–217

Valent QA et al. (1997) Nascent membrane and presecretory proteins synthesized in *Escherichia coli* associate with signal recognition particle and trigger factor. *Mol. Microbiol*. **25**, 53–64

Visser R G F **, Somhorst** I **, Kuipers GJ, Ruys** NJ **, Feenstra** WJ **Jacobsen** E (1991) Inhibition of the expression of the gene for granule-bound starch synthase in potato by antisense constructs. *Mol. Gen. Genet*. **225**, 289-296

Vrinten PL, Nakamura T (2000) Wheat granule-bound starch synthase I and II are encoded by separate genes that are expressed in different tissues. *Plant Physiol*. **122**, 255 - 264

Walters DA, Vetsch CS, Potts DE, Lundguist RC (1992) Transformation and inheritance of a hygromycin phosphotransferase gene in maize plants. *Plant Mol. Biol*. **18**, 189–200

Wagner S, Baars L, Ytterberg AJ, Klussmeier A, Wagner CS, Nord O, Nygren PA, van Wijk KJ, de Gier JW (2007) Consequences of membrane protein overexpression in *Escherichia coli*. *Mol. Cell Proteomics* **6**, 1527-1550

Wagner S, Klepsch MM, Schlegel S, Appel A, Draheim R, Tarry M, Högbom M, VanWijk KJ, Slotboom DJ, Persson JO, Gier JW (2008)Tuning Escherichia coli for membrane protein overexpression. *Proc. Natl. Acad. Sci.* **105**, 14371–14376

Wan Y, Lemaux PG. (1994) Generation of large numbers of independently transformed fertile barley plants. *Plant Physiol*. **104**, 37–48

Wang Z, Stutte GW (1992) The role of carbohydrates in active osmotic adjustment in apple under water stress. *J. Amer. Soc. Hort. Sci.***117**, 816-823

Weschke W, Panitz R, Sauer N, Wang Q, Neubohn B, Weber H, Wobus U (2000) Sucrose transporter into barley seeds: molecular characterization ot two transporters and implications for seed development and starch accumulation. *Plant J.* **21**, 455-467

Whalen MC, Innes RW, Bent AF, Staskwicz BJ (1991) Identification of Pseudomonas syringae pathogens of Arabidopsis and a bacterial locus determining avirulence on both Arabidopsis and soybean. *Plant cell* **3**, 49-59

Whister RL, Daniel JR. (1984) Molecular structure of starch. In RL Whister, JN Bemiller, EF Paschall, eds, Starch: Chemistry and Technology, Ed2. Academic Press, New York, PP 153-182

Winans SC, Kerstetter RA, Nester EW (1988) Transcriptional regulation of the *virA* and *virG* genes of *Agrobacterium tumefaciens*. *J. Bacteriol*. **170**, 4047–54

Winans SC (1990) Transcriptional induction of an *Agrobacterium* regulatory gene at tandem promoters by plant-released phenolic compounds, phosphate starvation, and acidic growth media. *J. Bacteriol*. **172**, 2433–38

Winkler HH, Neuhaus HE (1999) Non-mitochondrial ATP transport. *Trends Biochem Sci* **24**, 64–68

Wobus U, Weber H. (1999) Sugars as signal molecules in plant seed development. *Biol. Chem.* **390**, 937-944

Wu H, Doherty A, Jones HD (2009) *Agrobacterium*-mediated transformation of bread and durum wheat using freshly isolated immature embryos. *Methods in Molecular Biology, Transgenic wheat, barley and oats 478*, 93- 103

Yamamori M, Fujita S, Hayakawa K, Matsuki J, Yasui T. (2000) Genetic elimination of a starch granule protein, SGP-1, of wheat generates an altered starch with apparent high amylose. *Theor. Appl. Genet.* **101**, 21–29

Yemm EW, Willis AJ (1954) The estimation of carbohydrates in plant extracts by anthrone. *Biochem. J.* **57**, 508–514

Yun SH, Matheson NK (1993) Structure of the amylopectins of waxy, normal, amylose-extender, and wx:ae genotypes and of the phytoglycogen of maize. *Carbohydr. Res*. **243**, 307-321.

Yu-jun R, Jie Z. (2008) Optimization of electroporation paramerts for immature embryos of indica Rice (*Oryza sativa L.*). *Rice Sci.* **15**, 43-50

Zang S, Cho MJ, Koprek T, Yun R. (1999) Genetic transformation of commercial cultivars of oat (*Avena sativa L*) and barley (*Hordeum vulgare L.*) using in vitro shoot meristematic cultures derived from germinated seedlings. *Plant Cell Reports***18**, 959-966

Zeeman SC, Kossmann J, Smith AM (2010) Starch: Its metabolism, evolution and biotechnological modification in plants. *Annu. Rev. Plant Biol.* **61**, 209-234

Zhang S, Cho M-J, Koprek T, Yun R, Bregitzer P, Lemaux PG (2000) Genetic transformation of commercial cultivars of oat (*Avena sativa L.*) and barley (*Hordeum vulgare L.*) using in vitro shoot meristematic cultivars derived from germinated seedlings. *Plant Cell Rep*. **18**, 959–966

Zhang X, Colleoni C, Ratushna V, Sirghie-Colleoni M, James MG, Myers AM (2004) Molecular characterization demonstrates that the *Zea mays* gene *sugary2* codes for the starch synthase isoform SSIIa. *Plant Mol. Biol*. **54**, 865 - 879

Zupan JR, Zambryski PC (1995) Transfer of TDNA from Agrobacterium to the plant cell. *Plant Physiol*. **107**, 1041-1047

APPENDICES

Appendex 1. (chapter 2)
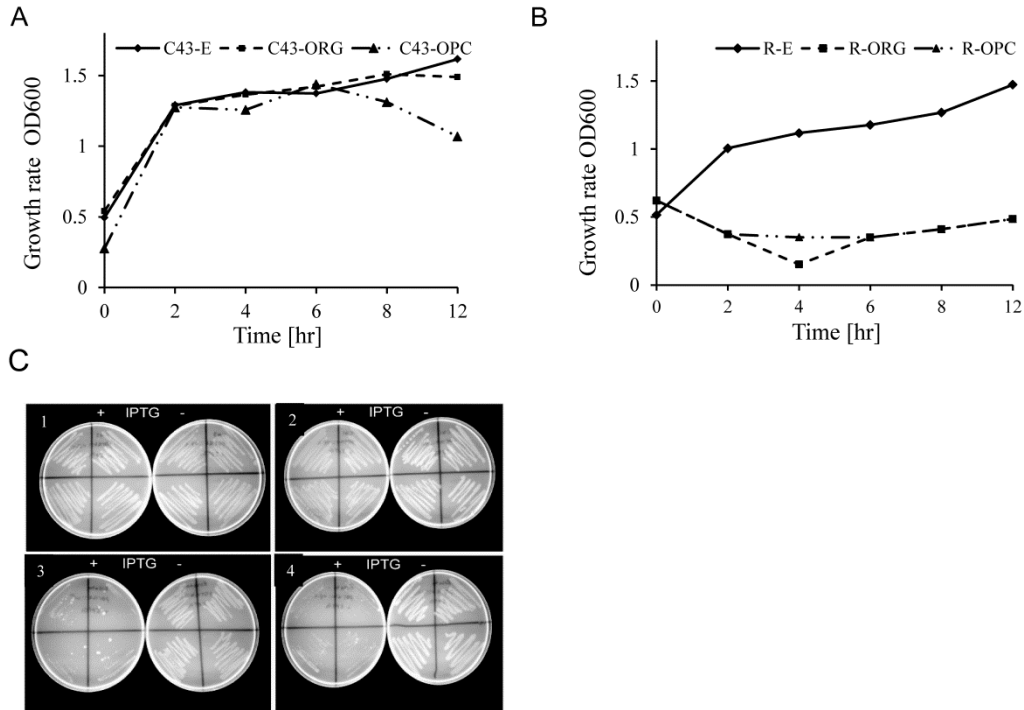
Inhibitory effect of HvBT1 on *E. coli* cells.

A: Growth curve of C43 cells; empty plasmid (C43-E), optimized ORF (C43-OPC), and original ORF (C43-ORG). **B**: Growth curve of Rosetta2 cells; empty plasmid (R-E), optimized ORF (R-OPC), and original ORF (R3-ORG). **C**: Growth of C43 and Rosetta2 cells on plate media. C 1 and 2 indicate the un-induced (-) and induced (+) C43 cells harboring original ORF and optimized ORF, respectively. C 3 and 4 indicate the un-induced (-) and induced (+) Rosetta2 cells harboring original ORF and optimized ORF, respectively.

Appendex 2. (chapter 2)

Barley genomic DNA sequence of *HvBT1* (1486 bp)

ATGGCGGCGGCAATGGCTGCAACGACAATGGTGACCAAGAACAACGGCGGCTCGCTCGCCAT
GGACAAGAAGAACTGGTTCTTTCGGCCGGCCCCTGAGGTCGCCTTCTCTTGGAGCTCGCAGCC
CGAGTCCAGGAGCTTGGAGTTCCCACGCAGGGCTCTGTTCGCCAGCGTCGGACTCAGCCTGTC
CCACGACGGGAAGGCTCGGCCCGCCGACGACGTCGCACACCAATTCGCAGCCGCGGGCGATG
CGGGCGTCCAGCAGGCCCAGAAGGCGAAAAAGGCCAAGAAGCAGCAGCTGGGTCTGAGGAA
GGTGAGGGTCAAGATCGGCAACCCGCACCTGCGTCGGCTGGTCAGCGGCGCCATCGCCGGCG
CCGTTTCGAGGACTTTCGTGGCGCCGCTGGAGACGATCAGGACGCACCTGATGGTGGGAAGCT
CCGGCGCCGACTCCATGGGCGGGGTTTTCCGGTGGATCATGCGGACGGAGGGGTGGCCCGGC
CTCTTCCGCGGCAACGCCGTCAACGTCCTCCGCGTCGCGCCGAGCAAGGCCATCGAGGCAAGC
CAGCCACCTCACGTGTTTTCCTTTGAAATTTCCTATAGTAGACGCGAGATGCATGCATGCATGC
AGCGTCGCTGATGATTCCACTTCCACATGCCGCGGTGCAGCACTTCACTTACGGCACGGCCAA
GAAGTACCTGACCCCGGAGGCCGGCGAGCCAGCCAAGGTCCCCATCCCCACGCCGCTTGTCG
CCAGAGCGCTCGCCGGAGTGGCCTCAACCCTGTGCACCTATCCCATGGAGCTCGTCAAGACCC
GTCTCACCATCGAGGTGAAGAAGACACAGAATTCTGCGCAGTCTCTACCAGTGGCAGTGCCAT
CTGATCAGGCTGACGGCCCCGTTGTGTTGTGTACTTGTGTTGCATGCAGAAGGATGTGTACGA
CAACCTCCTCCACGCGTTCGTCAAGATCGTGCGCGACGAGGGGCCCGGAGAGCTGTACCGCG
GGCTGGCGCCGAGCCTGATCGGCGTGGTGCCGTACGCGGCGGCCAACTTCTACGCCTACGAGA
CACTGCGGGGCGCGTACCGCCGCGCGTCGGGGAAGGAGGAGGTGGGCAACGTGCCGACGCTG
CTGATCGGGTCCGCGGCGGGCGCCATCGCCAGCACGGCCACCTTCCCGCTGGAGGTGGCGCG
GAAGCAGATGCAGGTGGGCGCCGTGGGCGGGAGGCAGGTGTACAAGAACGTCCTGCACGCCA
TGTACTGCATCCTCAACAAGGAGGGCGCCGCCGGGCTCTACCGCGGGCTCGGCCCCAGCTGCA
TCAAGCTCATGCCCGCCGCCGGCATCTCCTTCATGTGCTACGAGGCCTGCAAGAAGATACTCG
TCGACGACAAACAAGACGGCGAGCCCCAGGACCAGGAGGAGACGGAGACCGGACACACACA
AGGACAGGCGGCGCCCAAGAGCCCCAACGCCAACGGTGATCGACCATGA

Appendex 3. (chapter 2)

Barley complete cDNA sequence of *HvBT1* (1287 bp) (GenBank ID: AY560327.2)

ATGGCGGCGGCAATGGCTGCAACGACAATGGTGACCAAGAACAACGGCGGCTCGCTCGCCAT
GGACAAGAAGAACTGGTTCTTTCGGCCGGCCCCTGAGGTCGCCTTCTCTTGGAGCTCGCAGCC
CGAGTCCAGGAGCTTGGAGTTCCCACGCAGGGCTCTGTTCGCCAGCGTCGGACTCAGCCTGTC
CCACGACGGGAAGGCTCGGCCCGCCGACGACGTCGCACACCAACTCGCAGCCGCGGGCGATG
CGGGCGTCCAGCAGGCCCAGAAGGCGAAAAAGGCCAAGAAGCAGCAGCTGGGTCTGAGGAA
GGTGAGGGTCAAGATCGGCAACCCGCACCTGCGTCGGCTGGTCAGCGGCGCCATCGCCGGCG
CCGTTTCGAGGACTTTCGTGGCGCCGCTGGAGACGATCAGGACGCACCTGATGGTGGGAAGCT
CCGGCGCCGACTCCATGGGCGGGGTTTTCCGGTGGATCATGAGGACGGAGGGGTGGCCCGGC
CTCTTCCGCGGCAACGCCGTCAACGTCCTCCGCGTCGCGCCGAGCAAGGCCATCGAGCACTTC
ACTTACGACACGGCCAAGAAGTACCTGACCCCGGAGGCCGGCGAGCCAGCCAAGGTCCCCAT
CCCCACGCCGCTTGTCGCCGGAGCGCTCGCCGGAGTGGCCTCAACCCTGTGCACCTATCCCAT
GGAGCTCGTCAAGACCCGTCTCACCATCGAGAAGGATGTGTACGACAACCTCCTCCACGCGTT
CGTCAAGATCGTGCGCGACGAGGGGCCCGGAGAGCTGTACCGCGGGCTGGCGCCGAGCCTGA
TCGGCGTGGTGCCGTACGCGGCGGCCAACTTCTACGCCTACGAGACACTGCGGGGCGCGTACC
GCCGCGCGTCGGGGAAGGAGGAGGTGGGCAACGTGCCGACGCTGCTGATCGGGTCCGCGGCG
GGCGCCATCGCCAGCACGGCCACCTTCCCGCTGGAGGTGGCGCGGAAGCAGATGCAGGTGGG
CGCCGTGGGCGGGAGGCAGGTGTACAAGAACGTCCTGCACGCCATGTACTGCATCCTCAACA
AGGAGGGCGCCGCCGGGCTCTACCGCGGGCTCGGCCCCAGCTGCATCAAGCTCATGCCCGCC
GCCGGCATCTCCTTCATGTGCTACGAGGCCTGCAAGAAGATACTCGTCGACGACAAACAAGAC
GGCGAGCCCCAGGACCAGGAGGAGACGGAGACCGGACACACACAAGGACAGGCGGCGCCCA
AGAGCCCCAACGCCAACGGTGATCGACCATGA

159

Appendex 4. (chapter 2)

Gene Name: ADP-Glucose transporter gene, Length: 1287bp, Codon Optimization: No
Sequence:

CATATGGCAGCAGCGATGGCAGCAACGACGATGGTTACGAAAAACAACGGTGGCAGCCTGGC
AATGGATAAAAAAAACTGGTTCTTCCGCCCGGCTCCGGAAGTTGCGTTTAGTTGGAGCTCTCA
GCCGGAATCACGTTCGCTGGAATTTCCGCGTCGCGCACTGTTCGCCTCCGTGGGTCTGAGCCT
GTCTCATGATGGTAAAGCACGTCCGGCTGATGACGTCGCACACCAGCTGGCAGCAGCAGGTG
ACGCAGGTGTGCAGCAAGCGCAAAAAGCCAAAAAAGCGAAAAAACAGCAACTGGGCCTGCG
TAAAGTCCGCGTGAAAATTGGTAACCCGCATCTGCGTCGCCTGGTTTCAGGTGCAATCGCAGG
TGCAGTCTCGCGTACCTTTGTGGCACCGCTGGAAACCATTCGCACGCACCTGATGGTGGGCAG
TTCCGGTGCGGATTCCATGGGCGGTGTTTTTCGTTGGATCATGCGTACCGAAGGTTGGCCGGG
TCTGTTCCGTGGTAACGCAGTTAATGTCCTGCGCGTGGCCCCGAGCAAAGCAATTGAACATTT
CACCTATGATACGGCGAAAAAATACCTGACCCCGGAAGCTGGTGAACCGGCGAAAGTTCCGA
TCCCGACGCCGCTGGTCGCTGGTGCACTGGCCGGTGTGGCCAGCACCCTGTGCACGTATCCGA
TGGAACTGGTTAAAACCCGTCTGACGATTGAAAAAGATGTCTACGACAATCTGCTGCACGCGT
TTGTGAAAATCGTTCGTGATGAAGGTCCGGGTGAACTGTATCGTGGTCTGGCACCGTCACTGA
TTGGTGTGGTTCCGTACGCTGCGGCCAACTTCTATGCATACGAAACCCTGCGTGGTGCATATC
GTCGCGCATCGGGCAAAGAAGAAGTCGGTAATGTGCCGACCCTGCTGATTGGCAGTGCAGCT
GGTGCAATCGCTTCCACCGCTACGTTTCCGCTGGAAGTTGCGCGTAAACAGATGCAAGTTGGT
GCTGTCGGCGGTCGCCAGGTGTATAAAAACGTTCTGCATGCCATGTACTGCATTCTGAATAAA
GAAGGCGCAGCAGGTCTGTATCGTGGTCTGGGTCCGAGCTGTATTAAACTGATGCCGGCAGCT
GGCATCTCTTTCATGTGCTACGAAGCGTGTAAGAAAATTCTGGTGGATGACAAACAGGATGGT
GAACCGCAGGACCAAGAAGAAACCGAAACGGGTCATACCCAAGGTCAAGCAGCCCCGAAAT
CGCCGAACGCAAATGGTGATCGTCCGTAAGGATCC